

AN ABSTRACT OF THE DISSERTATION OF

Dong-Wan Kim for the degree of Doctor of Philosophy in Nuclear Engineering
presented on December 11, 2007.

Title: A Unified Model of One-Dimension Two-fluid Horizontal Flows and its
Stability Analysis.

Abstract approved: 

Qiao Wu

An improved version of the one-dimensional horizontal two-fluid flow model has been developed by incorporating physical terms for gravity and local void fraction profiles. Introduction of an interface mixing layer concept allows the one-dimensional two-fluid model to remain hyperbolic. This will overcome a major obstacle in using the current one-dimensional two-fluid horizontal flow model that was developed without considering the local void fraction information.

All these concepts allow the creation of a unified one-dimensional two-fluid model that would work over a wide range of flow structure and wide range of stable relative velocities. The unified formulation removes the unphysical instability caused by switching between flow regimes transition correlations. By eliminating the unphysical instability or numerical oscillations, a smooth transition near flow regime transition boundaries is possible. The unified interfacial model could significantly improve the numerical stability of a thermal-hydraulic code by eliminating the need for a subjective flow regime map and flow regime dependent correlations with the unified correlation.

It is shown that the proposed one-dimensional two-fluid horizontal flow model is stable in a range of flow regimes. To investigate the achieved physical stability, a theoretical characteristic stability analysis is performed with inviscous flow condition. The result is similar to the Kelvin-Helmholtz instability criterion, but closer to realistic

two-fluid natural stability. The unified two-fluid model could significantly improve the stability of horizontal flows and yield a more promising approach to a variety of practical problems.

©Copyright by Dong-Wan Kim

December 11, 2007

All Rights Reserved



**A Unified Model of One-Dimension Two-Fluid Horizontal Flows and its Stability
Analysis**

**by
Dong-Wan Kim**

**A DISSERTATION
submitted to
Oregon State University**

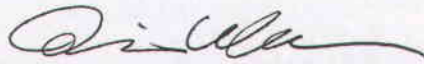
**in partial fulfillment of
the requirements for the
degree of**

Doctor of Philosophy

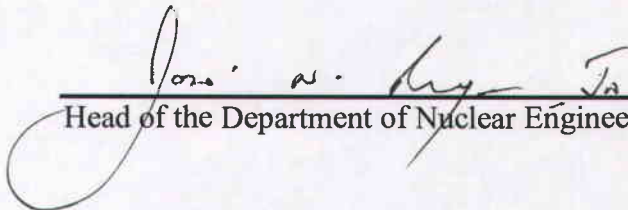
**Presented December 11, 2007
Commencement June 2008**

Doctor of Philosophy dissertation of Dong-Wan Kim presented on December 11 2007.

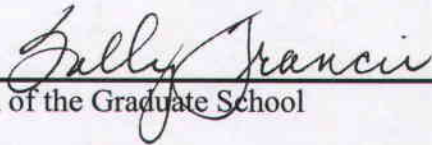
APPROVED:



Major Professor, representing Nuclear Engineering



Head of the Department of Nuclear Engineering and Radiation Health Physics



Dean of the Graduate School

I understand that my dissertation will become part of the permanent collection of Oregon State University libraries. My signature below authorizes release of my dissertation to any reader upon request.



Dong-Wan Kim, Author

ACKNOWLEDGMENTS

The author would like to first thank Dr. Wu for all of his help in formulation, review, and providing the impetus of this work. He has provided exceptional guidance through the model development portion of the work with both theoretical and applied information based upon his experience. Also, I would like to take opportunity to thank Dr. Reyes, Jr. and Dr. Palmer. It is a debt of gratitude for all of the continual support and guidance throughout the research studying phases, which I owed from them. They have been instrumental in my education. Many thank to the other members of my committee, Dr. Woods and Dr. Liburdy, for their valuable comments with a great deal of thought. I have had a large influence on my education, and I am thankful for all of that.

Lastly, I would like to thank my wife and two sons, Mi-Jeong, Woo-Jong, and Yoo-Jong for their great assistant, long lasting patience, and family love, which have been a major part of attaining this degree. They have made all things possible. The author also would like to greatly thank his friends for all the great support and encouragement that have been provided all over the research and studying years at OSU. It has also been my pleasure to have had many enjoyable conversations, which have stimulated and encouraged a large part of this dissertation and research.

TABLE OF CONTENTS

	<u>Page</u>
1 INTRODUCTION	1
2 LITERATURE REVIEW	3
2.1 TWO-FLUID FLOW MODELS	3
2.2 TWO-FLUID HORIZONTAL FLOW	5
2.3 ONE-DIMENSION FLOW MODEL INSTABILITY	7
2.3.1 Hyperbolicity of One-Dimension Two-Fluid Flow	8
2.3.2 Physical Instability and Unphysical Instability	9
2.3.3 Characteristic Stability Analysis	10
2.4 OBJECTIVES	12
3 ONE-DIMENSION TWO-FLUID MODELING	15
3.1 AVERAGING	16
3.2 BASIC RELATIONS OF LOCAL TWO-FLUID INDICATION	18
3.3 BASIC RELATIONS OF LOCAL TWO-FLUID FRACTION	21
3.4 LOCAL INSTANTANEOUS TWO-FLUID CONSERVATION	23
3.5 TIME-AVERAGED TWO-FLUID FLOW EQUATIONS	26
3.6 ONE-DIMENSION TWO-FLUID FLOW EQUATIONS	29
3.6.1 Mass Conservation Equations	30
3.6.2 Momentum Conservation Equations	33
3.6.3 Constitutive Equations	40
3.6.4 One-Dimension Two-Fluid Horizontal Flow	42
3.6.5 Stability Analysis with Delta Pressure	44
4 VOID DISTRIBUTION IN MIXTURE LAYER	48
4.1 LOCAL VOID PROFILES	49
4.2 VOID DISTRIBUTION EQUATION	50
4.3 VOID DISTRIBUTION EQUATION SOLUTION FORMS	55
4.4 PARAMETRIC STUDY OF VOID DISTRIBUTIONS	59
4.5 VOID DISTRIBUTION IN TWO-FLUID MIXTURE LAYER	63

TABLE OF CONTENTS (Continued)

	<u>Page</u>
5 UNIFIED ONE-DIMENSION HORIZONTAL FLOW MODEL	65
5.1 VOID FRACTION VARIATIONS	66
5.1.1 Void Fraction Weighted Average	67
5.1.2 Two-Fluid Flow Interfacial Pressure	67
5.1.3 Void Fraction Integral Parameters and Unification	68
5.2 LINEAR LOCAL VOID FRACTION MODEL.....	71
5.2.1 Stratified Separate and Well-Mixed Bubbly Flow.....	72
5.2.2 Wavy Flow.....	73
5.2.3 Mixed Flow.....	75
5.3 DELTA PRESSURE ON INSTABILITY ANALYSIS	77
5.4 UNIFIED ONE-DIMENSION HORIZONTAL FLOW MODEL	80
6 RESULTS	82
6.1 VOID FRACTION DISTRIBUTION.....	82
6.2 LOCAL VOID FRACTION PROFILE	85
6.2.1 Void Fraction Profiles.....	86
6.2.2 Void Fraction Profiles of Mixed Flow.....	88
6.3 DELTA PRESSURE VERIFICATION.....	91
6.4 STABILITY LIMIT.....	93
7 DISCUSSION AND FUTURE WORK.....	97
8 CONCLUSIONS.....	100
BIBLIOGRAPHY	102
NOMENCLATURE.....	115

LIST OF FIGURES

<u>Figure</u>	<u>Page</u>
2.1 Flow Map for Horizontal Flow [Mandhane et al., 1974]	7
3.1 Separate Flow Indication Function (Typical).....	19
3.2 Mixed Flow Indicator Function (Typical).....	19
3.3 Void Distribution Profiles (Typical)	20
3.4 Definitions of Coordination and Two-Fluid Interface.....	23
4.1 Void Distribution Profile of Different Flow Regimes.....	49
4.2 Void Distribution Equation Solution Forms.....	59
4.3 Void Fraction Diffusion (Diffusion Coefficient Variation)	60
4.4 Void Fraction Decrease (Turbulent Ratio Variations)	61
4.5 Void Fraction Swell (Froude Number Variation)	62
5.1 Linear Void Fraction Profile Model- Wavy Flow	74
5.2 Linear Void Fraction Profile Model-Mixed Flow	76
6.1 Mixture Flow Layer of Different Flow Regimes	83
6.2 Contours of Void Fraction Distribution	84
6.3 Experimental Void Fraction Profiles, $\langle j_f \rangle = 1.65$ m/s	86
6.4 Experimental Void Fraction Profiles, $\langle j_f \rangle = 3.8$ m/s	87
6.5 Experimental Void Fraction Profiles, $\langle j_f \rangle = 4.67$ m/s	89
6.6 Experimental Void Fraction Profiles, $\langle j_f \rangle = 5.0$ m/s	90
6.7 Comparison of Experimental and Theoretical Delta Pressures	92

LIST OF FIGURES (Continued)

<u>Figure</u>	<u>Page</u>
6.8 Comparison of Stability Limits (Experimental, Theoretical, Analytical, and Kevin-Helmholtz).....	94
6.9 Expansion of Analytical Stability Criteria Lines.....	95
D.1 Separated Flow Void Fraction Profile Model.....	133
E.1 Void Fraction Profile for Mixed Flow	136

LIST OF TABLES

<u>Table</u>	<u>Page</u>
2.1 Previous Work for Improving Stability of Two-Fluid Model	14

LIST OF APPENDICES

<u>Appendix</u>		<u>Page</u>
A	VOID FRACTION EQUATION.....	118
B	TWO-FLUID CONSERVATION EQUATIONS	120
C	ONE-D. TWO-FLUID CONSERVATION EQUATIONS.....	122
C.1	Mass Conservation Equation	122
C.2	Momentum Conservation Equation	124
C.3	Constitutive Equation	130
C.4	One-Dimension Horizontal Flow Model	131
D	INTEGRAL PARAMETERS FOR SEPARATED FLOW.....	133
E	INTEGRAL PARAMETERS FOR MIXED FLOW	136
F	DELTA PRESSURE EVALUATION	139

A Unified Model of One-Dimension Two-fluid Horizontal Flows and its Stability Analysis

1 INTRODUCTION

Two-fluid flow can be specified by two intractable single-fluid flows. These local instantaneous two-fluid flow fields can be characterized by their fluid motions, which can be coupled together through the interfacial boundary dependently. The two-fluid boundaries are dynamic, deformable, and continuous at the interface, having a large number or single number of interfaces, resulting in complex flow structures. In the modeling process, the probability of a single-fluid can be represented by single-fluid conservation with interdependent interfacial balance, respectively. These interactions, transferring flux, at interface can be expressed by a set of constitutive relationships. These two-fluid properties can be preserved with a set of mass, momentum, and energy conservation equations using their interface balance conditions.

Even if the resolving of local instantaneous two-fluid motions, it is rendering to more impractical or less useful in applications. A more practical method is necessary for more simplified formulations of the complex two-fluid interactions. This can be accomplished by averaging the two-fluid flow, making two independent fields by introducing some parameters, void fraction or etc. Fundamentally, the difficulties of resolving of the two-fluid interactions can be simplified by introducing a time-averaged parameter. By time-averaging, one of practical methods, a two-fluid flow conservation equation set can be made to an independent two-fluid flow conservation equation set that is engaged with an existing probability density function.

As it is well known, the averaging of these equation sets can depress the real physical governing laws of a two-fluid field in an averaged sense. Time-averaging of local instantaneous conservation equations produces a three-dimensional two-fluid conservation equation set, and area-averaging of the two-fluid conservation equation

set produces a one-dimension two-fluid conservation equation set. The one-dimension conservation equation sets have been used in important multiphase one-dimension computer code formulations.

With having average process and simplifying the complex interface interactions, the current one-dimension two-fluid horizontal flow formulation has unphysical instability problems in applying two-fluid flow numerical calculations. The cause of unphysical instability is the oversimplification of physical situations in dealing with the two-fluid flow or failure to express interfacial transfer terms in averaging processes. To solve these problems, some application codes use a large amount of empirical correlations or correlation factors dependent on flow regimes. The more extensive usages of an empirical correlation cause more numerical instability by switching correlations dependent on flow regimes. These code results could be incorrect when the flow regimes are no longer consistent and thus a numerical instability occurs in these calculations. In order to avoid these problems, a more reasonable physical approach is required to maintain consistence and a proper mechanical method is needed to unify these correlations.

The understanding of the interface interaction mechanisms is very important for determining the two-fluid flow characteristic. A proper averaging mechanism for interface balancing terms is required to correctly express the interfacial constitutive relationship. Averaging of many interfaces or a single interface, the interface distributions dependent on two-fluid flow structure, is required for the closure of these one-dimension equation sets. It will satisfy the necessary condition that a one-dimension two-fluid system equation needs to become closed, then the one-dimension two-fluid difference model can express two-fluid flow physical values well in averaged forms.

2 LITERATURE REVIEW

It has been shown in previous design or analysis of two-fluid flow applications that the dedicated prediction of averaged quantities would be sufficient. A local instantaneous behavior of various flow variables would be too expensive or require too much time even if it were possible. In these applications, some greatly useful parameters that should be known are average velocity, pressure, void fraction, and their gradients on two-fluid flow directions with accounting of instability problems. Unphysical instability can be caused by either unintentionally oversimplifying or neglecting the system physical situations and characteristics during a one-dimension modeling process. If the resultant modeling system is not stable, these models would be of little use under those flow conditions.

2.1 TWO-FLUID FLOW MODELS

As expected, a two-fluid flow consists of two Newtonian fluids with arbitrary viscosities, densities, and deformable interfaces. It is natural that these interfaces are more difficult to understand since their interaction is complex. These difficulties constitute closure problems which are related to the local interfacial terms that require expressing surface wave shapes and distributions of interfaces. In local instantaneous two-fluid flow, each fluid flow is considered separately along with interfacial boundaries with some relations of fluid conservational properties [Revankar and Ishii, 1992]. The basic properties are mass, momentum and energy of each of the two fluids. The transfer rates between the two fluids can be derived by their own conservations and interfacial balancing conditions. They can describe a changing or transferring of mass, momentum and energy of each fluid flow. The most important advantage of two-fluid model is a dynamic interaction between the fluids.

Another advantage is that the model can predict one-dimension-changes by area-averaging the time-averaged two-fluid flow and their interactions. Two-fluid modeling

is far more complicated not only in terms of field equations, but also in terms of these interfacial constitutive equations. Various approximations are usually made to simplify them. In the simplest approach, the two-fluid flows have been represented with a one-dimension single-pressure system form. In many practical applications, one-dimension single-pressure models are sufficiently accurate with only a little increase in the computational efforts compared to a single fluid simulation if without any unphysical instability problems.

These unphysical numerical instabilities are caused by the changing numerical correlations or constitutive equations from one regime to the other. Thus, a proper unified modeling of those complicated fluid structures is very important in achieving stability or finding instability. Using reasonable unified physical terms or a unified constitutive closure relationship, a smooth transition can be possible instead of unphysical oscillations that could occur near flow regime transitions. Furthermore, their numerical codes would no longer need a more subjective flow regime map or regime dependence correlation by eliminating regime dependences.

First of all, a useful two-fluid model that has been considered as a comprehensive two-fluid model that consists of six field equations. Averaging over time is considered mathematically or physically comprehensive of the two-fluid flow [Ishii, 1975; Ishii and Hibiki, 2006]:

● **Continuity Equation and the Interfacial Mass Transfer Condition:**

$$\frac{\partial \alpha_k \rho_k}{\partial t} + \nabla \cdot \alpha_k \rho_k \mathbf{u}_k = - \frac{1}{T_t} \sum_{T_k} \frac{\dot{m}_k}{|n_k \cdot \mathbf{u}_i|} \quad (2.1)$$

$$\dot{m}_k \equiv \mathbf{n}_k \cdot \rho_k (\mathbf{u}_k - \mathbf{u}_i)$$

$$\sum_{k=1}^2 \frac{1}{T_t} \sum_{T_k} \frac{\dot{m}_k}{|n_k \cdot \mathbf{u}_i|} = 0$$

● **Momentum Equation and Interfacial Momentum Transfer Condition:**

$$\begin{aligned} \frac{\partial \alpha_k \rho_k \mathbf{u}_k}{\partial t} + \nabla \cdot (\alpha_k \rho_k \mathbf{u}_k \mathbf{u}_k + \alpha_k \rho_k \tau_k^T + \alpha_k (\rho_k \bar{l} - \bar{r}_k)) - \mathbf{F}_k \alpha_k \\ = -\frac{1}{T_t} \sum_{T_k} \frac{1}{|n_k \cdot u_i|} (\dot{m} u_k + \mathbf{n}_k \cdot (\rho_k \bar{l} - \bar{r}_k)) \end{aligned} \quad (2.2)$$

$$\tau_k^T \equiv \mathbf{u}'_k \mathbf{u}'_k$$

$$\sum_{k=1}^2 \frac{1}{T_t} \sum_{T_k} \frac{1}{|n_k \cdot u_i|} (\dot{m} u_k + \mathbf{n}_k \cdot (\rho_k \bar{l} - \bar{r}_k)) = 0$$

● **Energy Equation and Interfacial Energy Transfer Condition:**

$$\begin{aligned} \frac{\partial}{\partial t} \alpha_k \rho_k (e_k + \frac{u_k^2}{2}) + \nabla \cdot (\alpha_k \rho_k (e_k + \frac{u_k^2}{2}) \mathbf{u}_k + \alpha_k (\rho_k \bar{l} - \bar{r}_k) \mathbf{u}_k + \alpha_k \mathbf{q}'_k) - \alpha_k \mathbf{F}_k \mathbf{u}_k \\ = -\frac{1}{T_t} \sum_{T_k} \frac{1}{|n_k \cdot u_i|} (\dot{m} (e_k + \frac{u_k^2}{2}) + \mathbf{n}_k \cdot (\rho_k \bar{l} - \bar{r}_k) \mathbf{u}_k + \mathbf{n}_k \cdot \mathbf{q}'_k) \end{aligned} \quad (2.3)$$

$$\mathbf{q}'_k \equiv \rho_k (e_k + \frac{u_k^2}{2})' \mathbf{u}'_k + (\rho_k \bar{l} - \bar{r}_k) \mathbf{u}'_k$$

$$\sum_{k=1}^2 \frac{1}{T_t} \sum_{T_k} \frac{1}{|n_k \cdot u_i|} (\dot{m} (e_k + \frac{u_k^2}{2}) + \mathbf{n}_k \cdot (\rho_k \bar{l} - \bar{r}_k) \mathbf{u}_k + \mathbf{n}_k \cdot \mathbf{q}'_k) = 0$$

In obtaining a time-averaged two-fluid flow model, it is needed to treat each of the two-fluid variables separately, including their deformable interfaces modeling. For example, the time-averaged interface pressure at a deformable interface is different from the time-average bulk phase pressure in principle. The truth may actually be quite appropriate in one-dimension two-fluid horizontal flow modeling.

2.2 TWO-FLUID HORIZONTAL FLOW

There are primary types of two-fluid flow patterns dependent on the definition of two-fluid horizontal flow. The most common types of two-fluid horizontal flow are

separated flow and mixed flow. By definition, the separated flow is typically considered as two local flow fields that are subdivided into single fluid regions with a varying number of moveable boundaries. Mixed flow has multiple local boundaries that subdivide into very small single fluid regions. These two-fluid flow types are often classified according to their natural characteristics [Ishii, 1975]: Basically, the three types are:

- Dispersed flow-particles or droplets or bubbles flow
- Separate flow-annular flow or stratified flows
- Transition flow

There are also other types of categorizations according to the interface distribution patterns. Dispersed flow types are characterized by the existence of dispersed bubbles in continuous fluid flow. Slug flow consists of larger bubbles in separating continuous fluid slugs with varied interfaces. Plug flow consists of a few big bubbles with few interface, even normally separate flow has a single interface. Also, all these are dependent on flow properties such as flow rates, channel geometry, density, surface tension, and flow orientations, etc. These flow points are typically determined by using a flow regime map. One of regime maps for horizontal flow is plotted in Figure 2.1. The flow regimes are plotted as a function of superficial velocities, which are determined by dividing volumetric flow rates by total flow cross section area.

From these complicated characteristics, knowing a unique flow pattern is important in a unified modeling or correlation developments in predicting the flow types. Also, it is important to know the point at which one flow pattern will take place from the other in pressure drop calculations. The pressure drop of mixed flow is an order magnitude higher than that of separated flow, especially, in horizontal flow [Taitel and Duker, 1987].

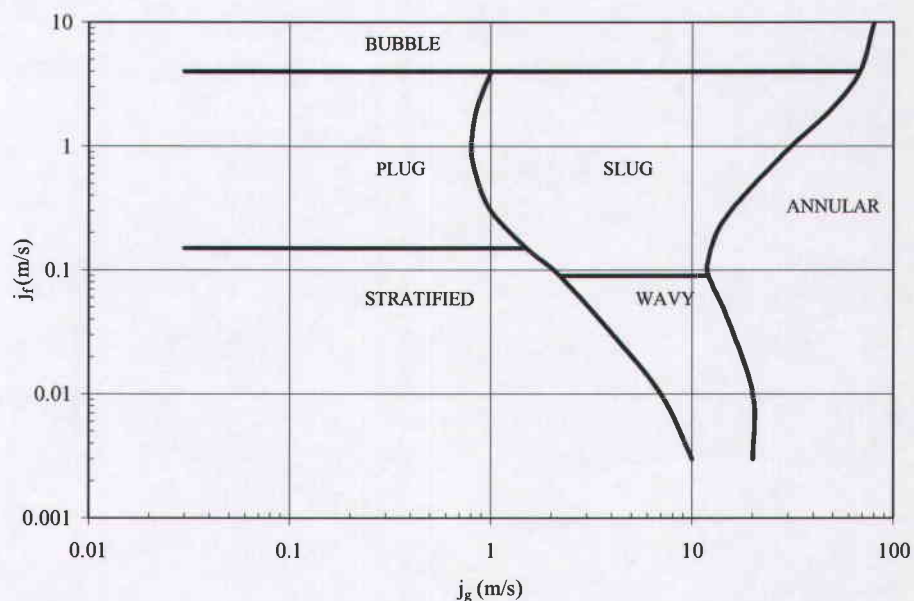


Figure 2.1: Flow Map for Horizontal Flow [Mandhane et al., 1974]

2.3 ONE-DIMENSION FLOW MODEL INSTABILITY

The previous one-dimension models have a few problems in respect to instability, even if one-dimension two-fluid horizontal flow models are very useful in industrial two-fluid calculation applications. These one-dimension models can be formulated by averaging three-dimensional two-fluid equations over the flow's cross-section area. Because of the oversimplification of the physical properties in the averaging process or modeling process, these models have unphysical instability characteristics and have a non-hyperbolic nature.

In one-dimension single-pressure modeling, it has been assumed that each fluid moves at its own uniform velocity with a uniform pressure. On the basis of these local boundary equilibriums, the model has been shown to be unstable for unequal fluid velocities [Gidaspow, 1974; Gidaspow et al., 1983; Lyczkowski et al., 1978; Song & Ishii, 2001]. In multiphase modeling, the main difficulties are due to the deformable

interfaces between the fluids and the discontinuities associated with them. They are directly associated with surface instability problems [Ishii & Mishima, 1984].

2.3.1 Hyperbolicity of One-Dimension Two-Fluid Flow

The introduced instability of a one-dimension model will be directly related to the well-posed or hyperbolic characteristics of the flow model. As an initial boundary value problem, a well-posed model has a solution which must satisfy the following three prerequisites [Drew, 1971; 1983].

- Solution must exist.
- Solution must be uniquely determined.
- Solution must depend continuously on the initial and boundary conditions.

This means that hyperbolic system has a unique solution over the system variables, also pointing out that hyperbolicity is main requirement to understand the characteristic solutions that are associated with their governing systems [Drew, 1971]. Hyperbolicity will correctly reflect what one expects to hold true for fundamental physics systems [Drew, 1983], even if an improper mathematical formulation can describe the physical phenomena. This means that if a one-dimension horizontal flow is modeled properly and has hyperbolicity, the model can simulate the motions of two-fluid flow well. Many other methods have been tried in order to get the system hyperbolicity by proper modeling. One of the attempts to create a realistic stable horizontal flow model is the use of compressible fluid [Gidaspow, 1974; Lyczkowski et al., 1978; Song and Ishii, 2001]. In these attempts of accounting for two-fluid compressibility, an increasing stability was achieved even though it is not a real situation. In the one-dimension two-fluid flow model field, these unequal fluid velocity instability problems have been studied for a long time.

2.3.2 Physical Instability and Unphysical Instability

As well known, the previous one-dimension two-fluid models have physical instability problems when the two-fluid velocities are not equal. These unphysical instabilities are due to a failure in one-dimension modeling such as pressure differences between the interface and phase pressure of two-fluids. If a model possesses a physical instability, the model becomes ill-posed and miss-estimation of two-fluid flow properties during the instability.

Another unphysical instability occurs when a two-fluid flow model is handled improperly. Some multiphase computer code uses one-dimension models that are incorporated with some flow related constitutive correlations. The constitutive relations came from experimental correlations that are dependent on the flow regimes. The correlations should be switched in response to two-fluid flow regime change. Sometimes, an improper commutation between these corrections occurs when an inaccurate flow regime prediction is made. This improper handling causes a numerical oscillation, an unphysical instability. If the model has an inconsistent numerical scheme creating oscillation, then problems become unsolvable [Lyczkowski et al., 1978]. In order to avoid the extensive use of empirical correlations, a more physical, reasonable and mechanical method is needed for unified constitutive relations.

Several attempts have been made to improve these instability properties by introducing some reasonable physical and mathematical terms. Some of the methods are adding a virtual mass term, accounting for a surface tension effect, adding a fluctuating velocity component [Trapp, 1986], introducing one-pressure model sets, assuming a continuous pressure across interface [Gidaspow, 1974], adding viscous stress terms [Ramshaw and Trapp, 1978], adding a virtual mass effect of heavier fluid and an interfacial drag for correcting the acceleration of light density flow in transient mode [Stuhmiller, 1977]. In another method with assuming that the pressure of two-fluid flow is equalized with an infinite pressure propagation speed and under hydrostatic conditions, an improved two-pressure model is presented with real characteristic roots [Ransom and Hicks, 1984]. All these attempts show that these

equations improved the appropriate two-fluid model. Table 2.1 shows some those attempts and improvements by appropriately choosing closure model forms. Some of these methods lead to a real characteristic root and have increased system stabilities.

2.3.3 Characteristic Stability Analysis

A physical instability lies on the prediction of the flow regime transition from stratified wavy flow to mixed slug flow [Trapp, 1986]. The physical mechanism behind flow regime transition is due to interfacial surface instability, when the inertia force overcomes the gravity force. In internal separate flow cases, the interfacial instability would cause growth of flow surface waves reaching the top of the cross section. The flow then transitions from a separated flow into a mixed flow, causing some instable intermittent flows. There is a strong need to determine at what conditions these instabilities occur. These can be analyzed by performing a characteristic analysis method of two-fluid flow equations [Gidaspow, 1974; Lyczkowski et al., 1978].

The characteristic stability analysis method is very similar to perturbation analysis methods, in determining whether a disturbance will amplify or decay a given two-fluid flow condition. For the determination of flow stability, the two-fluid system equations, mass and momentum equations need to line up with these closure relationships. The following procedures are used to change the governing equations to simplify the source term. Writing down mass and momentum conservation equations with these constitutive relationships, and applying incompressible, potential flow, and no body forces, the governing equations are made into a simple differential system of equations. The differential equations can be arranged in a characteristic matrix from which stability characteristic of the system can be found. Following the previous described simplification procedures, a previous model of one-dimension two-fluid horizontal flow can be written:

- **Continuity Equation:**

$$\frac{\partial \rho_k \alpha_k}{\partial t} + \frac{\partial \rho_k \alpha_k u_k}{\partial x} = 0 \quad (2.4)$$

- **Momentum Equation:**

$$\frac{\partial \alpha_k \rho_k u_k}{\partial t} + \frac{\partial \alpha_k \rho_k u_k u_k}{\partial x} + \alpha_k \frac{\partial p_k}{\partial x} = 0 \quad (2.5)$$

With definition of the system state vector \mathbf{x} ;

$$\mathbf{x} = [\alpha \quad u_k \quad u_{\bar{k}} \quad p]^T \quad (2.6)$$

the two-fluid flow differential equation can now be expressed in matrix form:

$$[A] \frac{\partial \mathbf{x}}{\partial t} + [B] \frac{\partial \mathbf{x}}{\partial x} = [C] \quad (2.7)$$

Based upon a prescribed set of initial values, the solution of the matrix equations can be reduced to investigate the roots of the following determinant:

$$|A\lambda - B| = 0 \quad (2.8)$$

For the determinant to be nontrivial, it should be equal to zero. While considering gravity, the determinant solution result gives a specific condition, Kelvin-Helmholtz stability criterion, for the system to remain hyperbolic and be well-posed:

$$u_r \equiv (u_1 - u_2) < \sqrt{\frac{\Delta\rho g H \alpha}{\rho_1}} \quad (2.9)$$

The result shows a criterion that is based on a relative velocity between the two fluids. Mainly two-fluid flow instability is due to the onset of competing dominant forces and the timely switching of them. The above transition criterion is a point where the buoyancy force takes over the inertia force of the two-fluid flow. In the separated flow case, the flow regime will change when buoyancy force dominates the inertia force. In mixed flow cases, a bubbly flow will appear when the liquid inertial-turbulence forces are dominated by the buoyancy force. This knowledge is required to determine the instability criteria, thus must be used in making a well-posed system.

2.4 OBJECTIVES

With literature review of previous works, the current basic one-dimension two-fluid model has an unphysical instability problem. The main cause of the unphysical instability is due to a failure to express the interface of a two-fluid and its interfacial transfer distribution in dealing with the model. In more detail, the cause of the unphysical instability is on the failure of the model is main force; the pressure difference between the bulk phase and the interface pressure that would govern forces of two-fluid flow stability. The pressure difference is between the void fraction-weighted average interfacial pressure and the bulk pressure. Once knowing the unique void fraction profiles from stratified flow to fully mixed flow and incorporating the phase unique distributions into the model, a unified one-dimension two-fluid model can be provided.

In cases of two-fluid codes, these also cause the unphysical instabilities in switching the correlations. They have flow a regime dependence on empirical correlations for flow regimes. When the numerical instability has occurred, the governing equations are not able to be correctly solved and thus, these solutions are no longer consistent. In order to avoid the extensive use of the empirical correlation, a more physical, reasonable and mechanically approached set of equations are needed to close the model equations. Proper modeling of those fluid structures is very important in determining system stability in many applications. With proper modeling of the void distributions, the computer codes will no longer need to be based on the more subjective flow regime maps and its flow regime dependence correlations. Instead, the unphysical instabilities that occur within the current basic one-dimension two-fluid model can be eliminated. By eliminating the unphysical oscillations that can occur near flow regime transition boundaries, a smooth transition from one flow regime type to another can be possible by the unified model. In proposing a unified one-dimension two-fluid horizontal flow formulation with an interface mixing layer concept will be introduced to produce and a unified pressure force in any flow regimes. The unified interfacial differential pressure model could significantly improve the numerical stability of the thermal-hydraulic code.

In this paper, using gravity and void fraction profiles, the author proposes a difference pressure model and furthermore, introduces a unified one-dimension two-fluid horizontal flow formulation with which achieving a physically stable system is possible.

Table 2.1: Previous Work for Improving Stability of Two-Fluid Model

Author	Year	Method	Result	Comment
Gidaspow Lyczkowski et al.	1974 1978	Added compressibility for both phases	Improvement of stability by a finite wave propagation speed	The two-fluid flow should be incompressible. ($Ma < 0.3$)
Ramshaw & Trapp	1978	Included Surface tension and compressibility for stability analysis,	Compares instability of system between short wavelength and long wavelength of two flows	Only short wavelength is stable.
Stumiller	1977	Interfacial pressure	Modified the interfacial pressure for improvement of stability	Used for bubbly flows. No separated flow consideration
Ransom and Hicks	1983	Interfacial pressure model	Shows the interfacial pressure by averaging the two phases pressure	Symmetric interfacial pressure
Thorley & Wiggert No & Kazimi Lahey	1985 1985 1991	Virtual mass	Includes the virtual mass force in interfacial force	Requires virtual mass coefficient No separated flow consideration
Song & Ishii Song & Ishii Song	2000 2001 2003	Momentum covariance of the convective term	Represents effects of void and momentum flux profile for the stabilized flow	Account for both void and velocity profile No separated flow consideration
Chung et al.	2001 2004	Surface tension and finite interface thickness	Introduces the modified surface tension term for instability	No separated flow consideration Requires interface thickness
Kent Abel	2005	Interfacial pressure model	Shows the interfacial pressure by considering gravity	Symmetric interfacial pressure model

3 ONE-DIMENSION TWO-FLUID MODELING

For a real industrial application of two-fluid flow, a more practical formulation or simplified method is necessary due to the complexity of two-fluid structures and interactions. This can be accomplished by making a mean two-fluid flow model with reasonable constitutive relation. Various methods can be applied in averaging local instantaneous formulations by more rigorous mathematical foundation [Ishii, 1981].

Two-fluid flow can be expressed by time-averaged conservation equation sets. Furthermore, one-dimension two-fluid models can be obtained by averaging a local instantaneous flow conservation mechanism over space and time. Mathematical derivation of these models is based on a fundamental time-space-averaging of two-fluid conservation with the same procedure for closure relations. Time-averaging of local instantaneous two-fluid flow provides local void fraction parametric two-fluid flow relationships, which are mass, momentum, and energy conservation. An auxiliary relationship is inter-fluid distributions such as a local void fraction distribution that distinguishes two-fluid mixture in an equilibrium state. By distinguishing two individual fluids, the void fraction is a mixture fraction or an existence probability of one of two single-fluids. A detailed derivation of two-fluid conservation equation will be described on the above point of view. Area-averaging of the void parametric two-fluid flow can produce a one-dimension two-fluid equation. The resulting averaged conservation equation has a simpler mathematical formulation than the original local instance equations. By making the readable formulations, some information could be lost with improper average handling. The lost information is needs to be complemented by carefully applying appropriate methods. With the auxiliary relationships, the one-dimension model can be used in multiphase computer codes without the previous instability problems. The derivation of these auxiliary relationships is a shift in moderating constitutive relationships, which is needed to close the relationship of the one-dimension two-fluid flow equation.

With the previous mathematical operations, various average terms will appear in a two-fluid modeling. Physically, time-averaging will separate mean values from a timely fluctuating, a sort of a noise single, quantity. The mean values can be measurable and, sometimes, invaluable in a mean average manner. Using these time-area-averaged definitions, a one-dimension two-fluid model can be developed. Practically, the developed one-dimension model can be used in calculation of multiphase flow, if the model does not show an unphysical instability.

3.1 AVERAGING

Averaging is integrating, normalizing, and smoothing a local instantaneous variation over a concerned domain. It will average, normalize, and smooth out the related value. By averaging methods, a mean two-fluid flow behavior can be obtained from a local instantaneous two-fluid flow. These are based on the following mathematical formulation method:

- Time- Averaging
- Space-Averaging

Both methods are commutative, interchangeable, and independent in the order that they applied. By integrating over flow cross-sectional area and dividing by the area, an area-averaged equation can be obtained. Similarly, by integrating over a sampling time, a time-averaged equation can be obtained. In these averaging processes, an additional variable can be introduced into the averaged equations like a time fraction or void fraction. The fractions are deeply dependent on each other, because a specific space occupation material in two-fluid flowing is one of two relative materials. Void fraction is commonly used in two-fluid modeling [Ishii 1975].

For illustrating the mathematical averaging procedure of two-fluid flow, the flow variables are required to be continuous and first order derivation. This means that the

local instantaneous flow variables need to be continuous over individual fluids and would be discontinuous at the interfaces. In these cases, these constituents are treated as superimposed continua and could be described by a mean variable, which can be obtained through averaging process. For a functional quantity, $F_k(x,t)$, the corresponding mathematical time-averaged quantity is defined:

$$\bar{F}_k \equiv \frac{1}{T} \int_{T_k} F_k dt \quad (3.1)$$

In the above equation, T is a total sampling time and T_k is the occupational time of k -fluid at a local point. With the definition of a time averaged quantity, the time-average of the time-fluctuation should be zero except for the averaging of these products. Also, the averaging of two variable products is different from the product of the two average variables:

$$\begin{aligned} F_k &= \bar{F}_k + F'_k \\ \bar{F}'_k &= 0 \\ \overline{F_k G_k} &= \bar{F}_k \bar{G}_k + \overline{F'_k G'_k} \end{aligned} \quad (3.2)$$

In the above equations, \bar{F}_k is the time-averaged value of any two-fluid variable F and F'_k is its timely fluctuation. These relations are very important to variables that are averaged in the deriving of average-product components, particularly, a fluctuating velocity product. In two-fluid flow, a velocity fluctuation term leads to a description of the Reynolds stress, one of the important properties in time-averaged momentum conservation. Similar to a time-average, an area-average quantity is defined:

$$\langle F_k \rangle \equiv \frac{1}{A} \int_{A_k} F_k dA \quad (3.3)$$

In the above equation, A is the total cross section area of a two-fluid flow and A_k is the summation of flow cross-section area of a k -fluid. Furthermore, a weighted area-average quantity is defined by:

$$\langle\langle F_k \rangle\rangle = \frac{\langle \alpha_k F_k \rangle}{\langle \alpha_k \rangle} \quad (3.4)$$

In the above equation, α_k is an average weighting factor and would be a time fraction or a void fraction of a two-fluid flow depending on the definition. These relations will be used in applying the important concept of a two-fluid fraction weighted average in defining two-fluid flow variations, and in expanding to the fraction-gradient-weight average.

3.2 BASIC RELATIONS OF LOCAL TWO-FLUID INDICATION

To indicate a specified single-fluid of a two-fluid flow over time and space domain, some special indication functions are needed. They have to be continuous in the individual fluid and discontinuous at the interfaces as shown Figure 3.1 and Figure 3.2. Graphically, they will show whole flow structure information through the local indication function, on or off two-fluid configuration over a flow cross section, for a separated and a mixed flow. One of them is an index function that is defined at a spatial position and a temporal time:

$$M_k(x,t) = \begin{cases} 1 & \text{if } x \text{ is in } k \text{ fluid at time } t \\ 0 & \text{otherwise} \end{cases} \quad (3.5)$$

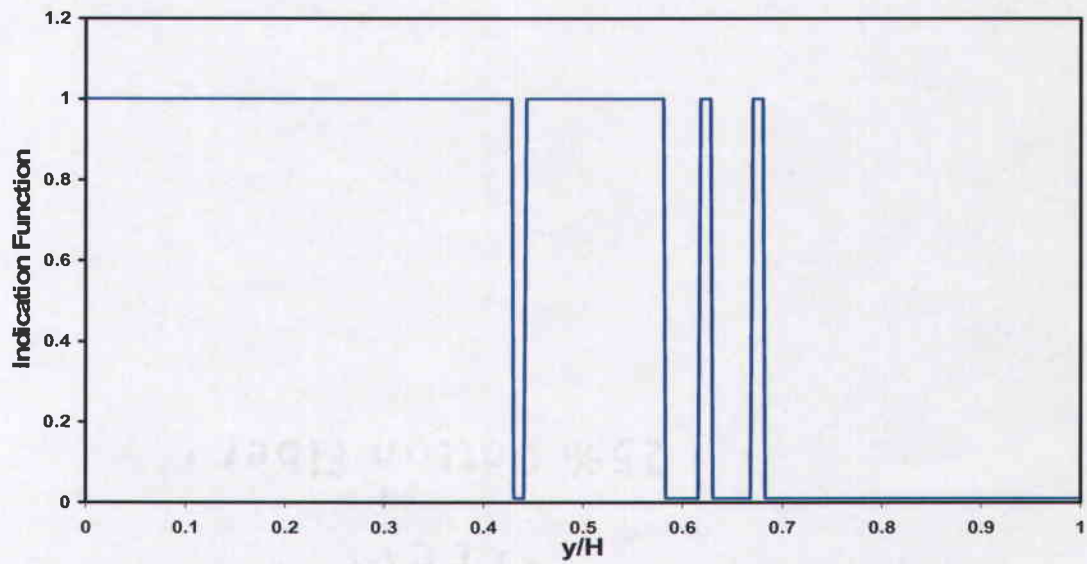


Figure 3.1: Separate Flow Indication Function (Typical)

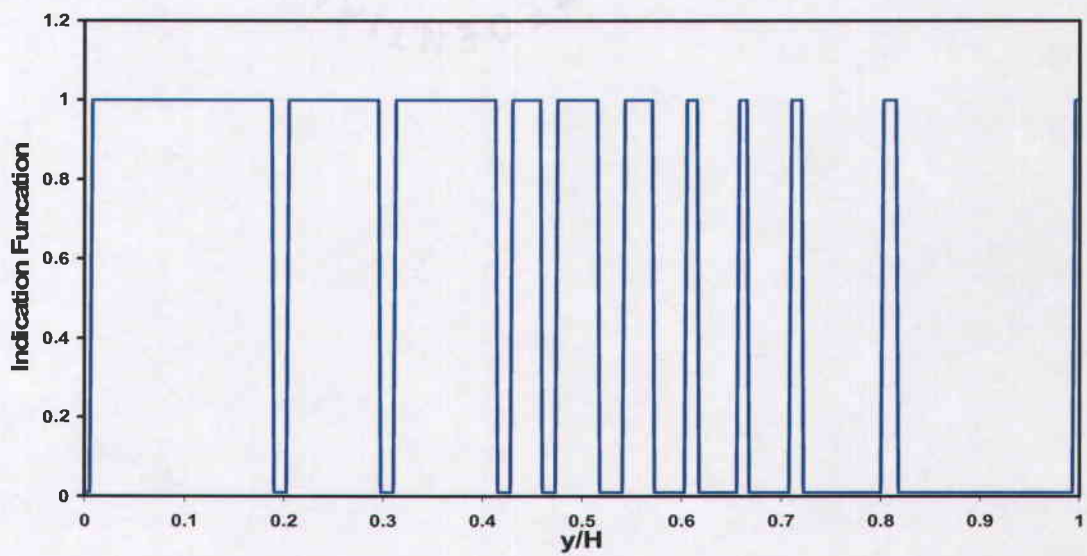


Figure 3.2: Mixed Flow Indicator Function (Typical)

With these definitions, the variations of two-fluid flow can be multiplied by the indication function. The corresponding mathematical time-average of the indication function, a local void fraction or time fraction of a specified k-fluid, is defined:

$$\alpha_k \equiv \frac{1}{T} \int_{T_k} M_k(\mathbf{x}, t) dt = \frac{T_k}{T} \quad (3.6)$$

In the above equation, T is a total sampling time and T_k is a k-fluid occupation time during the sampling time. From this definition, the local instantaneous two-fluid flow can then be treated as superimposed continua and can be expressed through average-smoothing processes. This time-averaging can be applied on a time fluctuating interface to obtain local void fraction, which will allow a simulation parameter of the time average interface motions in two-fluid flow [Ishii, 1975; Drew 1979, 1983].

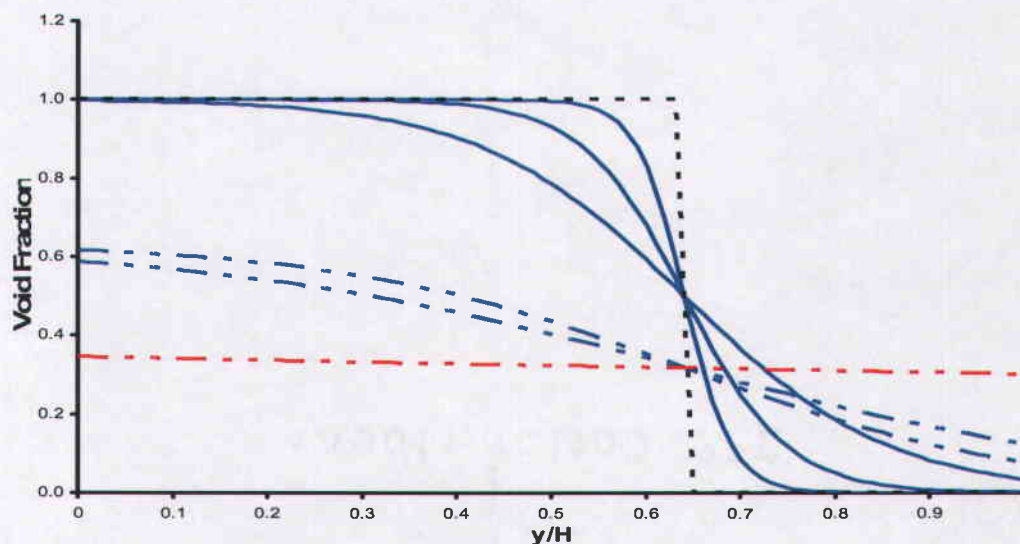


Figure 3.3: Void Distribution Profiles (Typical)

By the definition, time-averaging of the indication function is the probability of a fluid occupation over a relevant total time. The average function is continuous and is equal to zero outside of a single-fluid domain. Graphically, Figure 3.2 shows cross-sectional two-fluid flow time-average structure through the local void fraction function. It is the probability of existence of one of two single-fluids, for a separated and a mixed flow.

3.3 BASIC RELATIONS OF LOCAL TWO-FLUID VOID FRACTION

A time-averaging of local instantaneous two-fluid interactions allows a simple local two-fluid fraction formulation, which is very useable in mean formula algorithm. As shown in Figure 3.2, the higher order fluctuations are the results of multiple local instantaneous two-fluid interactions, mixing, and transitioning toward a local spontaneous equilibrium state. Time-averaging the flow arising flow fluctuations, an index function, can be suppressed as shown Figure 3.3. Mathematically, all these two-fluid interface relations can be obtained by applying Leibnitz's rule and Gauss theorem [Appendix A]:

- Leibnitz Rule:

$$\int_{T_k} \frac{\partial f_k}{\partial t} dt = \frac{\partial}{\partial t} \int_{T_k} f_k dt - \sum_{T_k} \frac{\mathbf{u}_i \cdot \mathbf{n}_k}{|\mathbf{u}_i \cdot \mathbf{n}_k|} f_k \quad (3.7)$$

- Gauss Theorem:

$$\int_{T_k} \nabla \cdot f_k dt = \nabla \cdot \int_{T_k} f_k dt + \sum_{T_k} \frac{\mathbf{n}_k}{|\mathbf{u}_i \cdot \mathbf{n}_k|} f_k \quad (3.8)$$

In the above equation, \mathbf{n}_k is the k-fluid normal vector, and $\mathbf{u}_i \cdot \mathbf{n}_k$ is the two-fluid interface surface displacement velocity. From the Leibniz rule, the averaging of the time-derivative indication function over a time sampling time can be written:

$$\frac{\partial \alpha_k}{\partial t} = \frac{1}{T_t} \sum_{T_k} \frac{\mathbf{u}_i \cdot \mathbf{n}_k}{|\mathbf{u}_i \cdot \mathbf{n}_k|} \quad (3.9)$$

With Gauss theorem, a space-derivative indication function can be derived similarly:

$$\nabla \cdot \alpha_k = -\frac{1}{T_t} \sum_{T_k} \frac{\mathbf{n}_k}{|\mathbf{u}_i \cdot \mathbf{n}_k|} \quad (3.10)$$

In the above equations, T_k is the occupation time of k-fluid during sampling time. By combining the above two terms, a void fraction conservation equation can be written:

$$\frac{\partial \alpha_k}{\partial t} + \mathbf{u}_i \cdot \nabla \alpha_k = 0 \quad (3.11)$$

The void fraction equation shows the local void fraction invariant. Also, a steady-state void fraction can vanish unless there is a timely void source [Ishii, 1975, 2006; Drew & Passman, 1999]. By setting the partial time derivative terms equal to zero, some stationary relations of the void fraction are obtained.

$$\begin{aligned} [1] \quad \frac{\partial \alpha_k}{\partial x} &= \frac{\partial \alpha_k}{\partial y} = 0 \\ [2] \quad \frac{\partial \alpha_k}{\partial x} + \frac{\partial \alpha_k}{\partial y} &= 0 \end{aligned} \quad (3.12)$$

The first equation sets lead to a solution that can be valid for both well mixed bubbly flow and separated single-fluid flow. The second form would lead to the solution of mixture or mixing zone.

$$\begin{aligned} [1] \quad & \alpha_k = \text{const} \\ [2] \quad & \frac{\partial \alpha_k}{\partial x} = -\frac{\partial \alpha_k}{\partial y} \end{aligned} \quad (3.13)$$

The above relations provide the foundation for deriving a one-dimension two-fluid flow model with a local interface relationship term. In next section, local instantaneous two-fluid flow conservation equation derivations are described.

3.4 LOCAL INSTANTANEOUS TWO-FLUID CONSERVATION

A two-fluid conservation equation set can be derived by manufacturing local instantaneous two single-fluid conservation equation sets. By adding each single-fluid conservation equation, a homogenized two-fluid local instantaneous conservation equation can be made. On the basis of a continuum of two-fluid, these attempts have been made in considering simple two-fluid flow models [Ishii, 1975; Drew 1979, 1983].

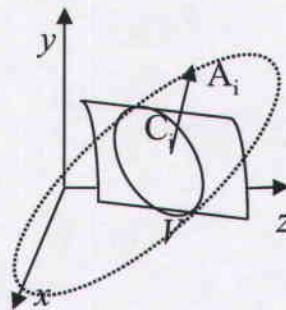


Figure 3.4: Definitions of Coordination and Two-Fluid Interface

An integral form of a single-fluid local instantaneous general conservation equation can be written with the following descriptions. The time change rates for the conservation quantity are equal to source rates minus sink rates over a control volume, including the flux over the surface of the control volume. Mathematically, the integral form of the single-fluid local instantaneous conservation equation can be written as

$$\frac{d}{dt} \int_V \rho_k \psi_k dV = \int_V s_k dV - \int_A \rho_k \psi_k (\mathbf{u}_k \cdot \mathbf{n}_k) dA - \int_A \mathbf{n}_k \cdot \mathbf{J}_k dA \quad (3.14)$$

In the above equation, $\rho_k \psi_k$ is the conservation quantity, and \mathbf{J}_k is the non-convective flux, with which the conservation quantity is transported over the control volume surface, and S_k is the production rate of the conservational quantity. By adding two single-fluid conservation equations with index k , an integral form of the two-fluid local instantaneous conservation equation can be written:

$$\sum_{k=1}^2 \frac{d}{dt} \int_V \rho_k \psi_k dV = - \sum_{k=1}^2 \int_A \rho_k \psi_k (\mathbf{u}_k \cdot \mathbf{n}_k) dA - \sum_{k=1}^2 \int_A \mathbf{n}_k \cdot \mathbf{J}_k dA + \sum_{k=1}^2 \int_V s_k dV \quad (3.15)$$

By rearranging the local instantaneous two-fluid equation, it can be reduced to a new two-fluid flow conservation equation:

$$\sum_{k=1}^2 \frac{d}{dt} \int_V \rho_k \psi_k dV + \sum_{k=1}^2 \int_A \mathbf{n}_k \cdot (\rho_k \psi_k \mathbf{u}_k + \mathbf{J}_k) dA = \sum_{k=1}^2 \int_V s_k dV \quad (3.16)$$

In the above equation, the first term is the time change rate of the conservation quantity, the second term is a net change rate over the two-fluid flow surface, and the

third is the source generation rate. Applying Leibnitz rule and Gauss theorem to the first and second terms, they can be rewritten, respectively:

- First Term :

$$\frac{d}{dt} \int_V \rho_k \psi_k dV = \int_V \frac{\partial \rho_k \psi_k}{\partial t} dV + \int_{A_i} \rho_k \psi_k (\mathbf{u}_i \cdot \mathbf{n}_k) dA \quad (3.17)$$

- Second Term:

$$\begin{aligned} & \int_A n_k \cdot (\rho_k \psi_k \mathbf{u}_k + \bar{\mathbf{J}}_k) dA \\ &= \int_V \nabla \cdot (\rho_k \psi_k \mathbf{u}_k + \mathbf{J}_k) dV - \int_{A_i} n_k \cdot (\rho_k \psi_k \mathbf{u}_k + \mathbf{J}_k) dA \end{aligned} \quad (3.18)$$

Combining the two previous terms:

$$\begin{aligned} & \sum_{k=1}^2 \left(\int_V \frac{\partial \rho_k \psi_k}{\partial t} dV + \int_{A_i} \rho_k \psi_k (\mathbf{u}_i \cdot \mathbf{n}_k) dA \right) \\ &+ \sum_{k=1}^2 \left(\int_V \nabla \cdot (\rho_k \psi_k \mathbf{u}_k + \mathbf{J}_k) dV - \int_{A_i} n_k \cdot (\rho_k \psi_k \mathbf{u}_k + \mathbf{J}_k) dA \right) = \sum_{k=1}^2 \int_V S_k dV \end{aligned} \quad (3.19)$$

By rearranging both sides in a control volume, the above conservation equation can be written:

$$\begin{aligned} & \sum_{k=1}^2 \int_V \left(\frac{\partial \rho_k \psi_k}{\partial t} + \nabla \cdot (\rho_k \psi_k \mathbf{u}_k + \mathbf{J}_k) - S_k \right) dV \\ & - \sum_{k=1}^2 \int_{A_i} n_k \cdot (\rho_k \psi_k (\mathbf{u}_k - \mathbf{u}_i) + \mathbf{J}_k) dA = 0 \end{aligned} \quad (3.20)$$

Because the control domain of the above two-fluid conservation equation is arbitrarily selected, the summation-integral terms can be divided into the control volume and the control surface, and both the summation-integral individual parts are zero:

$$\sum_{k=1}^2 \int_V \left(\frac{\partial \rho_k \psi_k}{\partial t} + \nabla \cdot (\rho_k \psi_k \mathbf{u}_k + \mathbf{J}_k) - S_k \right) dV = 0 \quad (3.21)$$

Further, by removing the summation notations using the previous argument, a simplified differential form of the two-fluid conservation equation can be obtained:

$$\frac{\partial \rho_k \psi_k}{\partial t} + \nabla \cdot (\rho_k \psi_k \mathbf{u}_k + \mathbf{J}_k) - S_k = 0 \quad (3.22)$$

Similarly, the integrand over the control surface can be reduced to a summation of a two-fluid balance equation:

$$\begin{aligned} \sum_{k=1}^2 \dot{m} \psi_k + \mathbf{n}_k \cdot \mathbf{J}_k &= 0 \\ \dot{m} &\equiv \rho_k \psi_k (\mathbf{u}_k - \mathbf{u}_i) \cdot \mathbf{n}_k \end{aligned} \quad (3.23)$$

With a mass transfer rate definition, the surface balance can be simplified. By time-averaging the above equation set, a two-fluid conservation equation can be obtained.

3.5 TIME-AVERAGED TWO-FLUID FLOW EQUATIONS

The main purpose of time-averaging a local instantaneous two-fluid equation is to remove the local flow fluctuations and get a two-fluid model equation representing a mean flow relation and base flow behavior [Trapp 1986]. By multiplying the

conservation equation sets by each fluid index function and applying time averaging over a sampling time, an integral form of time-averaged conservation can be obtained:

$$\frac{1}{T_t} \int_{\bar{t}_i} \frac{\partial \rho_k \psi_k M_k}{\partial t} dt + \frac{1}{T_t} \int_{\bar{t}_i} \nabla \cdot (\rho_k \psi_k \mathbf{u}_k M_k + \mathbf{J}_k M_k) dt = \frac{1}{T_t} \int_{\bar{t}_i} \mathbf{s}_k M_k dt \quad (3.24)$$

Applying Leibnitz rule and Gauss theorem [Appendix B], similar to deriving the differential two-fluid conservation equation, a differential form of time-averaged conservation equation can be obtained:

- First Term :

$$\frac{1}{T_t} \int_{\bar{t}_i} \frac{\partial \rho_k \psi_k M_k}{\partial t} dt = \frac{\partial}{\partial t} \left(\frac{\alpha_k}{T_k} \int_{\bar{t}_k} \rho_k \psi_k dt \right) - \frac{1}{T_t} \sum \frac{\mathbf{n}_k \cdot \mathbf{u}_i}{|\mathbf{n}_k \cdot \mathbf{u}_i|} \rho_k \psi_k \quad (3.25)$$

- Second Term:

$$\begin{aligned} & \frac{1}{T_t} \int_{\bar{t}_i} \nabla \cdot (\rho_k \psi_k \mathbf{u}_k + \mathbf{J}_k) M_k dt \\ &= \nabla \cdot \left(\frac{\alpha_k}{T_k} \int_{\bar{t}_k} (\rho_k \psi_k \mathbf{u}_k + \mathbf{J}_k) dt \right) + \sum \frac{\mathbf{n}_k \cdot (\rho_k \psi_k \mathbf{u}_k + \mathbf{J}_k)}{T_k |\mathbf{n}_k \cdot \mathbf{u}_i|} \end{aligned} \quad (3.26)$$

Combining the first two terms, the time-averaged equation can be written:

$$\begin{aligned} & \frac{\partial}{\partial t} \left(\frac{\alpha_k}{T_k} \int_{\bar{t}_k} \rho_k \psi_k dt \right) + \nabla \cdot \left(\frac{\alpha_k}{T_k} \int_{\bar{t}_k} (\rho_k \psi_k \mathbf{u}_k + \mathbf{J}_k) dt \right) - \frac{\alpha_k}{T_k} \int_{\bar{t}_k} \mathbf{s}_k dt \\ &= \frac{1}{T_t} \sum \frac{\mathbf{n}_k \cdot \mathbf{u}_i}{|\mathbf{n}_k \cdot \mathbf{u}_i|} \rho_k \psi_k - \sum \frac{\mathbf{n}_k \cdot (\rho_k \psi_k \mathbf{u}_k + \mathbf{J}_k)}{T_k |\mathbf{n}_k \cdot \mathbf{u}_i|} \end{aligned} \quad (3.27)$$

With the definitions of time-averaged quantities;

$$\begin{aligned}
 \frac{1}{T_k} \int_{T_k} \rho_k \psi_k dt &\equiv \overline{\rho_k \psi_k}^T \\
 \frac{1}{T_k} \int_{T_k} \rho_k \psi_k \mathbf{u}_k dt &\equiv \overline{\rho_k \psi_k \mathbf{u}_k}^T \\
 \frac{1}{T_k} \int_{T_k} \mathbf{J}_k dt &\equiv \overline{\mathbf{J}_k}^T \\
 \frac{1}{T_k} \int_{T_k} \mathbf{s}_k dt &\equiv \overline{\mathbf{s}_k}^T
 \end{aligned} \tag{3.28}$$

The integral form of the two-fluid conservation equations can be reduced to a more readable time-averaged differential conservation equation form:

$$\begin{aligned}
 &\frac{\partial}{\partial t} (\alpha_k \overline{\rho_k \psi_k}^T) + \nabla \cdot (\alpha_k \overline{\rho_k \psi_k \mathbf{u}_k}^T + \overline{\mathbf{J}_k}^T) - \alpha_k \overline{\mathbf{S}_k}^T \\
 &= \frac{1}{T_t} \sum_{T_t} \frac{-\mathbf{n}_k}{|\mathbf{n}_k \cdot \mathbf{u}_i|} (\rho_k (\mathbf{u}_k - \mathbf{u}_i) \psi_k + \mathbf{J}_k)
 \end{aligned} \tag{3.29}$$

The first three terms are the same form as the local instantaneous general conservation equations and the last term is very similar to the local instantaneous interface two-fluid balance equation. Using the definition of mass transfer rates, the time-averaged conservation two-fluid flow equation can be rewritten:

$$\begin{aligned}
 &\frac{\partial}{\partial t} (\alpha_k \overline{\rho_k \psi_k}^T) + \nabla \cdot (\alpha_k \overline{\rho_k \psi_k \mathbf{u}_k}^T + \alpha_k \overline{\mathbf{J}_k}^T) - \alpha_k \overline{\mathbf{S}_k}^T \\
 &= \frac{1}{T_t} \sum_{T_t} \frac{-1}{|\mathbf{n}_k \cdot \mathbf{u}_i|} (\dot{m}_k \psi_k + \mathbf{n}_k \cdot \mathbf{J}_k)
 \end{aligned} \tag{3.30}$$

The above equation is similar to the local instantaneous conservation equations multiplied by a local void fraction. Furthermore, by averaging fluctuation over time, a substantial conservation equation is obtained:

$$\begin{aligned} \frac{\partial}{\partial t} (\alpha_k \rho_k \bar{\psi}_k) + \nabla \cdot (\alpha_k \rho_k \bar{\psi}_k \bar{\mathbf{u}}_k + \rho_k \overline{\psi'_k \mathbf{u}'_k} + \alpha_k \bar{\mathbf{J}}_k) - \alpha_k \bar{s}_k \\ = \frac{1}{T_t} \sum_{T_i} \frac{-1}{|\mathbf{n}_k \cdot \mathbf{u}_i|} (\dot{m}_k \psi_k + \mathbf{n}_k \cdot \mathbf{J}_k) \end{aligned} \quad (3.31)$$

These formulations will hold that the two-fluid flow variation is indicated by long waves of local void fraction that is considered by averaging these flow variables over time. Averaging of the above time-averaged conservation equation over a two-fluid flow cross-sectional area will provide a one-dimension two-fluid equation.

3.6 ONE-DIMENSION TWO-FLUID FLOW EQUATIONS

By removing the over bar of the time-averaged equations for simplified notation, a time-average conservation equation can be written:

$$\begin{aligned} \frac{\partial}{\partial t} \alpha_k \rho_k \psi_k + \nabla \cdot (\alpha_k \rho_k \psi_k \mathbf{u}_k + \rho_k \psi'_k \mathbf{u}'_k + \alpha_k \mathbf{J}_k) \\ = \alpha_k s_k - \frac{1}{T_t} \sum_{T_i} \frac{1}{|\mathbf{n}_k \cdot \mathbf{u}_i|} (\dot{m} \psi_k + \mathbf{n}_k \cdot \mathbf{J}_k) \end{aligned} \quad (3.32)$$

In the above relations, it is assumed that the density does not change over the total sampling time. The first term is the local time change rate, the second term is the convective change rate, and the third term is the source generation rate. As shown in time-average procedures, an integral form of the area-averaged two-fluid conservation

equation can be created by integrating over the flow cross section area and by dividing both sides by the total two-fluid flow cross-sectional area:

$$\begin{aligned} & \frac{1}{A_A} \int \frac{\partial \alpha_k \rho_k \psi_k}{\partial t} dA + \frac{1}{A_A} \int \nabla \cdot (\alpha_k \rho_k \psi_k \mathbf{u}_k + \rho_k \psi'_k \mathbf{u}'_k + \alpha_k \mathbf{J}_k) dA \\ & = \frac{1}{A_A} \int s_k \alpha_k dA - \frac{1}{A_A} \int \frac{1}{T_t} \sum \frac{1}{|\mathbf{n}_k \cdot \mathbf{u}_i|} (\dot{m} \psi_k + \mathbf{n}_k \cdot \mathbf{J}_k) dA \end{aligned} \quad (3.33)$$

It has been assumed that the densities in the time-averaged conservation equations are constant over a small time distance. Such an assumption can also be applied in while deriving a one-dimension two-fluid conservation equation over a very small flow-direction distance. By introducing some related quantities and assumptions as shown in the previous time-averaging procedure, an integral form of the area-averaged conservation equation can be written. Each integral variation of the conservation equations be transformed to a differential form as be shown in two following subsections.

3.6.1 Mass Conservation Equations

Following the basic mathematical time-averaging procedures, a one-dimension conservation equation set for two-fluid flow can be obtained. Introducing the definition of mass related quantities, the integral form of one-dimension general conservation equation can be reduced to a differential form of a one-dimension mass conservation equation by applying Leibniz rule and Gauss theorem [Appendix C]. With the definition of mass conservation quantity, flux, and source terms:

$$\begin{aligned} \psi_k &= 1 \\ J_k &= 0 \\ S_k &= 0 \end{aligned} \quad (3.34)$$

the integral form of mass conservation equation can be written:

$$\frac{1}{A_A} \int \frac{\partial \alpha_k \rho_k}{\partial t} dA + \frac{1}{A_A} \int \nabla \cdot \alpha_k \rho_k \mathbf{u}_{\mathbf{x}} dA = - \frac{1}{A_A} \int \frac{1}{T_t} \sum_{T_k} \frac{\dot{m}}{|\mathbf{n}_k \cdot \mathbf{u}_i|} dA \quad (3.35)$$

By taking the dot product of flow-direction normal unit vector to the mass conservation equation and then applying Leibnitz rule and Gauss theorem on the first two terms respectively, the first two terms of the conservation equation become:

- First Term :

$$\frac{1}{A_A} \int \frac{\partial \rho_k \alpha_k}{\partial t} dA = \frac{\partial}{\partial t} \frac{1}{A_A} \int \alpha_k \rho_k dA - \frac{1}{A_{C_i}} \int \alpha_k \rho_k (\mathbf{u}_i \cdot \mathbf{n}_x) dC \quad (3.36)$$

- Second Term:

$$\frac{1}{A_A} \int \nabla \cdot \rho_k \mathbf{u}_{\mathbf{x}} \alpha_k dA = \frac{\partial}{\partial X} \left(\frac{1}{A_A} \int \rho_k \mathbf{u}_{\mathbf{x}} \alpha_k dA \right) + \frac{1}{A_{C_i}} \int \mathbf{n}_k \cdot \rho_k \mathbf{u}_{\mathbf{x}} \alpha_k dC \quad (3.37)$$

By combining these terms, the integral form of the mass conservation equation can be reduced to a differential form of the equation:

$$\frac{\partial}{\partial t} \frac{1}{A_A} \int \rho_k \alpha_k dA + \frac{\partial}{\partial X} \left(\frac{1}{A_A} \int \rho_k \mathbf{u}_{\mathbf{x}} \alpha_k dA \right) = - \frac{1}{A_A} \int \frac{1}{T_t} \sum_{T_k} \frac{\dot{m}}{|\mathbf{n}_k \cdot \mathbf{u}_i|} dA \quad (3.38)$$

Assuming that density does not change over the flow cross-section area, the following mass conservation equation can be obtained:

$$\underbrace{\frac{\partial}{\partial t} \frac{\rho_k}{A} \int \alpha_k dA}_{[1]} + \underbrace{\frac{\partial}{\partial x} \left(\frac{\rho_k}{A} \int \mathbf{u}_{xk} \alpha_k dA \right)}_{[2]} = - \underbrace{\frac{1}{A} \int \frac{1}{T_i} \sum \frac{\dot{m}}{|\mathbf{n}_k \cdot \mathbf{u}_i|} dA}_{[3]} \quad (3.39)$$

Using definitions of an average void fraction and a void fraction weight average quantity, the terms of the mass conservation equation can be written:

$$[1] \quad \frac{\partial}{\partial t} \frac{\rho_k}{A} \int \alpha_k dA = \frac{\partial}{\partial t} \rho_k \langle \alpha_k \rangle \quad (3.40)$$

$$[2] \quad \frac{\partial}{\partial x} \left(\frac{\rho_k}{A} \int u_{xk} \alpha_k dA \right) = \frac{\partial}{\partial x} \left(\frac{\rho_k}{A} \int u_{xk} \alpha_k dA \right) = \frac{\partial}{\partial x} \rho_k \langle \alpha_k \rangle \langle \langle \mathbf{u}_{xk} \rangle \rangle \quad (3.41)$$

$$[3] \quad - \frac{1}{A} \int \frac{1}{T_i} \sum \frac{\dot{m}}{|\mathbf{n}_k \cdot \mathbf{u}_i|} dA = \frac{1}{A} \int \Gamma_k dA \equiv \langle \Gamma_k \rangle \quad (3.42)$$

In Equation [3], a new two-fluid mass source term, mass transfer rates per unit interface length, are defined.

$$\Gamma_k \equiv - \frac{1}{T_i} \sum \frac{\dot{m}}{|\mathbf{n}_k \cdot \mathbf{u}_i|} \quad (3.43)$$

This definition takes into account of the mass transfer rate which is due to the effect of the interface surface displacement velocity between the two fluids by the contraction or expansion of interface surfaces. It is induced by the velocity difference between the interfaces and the single-fluid phase [Ishii, 1975]. By combining all the above terms

and including the mass transfer rates, a differential form of the one-dimension mass conservation equation can be obtained:

$$\frac{\partial}{\partial t} \rho_k \langle \alpha_k \rangle + \frac{\partial}{\partial x} \rho_k \langle \alpha_k \rangle \langle u_{xk} \rangle = \langle \Gamma_k \rangle \quad (3.44)$$

Both the lighter upper (dispersed) flow and the heavier bottom (continuous) flow can be indicated by replacing the subscript “k” with the subscripts “d” and “c”, respectively. The one-dimension mass conservation equations are:

$$\begin{aligned} \frac{\partial}{\partial t} \rho_d \langle \alpha_d \rangle + \frac{\partial}{\partial x} \rho_d \langle \alpha_d \rangle \langle u_d \rangle &= \langle \Gamma_d \rangle \\ \frac{\partial}{\partial t} \rho_c \langle \alpha_c \rangle + \frac{\partial}{\partial x} \rho_c \langle \alpha_c \rangle \langle u_c \rangle &= \langle \Gamma_c \rangle \end{aligned} \quad (3.45)$$

These equations can be applied to a real problem if a constitutive relation of the mass production and exchange rate is known. Beside an interfacial mass exchange due to unequal two-fluid velocity, the mass change rate that can be induced by phase-change.

3.6.2 Momentum Conservation Equations

A two-fluid momentum equation can be derived by incorporating the definition of momentum conservation quantity, flux, and source into the time-averaged general conservation equation:

$$\begin{aligned} \psi_k &\equiv \mathbf{u}_k \\ \bar{\mathbf{J}}_k &\equiv \rho_k \bar{\mathbf{I}} - \bar{\boldsymbol{\tau}}_k \\ \mathbf{s}_k &\equiv \mathbf{F}_k \\ \bar{\boldsymbol{\tau}}_k^T &\equiv \bar{\boldsymbol{\tau}}_k + \rho_k \overline{\mathbf{u}'_k \mathbf{u}'_k{}^T} \end{aligned} \quad (3.46)$$

By integrating the general conservation equation and taking the dot product of the flow directional normal unit vector the momentum equation, and dividing the momentum equation over the flow cross section area, the integral form of the one-dimension momentum conservation equation becomes:

$$\begin{aligned} & \frac{1}{A} \int \frac{\partial \rho_k \mathbf{u}_{xk} \alpha_k}{\partial t} dA + \frac{1}{A} \int \nabla \cdot \alpha_k (\rho_k \mathbf{u}_k \mathbf{u}_{xk} + \mathbf{n}_x \cdot \rho_k \bar{\mathbf{I}} - \mathbf{n}_x \cdot \bar{\boldsymbol{\tau}}_k) dA \\ &= \frac{1}{A} \int \mathbf{F}_{xk} \alpha_k dA - \frac{1}{A} \int \frac{1}{T_t} \sum_{T_i} \frac{\mathbf{n}_x}{|\mathbf{n}_k \cdot \mathbf{u}_i|} (\dot{m} \mathbf{u}_k + \mathbf{n}_k \cdot \rho_k \bar{\mathbf{I}} - \mathbf{n}_k \cdot \bar{\boldsymbol{\tau}}_k) dA \end{aligned} \quad (3.47)$$

By applying Leibniz rule and Gauss theorem, each term of the integral form of area-averaged momentum conservation equation can be written:

- First Term :

$$\frac{1}{A} \int \frac{\partial \rho_k \mathbf{u}_{xk} \alpha_k}{\partial t} dA = \frac{\partial}{\partial t} \frac{1}{A} \int \alpha_k \rho_k \mathbf{u}_{xk} dA - \frac{1}{A_{C_i}} \int (\mathbf{n}_k \cdot \mathbf{u}_i) \alpha_k \rho_k \mathbf{u}_{xk} dC \quad (3.48)$$

- Second Term:

$$\frac{1}{A} \int \nabla \cdot \alpha_k \rho_k \mathbf{u}_k \mathbf{u}_{xk} dA = \frac{\partial}{\partial X} \frac{1}{A} \int \alpha_k \rho_k u_{xk}^2 dA + \frac{1}{A_{C_i}} \int \mathbf{n}_k \cdot \alpha_k \rho_k \mathbf{u}_i \mathbf{u}_{xk} dC \quad (3.49)$$

- Third Term:

$$\frac{1}{A} \int \nabla \cdot \alpha_k \mathbf{p}_{xk} dA = \frac{\partial}{\partial X} \frac{1}{A} \int \alpha_k p_k dA + \frac{1}{A_{C_i}} \int \mathbf{n}_x \cdot \alpha_k \mathbf{p}_k dC \quad (3.50)$$

- Fourth Term:

$$\begin{aligned} & \frac{1}{A_A} \int \nabla \cdot \alpha_k \bar{\tau}_{xk}^T dA \\ & \cong \frac{\partial}{\partial X} \frac{1}{A_A} \int \alpha_k (\bar{\tau}_{xk} + \rho_k \overline{u'u_x^T}) dA + \frac{1}{A_{C_i}} \int \mathbf{n}_x \cdot \alpha_k \bar{\tau}_k dC + \frac{4}{D_o} \alpha_{wk} T_{wk} \end{aligned} \quad (3.51)$$

In the above equation, the wall shear stress's constitutive relationship is needed to obtain a realistic analysis of the transient response of viscous flows. By combining the above four terms including, a more manageable form of the area-averaged momentum conservation equation can be written:

$$\begin{aligned} & \frac{\partial}{\partial t} \frac{1}{A_A} \int \alpha_k \rho_k u_{xk} dA + \frac{\partial}{\partial X} \frac{1}{A_A} \int \alpha_k \rho_k u_{xk}^2 dA \\ & = - \frac{\partial}{\partial X} \frac{1}{A_A} \int \alpha_k \rho_k dA - \frac{4\alpha_{wk} T_{wk}}{D_o} - \frac{\partial}{\partial X} \frac{1}{A_A} \int \alpha_k (\bar{\tau}_{xk} + \rho_k \overline{u'u_x^T}) dA \\ & + \frac{1}{A_A} \int F_{xk} \alpha_k dA - \frac{1}{A_A} \int \frac{1}{T_f} \sum \frac{\mathbf{n}_x \cdot}{|\mathbf{n}_k \cdot \mathbf{u}_i|} (\dot{m} \mathbf{u}_{ki} + \mathbf{n}_k \cdot \rho_{ki} \bar{\mathbf{I}} - \mathbf{n}_k \cdot \bar{\tau}_{ki}) dA \\ & - \frac{1}{A_{C_i}} \int \mathbf{n}_x \cdot \alpha_k (\rho_k \bar{\mathbf{I}} - \bar{\tau}_k) dC \end{aligned} \quad (3.52)$$

The above equation shows a void fraction weighted integral that is useful in deriving a one-dimension equation. The integral can be used for deriving a more readable and manageable average void fraction parameter. By assuming that the density does not change over a very small flow distance, the momentum conservation equation can be written:

$$\begin{aligned}
& \underbrace{\frac{\partial \rho_k}{\partial t} \int_A \alpha_k \mathbf{u}_{xk} dA}_{[1]} + \underbrace{\frac{\partial \rho_k}{\partial x} \int_A \alpha_k u_{xk}^2 dA}_{[2]} \\
&= \underbrace{-\frac{\partial}{\partial x} \frac{1}{A_A} \int_A \alpha_k \rho_k dA}_{[3]} - 4 \frac{\alpha_{wk} T_{wk}}{D_e} - \underbrace{\frac{\partial}{\partial x} \frac{1}{A_A} \int_A \alpha_k (\bar{\tau}_{xk} + \rho_k \overline{\mathbf{u}' \mathbf{u}'_x}) dA}_{[4]} \\
&+ \underbrace{\frac{1}{A_A} \int_A F_{xk} \alpha_k dA}_{[5]} - \underbrace{\frac{1}{A_A} \int_A \frac{1}{T_t} \sum_i \frac{\mathbf{n}_x \cdot \mathbf{n}_i}{|\mathbf{n}_k \cdot \mathbf{u}_i|} (\dot{m} \mathbf{u}_{ki} + \mathbf{n}_k \cdot \rho_{ki} \bar{\mathbf{I}} - \mathbf{n}_k \cdot \bar{\tau}_{ki}) dA}_{[6]} \\
&- \underbrace{\frac{1}{A_{C_i}} \int_{C_i} \mathbf{n}_x \cdot \alpha_k (\rho_k \bar{\mathbf{I}} - \bar{\tau}_k^T) dC}_{[6]}
\end{aligned} \tag{3.53}$$

The first five terms of the integral one-dimension two-fluid momentum equation become:

$$[1]. \quad \frac{\partial \rho_k}{\partial t} \int_A \mathbf{u}_{xk} \alpha_k dA = \frac{\partial}{\partial t} \rho_k \langle \alpha_k \rangle \langle \langle u_{xk} \rangle \rangle \tag{3.54}$$

$$[2]. \quad \frac{1}{A_A} \int_A u_{xk}^2 \alpha_k dA = \langle \alpha_k \rangle \langle \langle u_{xk}^2 \rangle \rangle \equiv c_m \langle \alpha_k \rangle \langle \langle u_{xk} \rangle \rangle^2 \tag{3.55}$$

$$[3]. \quad \frac{\partial}{\partial x} \frac{1}{A_A} \int_A \mathbf{n}_x \cdot \alpha_k \rho_k \bar{\mathbf{I}} dA = \frac{\partial}{\partial x} \frac{1}{A_A} \int_A \rho_k \alpha_k dA = \frac{\partial}{\partial x} \langle \alpha_k \rangle \langle \langle \rho_k \rangle \rangle \tag{3.56}$$

$$[4]. \quad \frac{\partial}{\partial x} \frac{1}{A_A} \int_A \alpha_k (\bar{\tau}_{xk} + \rho_k \overline{\mathbf{u}' \mathbf{u}'_x}) dA = \frac{\partial}{\partial x} \langle \alpha_k \rangle \langle \langle \bar{\tau}_{xk} + \rho_k \overline{\mathbf{u}' \mathbf{u}'_x} \rangle \rangle \tag{3.57}$$

$$[5]. \quad \frac{1}{A_A} \int_A (F_k \cdot \mathbf{n}_x) \alpha_k dA = \frac{1}{A_A} \int_A F_{xk} \alpha_k dA = \langle \alpha_k \rangle \langle \langle F_{xk} \rangle \rangle \tag{3.58}$$

In the second term, an important auxiliary relation comes from the separation of the average of products into the product of averages, representing the average products of dependent variables to the products of the averages ratio. With the definition of the covariance coefficient as the rate of the average of products velocity to the product of averages of the velocity, the second term becomes more simplified. A more detailed covariance coefficient can be introduced by evaluating the local instantaneous two-fluid velocity profiles. The third term shows the normal stress contribution at the interface and the fourth term shows viscous stress terms that consists of a wall interface shear stress and a timely velocity fluctuation. Since all terms are related to the two-fluid interfacial momentum sources, these five items need more detailed evaluations:

- First Term :

$$\frac{1}{A_A} \int \frac{1}{T_t} \sum \frac{\dot{m} \mathbf{u}_{xk}}{|\mathbf{n}_k \cdot \mathbf{u}_i|} dA = \frac{1}{A_A} \int \Gamma_k u_{xk} dA = \langle \Gamma_k \rangle \langle \langle u_{xk} \rangle \rangle \quad (3.59)$$

- Second Term :

$$-\frac{1}{A_A} \int \frac{1}{T_t} \sum \frac{\mathbf{n}_k \cdot \mathbf{n}_x p_{ki}}{|\mathbf{n}_k \cdot \mathbf{u}_i|} dA = \langle \langle p_{ki} \rangle \rangle \frac{\partial \langle \alpha_k \rangle}{\partial x} \quad (3.60)$$

- Third Term:

$$\frac{1}{A_A} \int \frac{1}{T_t} \sum \frac{\mathbf{n}_k \cdot \bar{\boldsymbol{\tau}}_{xi}}{|\mathbf{n}_k \cdot \mathbf{u}_i|} dA = -\frac{1}{A_A} \int \bar{\boldsymbol{\tau}}_i \frac{\partial \alpha_k}{\partial x} dA \quad (3.61)$$

- Fourth Term :

$$-\frac{1}{A} \int_C \mathbf{n}_k \cdot \alpha_k \mathbf{p}_{xk} dC = -\frac{1}{A} \int_A \frac{\partial}{\partial X} \alpha_k \rho_{ki} dA \equiv -\langle \mathbf{n}_x \cdot \nabla \alpha_k \rho_{ki} \rangle \quad (3.62)$$

- Fifth Term:

$$\frac{1}{A} \int_{C_i} \mathbf{n}_x \cdot \alpha_k \bar{\tau}_k dC = \langle \bar{\tau}_{ki} \nabla \alpha_k \cdot \mathbf{n}_x \rangle + \frac{1}{A} \int_A \alpha_k \frac{\partial \bar{\tau}_{ik}}{\partial X} dA \quad (3.63)$$

By summing the terms, a differential form of the one-dimension two-fluid momentum equation can be obtained:

$$\begin{aligned} & \frac{\partial}{\partial t} \rho_k \langle \alpha_k \rangle \langle \langle u_{xk} \rangle \rangle + \frac{\partial}{\partial x} c_m \rho_k \langle \alpha_k \rangle \langle \langle u_{xk} \rangle \rangle^2 - \langle \alpha_k \rangle \langle \langle F_{xk} \rangle \rangle \\ & + \frac{\partial}{\partial x} \langle \alpha_k \rangle \langle \langle \rho_k \rangle \rangle - \langle \langle \rho_{ki} \rangle \rangle \frac{\partial \langle \alpha_k \rangle}{\partial x} + \frac{\partial}{\partial x} \langle \alpha_k \rangle \langle \langle \bar{\tau}_{xk} + \rho_k \overline{\mathbf{u}' \mathbf{u}'^T} \rangle \rangle \\ & = \langle \Gamma_k \rangle \langle \langle u_{xk} \rangle \rangle - 4 \frac{\alpha_{wk} \Gamma_{wk}}{D_e} - \langle \mathbf{n}_x \cdot \nabla \alpha_k \rho_{ki} \rangle - \langle \bar{\tau}_{ki} \nabla \alpha_k \cdot \mathbf{n}_x \rangle \end{aligned} \quad (3.64)$$

In the above momentum equation, the total drag forces at the interface can be expressed by the combination of the pressures and viscous stress terms, in which variations are induced by void fraction gradients [Ishii, 1975; Ishii and Hibiki, 2006]:

$$M_{xk}^d = -\mathbf{n}_x \cdot \nabla \alpha_k \rho_{ki} - \bar{\tau}_{ki} \nabla \alpha_k \cdot \mathbf{n}_x \quad (3.65)$$

It is noted that void fraction variations along the two-fluid flow direction would play

major roles for interface roughness. By combining the above definition of interface drag force, the one-dimension momentum equation can be reduced to:

$$\begin{aligned}
 & \frac{\partial \langle \alpha_k \rangle}{\partial t} \rho_k \langle \langle u_{xk} \rangle \rangle + \frac{\partial \langle \alpha_k \rangle}{\partial x} c_{mk} \rho_k \langle \langle u_{xk} \rangle \rangle^2 - \langle \alpha_k \rangle \langle \langle F_{xk} \rangle \rangle \\
 & + \frac{\partial \langle \alpha_k \rangle}{\partial x} \langle \langle \rho_k \rangle \rangle - \langle \langle \rho_{ki} \rangle \rangle \frac{\partial \langle \alpha_k \rangle}{\partial x} + \frac{\partial \langle \alpha_k \rangle}{\partial x} \langle \langle \bar{\tau}_{xk} + \rho_k \overline{u' u'^T} \rangle \rangle \\
 & = \langle \Gamma_k \rangle \langle \langle u_{xk} \rangle \rangle - 4 \frac{\alpha_{wk} T_{wk}}{D_e} + \langle M_{xk}^d \rangle
 \end{aligned} \tag{3.66}$$

For a two-fluid flow, the two one-dimension momentum equations can be obtained by replacing the k with c and d:

$$\begin{aligned}
 & \frac{\partial \langle \alpha_c \rangle}{\partial t} \rho_c \langle \langle u_{xc} \rangle \rangle + \frac{\partial \langle \alpha_c \rangle}{\partial z} c_{mc} \rho_c \langle \langle u_{xc} \rangle \rangle^2 - \langle \alpha_c \rangle \langle \langle F_{xc} \rangle \rangle \\
 & + \frac{\partial \langle \alpha_c \rangle}{\partial x} \langle \langle \rho_c \rangle \rangle - \langle \langle \rho_{ic} \rangle \rangle \frac{\partial \langle \alpha_c \rangle}{\partial z} + \frac{\partial \langle \alpha_c \rangle}{\partial x} \langle \langle \bar{\tau}_{xkc} + \rho_k \overline{u' u'^T} \rangle \rangle \\
 & = \langle \Gamma_c \rangle \langle \langle u_{xc} \rangle \rangle - 4 \frac{\alpha_{wc} T_{wc}}{D_e} + \langle M_{xc}^d \rangle
 \end{aligned} \tag{3.67}$$

$$\begin{aligned}
 & \frac{\partial \langle \alpha_d \rangle}{\partial t} \rho_d \langle \langle u_{xd} \rangle \rangle + \frac{\partial \langle \alpha_d \rangle}{\partial z} c_{md} \rho_d \langle \langle u_{xd} \rangle \rangle^2 - \langle \alpha_d \rangle \langle \langle F_{xd} \rangle \rangle \\
 & + \frac{\partial \langle \alpha_d \rangle}{\partial x} \langle \langle \rho_d \rangle \rangle - \langle \langle \rho_{id} \rangle \rangle \frac{\partial \langle \alpha_d \rangle}{\partial z} + \frac{\partial \langle \alpha_d \rangle}{\partial x} \langle \langle \bar{\tau}_{xkd} + \rho_k \overline{u' u'^T} \rangle \rangle \\
 & = \langle \Gamma_d \rangle \langle \langle u_{xd} \rangle \rangle - 4 \frac{\alpha_{wd} T_{wd}}{D_e} + \langle M_{xd}^d \rangle
 \end{aligned} \tag{3.68}$$

With the exception of the drag force sign and index, the dispersed momentum equation is the same as the continuous momentum equation. The interfacial drag force is a function of the interface shape, interface pressure, and interface shear stress.

It is needed to provide constitutive relationships to close the system for realistic analysis. Even if a full description of momentum change would require the considerations of various phenomena such as added-mass effects, Basset forces, drag forces, and phase-change effects, they are all local instantaneous forces and needed in an additional local instantaneous modeling. These local instantaneous two-fluid models are out of the scope of this research and the attention is restricted to one-dimension two-fluid horizontal flow model. In one-dimension flow, a dominated momentum exchange would arise when the two-fluids have different mean velocities unless a realistic mass transfer or phase change term is taken into account. The one-dimension model can be applied to a real problem if these corresponding constitutive relations are known.

3.6.3 Constitutive Equations

As shown in previous sections, a reasonable constitutive relationship is required to close the one-dimension conservation equations. Specifically, one-dimension constitutive relationship are strongly desired since a local instantaneous relation and its combinations could be impractical to use as a one-dimension constitutive relation corresponding to the one-dimension equations. For example of local instantaneous , it has been assumed that interfaces have no thickness and no mass, hence the conservation quantities like mass, momentum or energy can not be stored in local instantaneous two-fluid flow interfaces. From these relationships, some local instantaneous constitutive relationship could be obtained. However, they can not directly preserve their three dimensional characteristics in one-dimension flow modeling.

By averaging a local instantaneous interfacial transfer conditions with the same method, one-dimension conservation equation deriving methods, a conservative one-dimension instantaneous interfacial transfer condition will be obtained. By starting

with a local instantaneous interfacial condition, a general conservation equation across the interface can be written:

$$\sum_{k=1}^2 [\dot{m}_k \psi_k + \mathbf{J}_k \cdot \mathbf{n}_k] = 0 \quad (3.69)$$

The first two terms in the above equation denote a mass production flux and an interfacial flux. With a definition of mass related quantity and flux, a mass interface condition can be written [Appendix C]:

$$\sum_{k=1}^2 \dot{m}_k = 0 \quad (3.70)$$

By inserting the definition of mass transfer rate equation and by taking the normal directional property of the two-fluid interface, the interface velocity relationship of two-fluid flow can be obtained:

$$u_i = \frac{\rho_2 u_2 - \rho_1 u_1}{\rho_2 - \rho_1} \quad (3.71)$$

It is shown that the interface velocity is due to the effects of density difference as well as the two-fluid velocity difference. This relationship can be used in making an approximation of interface velocity. Also, it has been usually assumed that there is no mass transfer in a two-fluid flow equation unless two-fluid phase-changes. This can be proven by time-averaging the mass transfer condition. By multiplying the local instantaneous mass transfer term by the indication function and averaging this equation over a sampling time, a time-averaged interfacial mass transfer rate can be obtained:

$$0 = \sum_k \frac{1}{T_s} \int_{T_s} \dot{m} M_k dt = \bar{m}_k^T + (\bar{m}_k^T - \bar{m}_k^T) \alpha_k \quad (3.72)$$

With the condition of non-zero void fractions, the time-averaged mass transfer rates can be reduced to zero:

$$0 = \bar{\dot{m}}_k^T = \bar{\dot{m}}_k^T \quad (3.73)$$

The above expression yields a very important two-fluid flow condition. In the quasi-steady-state sense, any time-average interfacial mass transfer rates should be no interface mass transfer rate conditions without phase-changes.

3.6.4 One-Dimension Two-Fluid Horizontal Flow

A one-dimension two-fluid flow model can be formulated by time-area-averaging, even with a two-fluid flow consisting of two single-phase regions bounded by dynamic interfaces. In the incompressible flow limit, the densities of the two-fluids can be taken outside of all derivative terms. In considering one-dimension interface force balancing condition with average void fraction variations, two important pressure gradient constitutive relations are need. A pressure variation condition is more important to the results of one-dimension constitutive modeling. The variation is caused by a net transverse momentum balance and by a net flow-direction momentum balance. It will supplement the one-dimension horizontal model as basic constitutive relations.

$$\frac{\partial p_1}{\partial x} = \frac{\partial p_2}{\partial x} \quad (3.74)$$

Furthermore, in the one-dimension two-fluid horizontal flow momentum equation the available choice of the effective external body force and the mass transfer rates are zero without phase-change situations:

$$\begin{aligned}\Gamma_k &= 0 \\ F_x &= 0\end{aligned}\tag{3.75}$$

Since the mass interface transfer in two-fluid flow is statements of the local instantaneous interfacial velocity difference between the fluids, the time-average mass transfer rates will disappear. For fully developed flow applications, the covariance coefficients are set equal to one. With the two-fluid flow situations, the mass and momentum equations of the one-dimension two-fluid flow equations become:

$$\begin{aligned}\frac{\partial}{\partial t} \rho_1 \alpha_1 + \frac{\partial}{\partial x} \rho_1 \alpha_1 u_2 &= 0 \\ \frac{\partial}{\partial t} \rho_2 \alpha_2 + \frac{\partial}{\partial x} \rho_2 \alpha_2 u_2 &= 0 \\ \frac{\partial}{\partial t} \rho_1 \alpha_1 u_1 + \frac{\partial}{\partial x} \rho_1 \alpha_1 u_1^2 - \Delta p \frac{\partial \alpha_1}{\partial x} &= -\frac{\partial p}{\partial x} \\ \frac{\partial}{\partial t} \rho_2 \alpha_2 u_2 + \frac{\partial}{\partial x} \rho_2 \alpha_2 u_2^2 + \Delta p \frac{\partial \alpha_2}{\partial x} &= -\frac{\partial p}{\partial x}\end{aligned}\tag{3.76}$$

These relationships are expressed without a bracket and over bar, by using delta pressure definition for simple notations. In the simplifications of the above two-fluid flow equation set, the delta pressure expression would be an effective pressure difference between the interface and phase pressure. It has been evident that the delta pressure is an amplification factor of the void gradient and an important factor of two-fluid stability. With all these previous relationships, the number of dependent variable and system sizes can be changed.

3.6.5 Stability Analysis with Delta Pressure

A characteristic analysis method is one of the well known methods for determining two-fluid flow stability as well as the linear perturbation method. More specifically, whether an interface wave has been amplified or decayed needs to be determined by interface transfer relationships. The impact of the pressure on instability of the model needs to be determined since delta pressure is one of the important constitutive relations of the current one-dimension two-fluid horizontal flow model. In the characteristic analysis, this section will show how delta pressure could be involved in one-dimension two-fluid models with the pressure gradients.

- **Continuity Equation:**

$$\begin{aligned}\frac{\partial \alpha_1}{\partial t} + u_1 \frac{\partial \alpha_1}{\partial x} + \alpha_1 \frac{\partial u_1}{\partial x} &= 0 \\ \frac{\partial \alpha_2}{\partial t} + u_2 \frac{\partial \alpha_2}{\partial x} + \alpha_2 \frac{\partial u_2}{\partial x} &= 0\end{aligned}\quad (3.77)$$

- **Momentum Equation:**

$$\begin{aligned}u_1 \frac{\partial \alpha_1}{\partial t} + \alpha_1 \frac{\partial u_1}{\partial t} + (u_1^2 + \Delta p_1) \frac{\partial \alpha_1}{\partial x} + 2\alpha_1 u_1 \frac{\partial u_1}{\partial x} + \frac{\alpha_1}{\rho_1} \frac{\partial p}{\partial x} &= 0 \\ u_2 \frac{\partial \alpha_2}{\partial t} + \alpha_2 \frac{\partial u_2}{\partial t} + (u_2^2 - \Delta p_2) \frac{\partial \alpha_2}{\partial x} + 2\alpha_2 u_2 \frac{\partial u_2}{\partial x} + \frac{\alpha_2}{\rho_2} \frac{\partial p}{\partial x} &= 0\end{aligned}\quad (3.78)$$

With the simplified velocity coefficients and assumptions, a simplified set of differential one-dimension two-fluid horizontal flow equation sets can be made. As can be seen in the above momentum equations, the delta pressure and inertial forces cause the space void variation in making equilibrium momentum even if the inertial

force term is only a coefficient or a temporal growth factor of void fractions. To perform a characteristic analysis, a matrix form of the equations can be written with a simplified external source. These one-dimension mass and momentum conservation equation sets can be written in a simple matrix form:

$$[A] \frac{\partial S}{\partial t} + [B] \frac{\partial S}{\partial x} = 0$$

$$S = [\alpha \quad u_1 \quad u_2 \quad p]^T$$

$$[A] = \begin{bmatrix} 1 & 0 & 0 & 0 \\ 1 & 0 & 0 & 0 \\ \rho_1 u_1 & \alpha \rho_1 & 0 & 0 \\ \rho_2 u_2 & 0 & (\alpha - 1) \rho_2 & 0 \end{bmatrix}$$

$$[B] = \begin{bmatrix} u_1 & \alpha & 0 & 0 \\ u_2 & 0 & (\alpha - 1) & 0 \\ \rho_1 u_1 + \Delta p_1 & 2\alpha \rho_1 u_1 & 0 & \alpha \\ \rho_2 u_2 - \Delta p_2 & 0 & 2(\alpha - 1) \rho_2 u_2 & (\alpha - 1) \end{bmatrix} \quad (3.79)$$

As noted in the above matrix, there are no external source terms. Mathematically, the characteristic analysis is not dependent on external sources since the analysis shows only overall system characteristics as complementary solutions. The solutions are reduced to the investigation of the determinant roots:

$$(\Delta p_1 - \rho_1 (u_1 - \lambda)^2) (1 - \alpha) + (\Delta p_2 - \rho_2 (u_2 - \lambda)^2) \alpha = 0 \quad (3.80)$$

To solve the above equation, an appropriate expression of the delta pressure term is necessary. The delta pressure is effective pressure difference between the interfacial

and phase pressure, and could be derived from a local void fraction relation with involved body forces. In an air-water two-fluid case, the air-phase delta pressure can be set to zero with the following liquid-phase delta pressure expression:

$$\Delta p_2 = \Delta p \quad (3.81)$$

The previous determinate equation that has the unstable solution forms for a long time can be recast:

$$(-\rho_1(u_1 - \lambda)^2)(1 - \alpha) + (\Delta p - \rho_2(u_2 - \lambda)^2)\alpha = 0 \quad (3.82)$$

For an appropriate solution of the physical stability, expressions of the delta pressure are necessary. These could be derived from two-fluid physical modeling. By accounting for a non-zero unspecified delta pressure expression, a second order characteristic equation can be obtained:

$$\left(\frac{\rho_1}{\alpha} + \frac{\rho_2}{1-\alpha}\right)\lambda^2 - 2\left(\frac{\rho_1 u_1}{\alpha} + \frac{\rho_2 u_2}{1-\alpha}\right)\lambda + \left(\frac{\rho_1 u_1^2}{\alpha} + \frac{\rho_2 u_2^2}{1-\alpha}\right) = \frac{\Delta p}{1-\alpha} \quad (3.83)$$

A parametric equation of one-dimension two-fluid horizontal flow model can be obtained by a system characteristic method. The roots of the above equation can be found using quadratic equation:

$$\lambda_{1,2} = \frac{\left(\frac{\rho_1 u_1}{\alpha} + \frac{\rho_2 u_2}{1-\alpha}\right) \pm \sqrt{-\frac{\rho_1 \rho_2}{\alpha(1-\alpha)}(u_1 - u_2)^2 + \frac{\Delta p}{1-\alpha} \left(\frac{\rho_1}{\alpha} + \frac{\rho_2}{1-\alpha}\right)}}{\left(\frac{\rho_1}{\alpha} + \frac{\rho_2}{1-\alpha}\right)} \quad (3.84)$$

The main interest resides in the terms under the square roots. By definition of the determinant, the solutions are the system roots. When the one-dimension horizontal flow has imaginary solutions, flow instability would exist. Since an imaginary solution is the signature of system instability, determining whether the solutions of the quadratic formulation have imaginary parts is very important. This means that the instability is dependent on the sign of the square root. For the determinant, the following equations can be obtained by the square root:

$$(u_1 - u_2)^2 \leq \frac{\Delta p}{\rho_1} \left(\frac{\rho_1}{\rho_2} + \frac{\alpha}{1-\alpha} \right) \quad (3.85)$$

When the equality of the above equation is violated, interface instability appears and grows. This means that the delta pressure has a positive pressure expression unless the relative velocity has a zero tolerance of stability, which should be handed correctly. If the two-fluid flow has a large density difference, then the above equation can be further simplified:

$$(u_1 - u_2) \leq \pm \sqrt{\frac{\Delta p}{\rho_1} \frac{\alpha}{1-\alpha}} \quad (3.86)$$

This result shows that the delta pressure is the main factor in stabilizing the flow and shows how the delta pressure term helps to stabilize the flow. By incorporating the delta pressure expression, the characteristic stability analysis method will show the important flow stability mechanism that is needed to be determined. In order to obtain a more reliable result, delta pressure correlations should be explicitly expressed. With any positive delta pressure, the delta pressure expression in the square root equation would help to stabilize the flow. This expression can be refined by additionally considering an available body force distribution by the definition of the delta pressure.

4 VOID DISTRIBUTION IN MIXTURE LAYER

This section will explore the optional void fraction governing relationships incorporating gravity, which can be used to determine overall void distribution profiles in the mixture layer of horizontal two-fluid flows. In order to obtain a useful void distribution profile, it is essential to determine what two-fluid flow parameter is the main factor and how it can be obtained. Ideally, the best way to perform this is the use of analytical functional forms in terms of known parameters such as average void fraction, pipe diameter, gravity, and superficial velocities. However, this may be difficult since the physical process within the two-fluid flow is a very complicated interaction in real situations.

Proper mathematical or mechanical modeling allows the explanations of various void variations of two-fluid interactions in horizontal flows. The main motivation of this section is to obtain void fraction distribution governing equations by approximation of void immigration processes when the two-fluid flow is within mixing layer. The modeling is started by considering a transportable bubble which can switch the positions to the liquid phase with effectively involved forces. One of the void immigration mechanisms in mixture flow is the liquid fluctuations with suspended voids. The velocity fluctuation of suspended voids could be expressed by void concentration variations [Lahey et al, 1993; Anglart et al, 1997; Bostjan Koncar et al, 2004;].

The void immigrations can be formulated by adding two two-fluid momentum equations, analytically making a net momentum equation of void dominant force relations. They can be used to describe a relationship among a local void fraction, liquid turbulence, and buoyancy. An advantage of this formulation is that it can easily include the void immigration mechanisms, void diffusivities and liquid turbulence, etc. The formulations allow the dominant force dependent void fraction profiles, higher flat void profiles for higher buoyancy forces and lower void profiles for higher liquid

turbulence. These contributions will play a more important role as turbulent-diffusivities vary.

Specifically in model developments, these liquid-velocity fluctuations can be taken into account within an expected force variation range. Another natural characteristic of these void immigration mechanisms is the terminal velocity of raising suspensions. The terminal velocity of the suspended voids would be constant and in steady-state suddenly, depending on the two-fluid properties such as densities, void concentrations, etc. All these relations can be assumed to be held in near stationary states due to the fact that the flow pattern is re-established, and instantaneously feels the influence of mixing forces; the same things can be observed inside mixing layer flows [Buckingham, 1997].

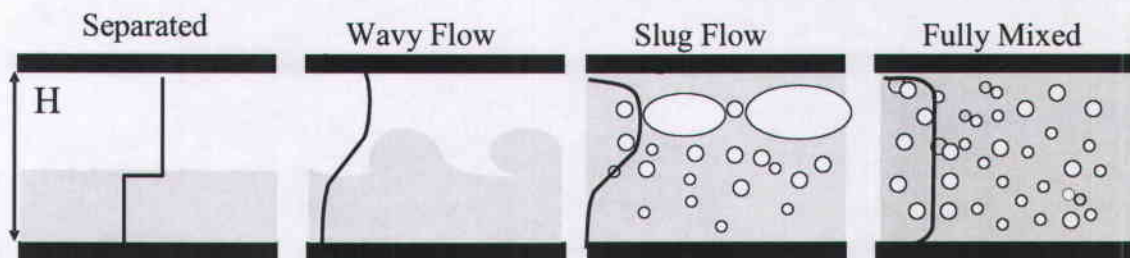


Figure 4.1: Void Distribution Profile of Different Flow Regimes

4.1 LOCAL VOID PROFILES

Some typical relationships among different two-fluid flow regimes are shown in Figure 4.1 with their typical local void profiles. The void distribution of a wavy flow, for example, can be represented by a smoothly varying line over the two-fluid flow cross area, dominated by long surface waves. Also, the two-fluid flow generates fluctuation ripples, which would have a much smaller wave than the long surface wave even if the main wave of a stratified separate flow is a surface fluctuation ripple.

Normally, the wave is composed of long waves over which fluctuation ripples are superimposed. Without knowing the detail constitutive relations of the void distributions, the best way is evaluating the momentum balance between the two horizontal flow fluids.

Since coupling of the two-fluid flow can occur at the two-fluid interface only, local two-fluid interfacial transfer is strongly dependent on the two-fluid interfacial fractions. It can be an important connection in developing a two-fluid fraction related closure, specifically, when the ratio of disperse to continuous density is very small so the turbulence of the disperse phase would be neglected over the whole mixing layer flow. The relative strength of fluctuation ripples will influence the amount of void fraction immigration, even if the immigration amount is induced by retractably and manageably small turbulent ripples. These approaches require knowledge of relationships between turbulence and void fraction variations as any interfacial transfer terms that would be directly related to its surface area and governing force. They are also required to find a net interfacial void immigration force. It has been assumed that turbulence can influence void fraction immigration or void fraction distribution [Buckingham, 1997]. From these approaches, the relationship between a void fraction gradient and a velocity fluctuation can be found.

4.2 VOID DISTRIBUTION EQUATION

In steady-state with no net flow in the vertical direction, the local void distribution over the two-fluid mixture could be determined using momentum conservation in the vertical direction. The most reasonable way to obtain the constitutive of two-fluid fraction is by deriving a momentum balance between two fluids or a net momentum balance in mixture flow. The net momentum balance can be obtained by adding the individual momentum balance among the turbulence, the turbulent gradient, and buoyancy forces between the two flow fluids, all making a two fluid force balance and fraction relationship. In more details, the total momentum

equation can be modified by considering each-phase turbulent strength, even if the outside of mixture flow is governed by their individual-phase dominant force relationships. For example, the governing force terms of a mixture flow are continuous-phase turbulent force since the continuous-phase turbulent forces are larger than that of dispersed-phase turbulence due to density effects. If the turbulent strength is much smaller than gravity, void fraction immigration would be derived primarily with buoyancy; thus void rising is significantly affected by net gravity forces. In the case of strong turbulence, the gravity force is limited to balancing the turbulent deficiency of disperse phase flow. In all the above cases, the two-fluid total momentum balance plays a main role on void fraction distributions. As a starting point, the gravitational-direction two-fluid momentum equation was obtained from a general momentum conservation equation [Ishii & Hibiki, 2006].

$$\begin{aligned}
& \alpha_k \rho_k \left(\frac{\partial u_{yk}}{\partial t} + u_{yk} \frac{\partial u_{yk}}{\partial x} + u_{yk} \frac{\partial u_{yk}}{\partial y} \right) + \alpha_k \frac{\partial p_k}{\partial y} - (\rho_{ik} - \rho_k) \frac{\partial \alpha_k}{\partial y} \\
& = \frac{\partial}{\partial x} \alpha_k (\bar{\tau}_{yk} + \bar{\tau}_{yk}^{Re}) + \frac{\partial}{\partial y} \alpha_k (\bar{\tau}_{yk} + \bar{\tau}_{yk}^{Re}) + M_{ik} \\
& \quad - \left(\bar{\tau}_{xyi} \frac{\partial \alpha_k}{\partial x} + \bar{\tau}_{yyi} \frac{\partial \alpha_k}{\partial y} \right) + \rho_k \alpha_k g
\end{aligned} \tag{4.1}$$

In the above equation, the subscript indicates correspond to phases, α_k is a local void fraction, $\bar{\tau}_{yk}$ is the vertical-direction viscous stress, $\bar{\tau}_{yk}^{Re}$ is Reynolds stress, and $\bar{\tau}_{xyi}$ is the interface shear stress, respectively. It is worth noting that void raising velocity is assumed to be finite due to buoyancy effects, to be fully developed condition. With these approximations, the momentum equation can be rewritten:

$$0 = -\alpha_k \frac{\partial p_k}{\partial y} + \frac{\partial}{\partial y} \alpha_k (\bar{\tau}_{yk} + \bar{\tau}_{yk}^{Re}) + (\rho_{ik} - \rho_k) \frac{\partial \alpha_k}{\partial y} + \rho_k \alpha_k g + M_{ik} \tag{4.2}$$

This means that in steady-state with no net flows in the vertical direction, the local void distribution can be determined by the vertical directional momentum conservation equations.

Each of the above momentum equation terms need to be constituted in order to achieve exact solutions mathematically, even if some weak force terms must be neglected to physical understand the solutions. For example, the dynamic pressure variation and viscous terms can be neglected in inviscous incompressible two-fluid flow cases. When considering a vertical momentum equation, the dynamic pressure difference between phase pressures and its counterpart interfacial pressure will be negligibly small unless there are some considerable body forces. In these situations, most other terms are negligible with the exception of gravity, turbulence (Reynolds stress), and interfacial drag (interfacial source). By rearranging and applying these considerations, the two-fluid momentum equation can be reduced to two simple single-fluid momentum equations:

$$0 = \frac{\partial}{\partial y} \alpha_1 \bar{r}_{y1}^{Ro} + \rho_1 \alpha_1 g + M_{iy1} \quad (4.3)$$

$$0 = \frac{\partial}{\partial y} (1 - \alpha) \bar{r}_{y2}^{Ro} + \rho_2 (1 - \alpha) g + M_{iy2}$$

With the approximation that all interfaces can be homogenized without considering interfacial forces, surface tension force, etc, the net momentum equation can be further simplified. Because these two interfacial momentum sources would be equal in magnitude and opposite in sign, the net two-fluid momentum of mixture flow can be obtained by adding the each-phase momentum in considering a homogenized mixture flow. Without heterogeneous interfaces, all of the previous features made the net momentum equation a dominant equation in which the interfacial momentum source can canceled each other.

If the disperse-phase density is much smaller than the liquid continuous-phase in two-fluid flow, the density-related forces would be relatively small and negligible. The magnitude of disperse-turbulence forces can be neglected to relative liquid-turbulence forces. The liquid-turbulent turbulence can produce void immigration forces compared to the disperse-turbulence. Summing up the all above features, a dominant force momentum equation can be determined:

$$0 = -\bar{\bar{\tau}}_{y2}^{R0} \frac{\partial \alpha}{\partial y} + (1 - \alpha) \frac{\partial}{\partial y} \bar{\bar{\tau}}_{y2}^{R0} + \alpha \rho_1 g + (1 - \alpha) \rho_2 g \quad (4.4)$$

The above equation shows that the liquid-phase turbulence is dominated forces by gravity. Since the turbulence is a timely resolved velocity fluctuation, a closure relationship is needed to take into account how the liquid-fluid fluctuation dispersed mixture flows. Thus, the above momentum equation can be turned in to a void fraction parametric equation. By incorporating void-diffusivity in liquid-turbulence, the turbulence can get void constitutive closure [Lahey et al, 1993; Anglart et al, 1997; Buckingham, 1997; Bostjan Koncar et al, 2004, Ishii & Hibiki, 2006]:

$$\bar{\bar{\tau}}_{y2}^{R0} = -(C_{TD} \rho_2 k) \frac{\partial \alpha}{\partial y} \quad (4.5)$$

In the above equation, k is the turbulent kinetic energy of the liquid-phase and C_{TD} is its dispersion coefficient. Indeed, the closure relationships should provide migration mechanisms of void fraction towards the lower parts of the flow. This relation can be introduced to compensate for an averaged two-phase continuity that does not allow phase diffusion effects [Ishii & Hibiki, 2006]. This means that a downward void flux is due to liquid-turbulence and an upward void flux is due to buoyancy force [Buckingham, 1997]. The turbulent-void relationship can also support a liquid-

turbulence can be expressed in two parts, a constant turbulence term and a void proportional term:

$$\bar{\tau}_{y2}^{Re} = \bar{\tau}_0^{Re} - D \frac{\partial \alpha}{\partial y} \quad (4.6)$$

By substituting the above relation to the net momentum equation, the net momentum equation can turn to a void distribution equation:

$$(1 - \alpha) \frac{\partial}{\partial y} \left(\bar{\tau}_0 - D \frac{\partial \alpha}{\partial y} \right) \frac{\partial \alpha}{\partial y} - \left(\bar{\tau}_0 - D \frac{\partial \alpha}{\partial y} \right) \frac{\partial \alpha}{\partial y} - (\rho_2 - \rho_1) g \alpha = -\rho_2 g \quad (4.7)$$

By assuming homogenous two-fluid flow and even mixture of the two-fluid flow, the above distribution equation can be changed to a diffusion equation:

$$\begin{aligned} \varepsilon \frac{\partial}{\partial y} \left(\frac{\partial \alpha}{\partial y} \right) + c \frac{\partial \alpha}{\partial y} + \frac{(\rho_2 - \rho_1) g}{\rho_2 u_2^2} \alpha &= \frac{\rho_2 g}{\rho_2 u_2^2} \\ \varepsilon &\equiv D(1 - \alpha) / \rho_2 u_2^2 \\ c &\equiv \bar{\tau}_0 / \rho_2 u_2^2 \end{aligned} \quad (4.8)$$

The last two coefficients define diffusivity and turbulent ratio to liquid inertial force. The turbulent coefficient, c , is the percentage of turbulent associate forces to inertial force, and the proportional coefficient, D , is the turbulent-diffusivity of the disperse-phase to overcome the inertial forces in the continuous-phase. With the definitions of the relative force coefficients, the above equation can be reduced to a simple parametric void distribution equation:

$$\varepsilon \frac{\partial^2 \alpha}{\partial y^2} + c \frac{\partial \alpha}{\partial y} + \frac{1}{H Fr_{\Delta}^2} \alpha = \frac{1}{Fr^2} \quad (4.9)$$

$$Fr_{\Delta}^2 \equiv \frac{\rho_2 u_2^2}{\Delta \rho g H}, \quad Fr^2 \equiv \frac{\rho_2 u_2^2}{\rho_2 g H}$$

The above void equation is similar to one which has been modeled as a diffusive-transport equation [Picart et al, 1985]. In the above, the Froude numbers provide the important linkages between the dispersed void dominate force and the continuous liquid force, where the inertial force to gravity ratio is introduced as an external source. The Froude number contains the orthogonal force ratio of the horizontal inertial force to vertical gravitational force and justifies the ratio of the continuous liquid force to the dispersed void body force. In mixed two-fluid flow, these features will be illustrated with the solution of the obtained total momentum equation. They also provide direct relations to the void moving mechanisms horizontally and vertically.

4.3 VOID DISTRIBUTION EQUATION SOLUTION FORMS

In the previous section, it is clearly shown that the amount of disperse void immigration is influenced by turbulence and buoyancy forces. The void distribution equation is represented by the dominate force parameters. The parameters are defined with a function of continuous-phase turbulent force, including its gradients. The turbulent force is expressed additionally through the void diffusion term in the distribution equation. The raising nature of dispersed voids is taken into account by introducing buoyancy, even with turbulence specifying diffusivity. There are main advantages of the void diffusion-distribution formulation. It does not utilize any raising two-fluid velocity and incorporate local instantaneous behaviors of voids. Since these void raising velocities and behaviors would be unknown functionalities of two-fluid concentrations, densities, and viscosity, all these complex aspects would need to be studied in further research.

As the previous discussion deals with some of the most important fundamentals of void distribution, these ideas can be furthermore manufactured with simple mathematical studies of the void distribution equation itself and its solution forms. In these mathematical formulations, it is worth while to note that the continuous liquid turbulence should be included in finding some meaningful solution forms. If void fraction solution is a constant, the second order differential equation leads to particular solution.

$$\alpha = H \frac{Fr_{\Delta}^2}{Fr^2} \quad (4.10)$$

The solution could be found while considering over a long distance value that can be reached by. In deriving a one-dimension two-fluid flow model, the above relation is an important base relation in a constant void fraction zones. Furthermore, the void distribution equation can be associated the following homogeneous equation form.

$$\varepsilon \frac{\partial^2 \alpha}{\partial y^2} + c \frac{\partial \alpha}{\partial y} + \frac{1}{HFr_{\Delta}^2} \alpha = 0 \quad (4.11)$$

With the homogenous equation, some complementary solutions can be found. In case of very small diffusion coefficients, the void distribution equation can be limited to first order difference equations, since the second order term becomes very small or zero. By setting the diffusion coefficients to zero, the void distribution equation can be the simplified differential equation below:

$$c \frac{\partial \alpha}{\partial y} + \frac{1}{HFr_{\Delta}^2} \alpha = 0 \quad (4.12)$$

Physically, the equation shows that a large amount of disperse void immigration is influenced by buoyancy and turbulent forces, specifically by the factor of liquid-phase turbulence. The first order differential equation has the following solution:

$$\alpha(y) = Ae^{\left(\frac{1}{cFr_{\Delta}^2 H} y\right)} \quad (4.13)$$

By choosing a suitable internal boundary condition, this solution agrees with long range solution well. However, it cannot satisfy the external boundary condition. This is because the solution is an entire long range solution. For a very short range solution, a simplified differential equation can be derived by modifying the void distribution equation as done in previous for small diffusion coefficient. To this end a new inner variable is introduced by stretching the void distribution coordinates:

$$\hat{y} = y/\varepsilon \quad (4.14)$$

This means that the coordinate is scaled in proportion to a very small coefficient, and that the coordinates are expanded for very small range solutions as the coefficients are going to small value. Using this relation, the void distribution equation can be written:

$$\frac{\partial^2 \alpha}{\partial \hat{y}^2} + c \frac{\partial \alpha}{\partial \hat{y}} + \frac{\varepsilon}{HFr_{\Delta}^2} \alpha = 0 \quad (4.15)$$

Setting the diffusion coefficient zero, the void distribution equation can be written for a very small range solution:

$$\frac{\partial^2 \alpha}{\partial \hat{y}^2} + c \frac{\partial \alpha}{\partial \hat{y}} = 0 \quad (4.16)$$

In spite of simplification, this equation still remains second order, and then the general solution can be written as:

$$\alpha(\hat{y}) = Ae^{-c\hat{y}} + B \quad (4.17)$$

It is worth while to note that this solution form can satisfy the external boundary conditions as well. Determining the constant B is carried out by matching the short range solution and the long range solution since these two solutions must be equal in an overlap range region. It immediately makes the short range solution and the following relation should be hold:

$$\alpha(\hat{y}) = A(1 - e^{-c\hat{y}}) \quad (4.18)$$

These two solutions represent the entire solution when each is applied in their regions of validity. The composite solution is shown graphically in Fig. 4.2, where the blue solid curve is the long range solution and the black, green solid curves are the short range solution and the composition solution. The long range solution corresponds to the strong turbulence and buoyancy zone which do not satisfy the external boundary conditions at the wall. The short range solution is valid in a very narrow zone attached to the wall, and corresponds to the interface layer between the wall and very short range zone which is determined by turbulence gradients. However, it is only by including this short range solution that the external boundary condition at wall can be satisfied. As the diffusion coefficient is vanishing, the void distribution solution passes over to the long range solution. The obtained entire solution can be

valid for the whole region by adding both partial range solutions: making the composite solution. In parametric studies, the specific characters of local void fraction profiles will be shown due to the relation of turbulence and gravity force at two-fluid mixture flow region.

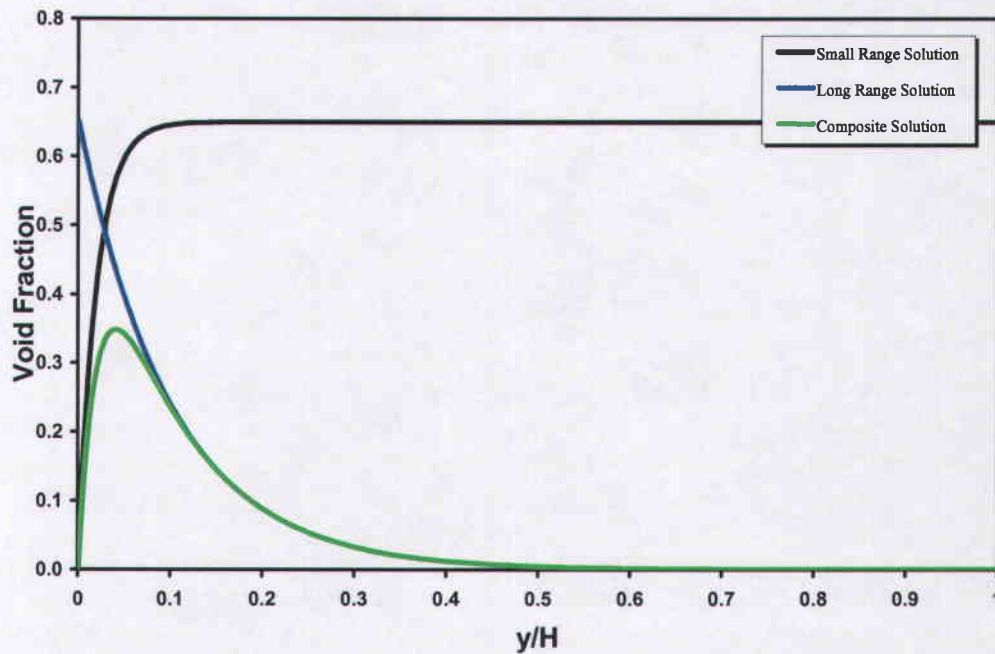


Figure 4.2: Void Distribution Equation Solution Forms

4.4 PARAMETRIC STUDY OF VOID DISTRIBUTIONS

As implied in the previous section, it can be mentioned that these asymptotic analytical solutions can show the overall void fraction profiles inside the mixture layer. Numerically, some parametric studies can be performed with adjusting all of the void distribution coefficients. As is well known, a stratified separate flow can only exist when the two-fluid inertia force dominates over the buoyancy force. But, inside of the mixture flow zone, two-fluid flow structures can be constructed when the continuous-

phase turbulence becomes one of the main important factors. The turbulence becomes an important parameter in profiling flow structures as well as buoyancy. There is need to predict different turbulent regions, one is the lower liquid turbulent region and the other is the higher turbulent region. The behaviors of a uniform or non-uniform void fraction profile are different since they stem from the differences in the spatial turbulence force throughout the flow cross-section domain. Figure 4.3 through 4.5 show these effects taken into account, the expected variation of turbulent diffusivity, turbulent strength, and the contributions on momentum, thus on void fraction distributions at a two-fluid mixture flow region.

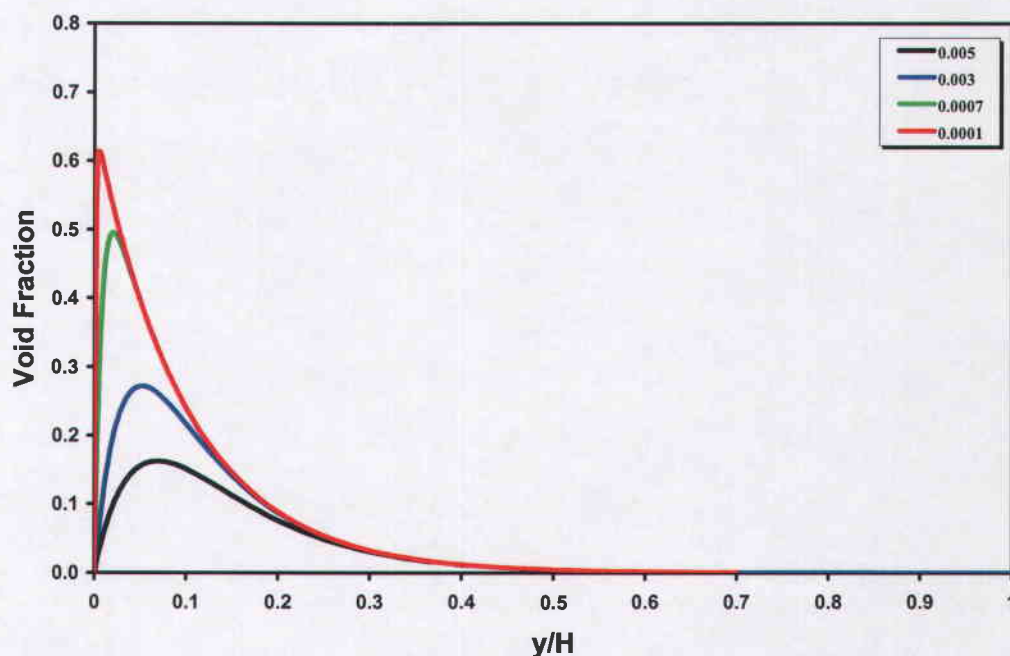


Figure 4.3: Void Fraction Diffusion (Diffusion Coefficient Variation)

Figure 4.3 shows some turbulent-diffusion coefficient effects on local void fraction profiles, which are evaluated by fixing the other contributing factors. As the

turbulent-diffusion coefficient increases, the void fraction profile peak broadens with keeping overall profile shape. This implied that the turbulent coefficient affects the location and magnitude of the peak void fraction of two-fluid mixture flow. This is because the active diffusivity of void increases, diffusing to a lower part of the flow area, as the diffusion coefficient of the two-fluid flow is increased. As diffusivity moves downward, the changing of flow structure can be accompanied by active mixing of the lower-density phase: hence a lower void fraction peak, flatter mixture ratios, and lower peak void fractions can be observed.

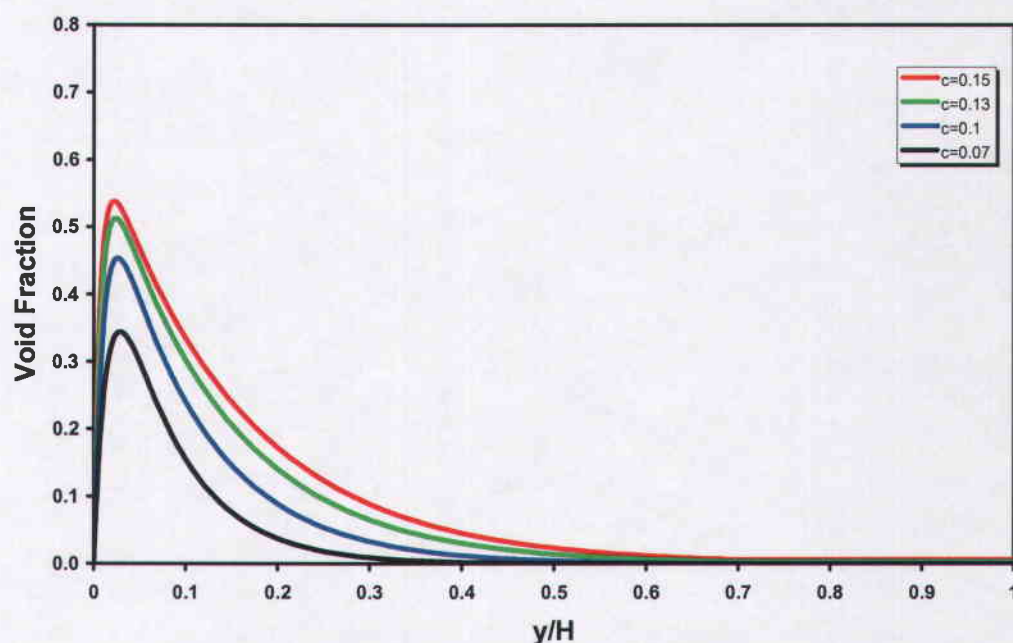


Figure 4.4: Void Fraction Decrease (Turbulent Ratio Variations)

Figure 4.4 shows the effects of variation of the ratio of liquid-phase turbulence to inertial force, liquid-phase turbulent ratio. As the turbulent ratio increases, the overall shape of the void fraction profile decreases. It is clearly shown that liquid-phase

turbulence affects the overall void fraction profiles without changing the maximum void fraction locations in the cross-section area. It is further explained that as the ratio increases, thus increasing turbulent force, the immigration of voids is increased and the relative diffusivity of the disperse-phase is increased. The overall void fraction profile is lowered by a given two-fluid flow amount. Even if the decrease in void fraction profiles happen, the overall void distribution profile is still maintained in any case. The usage of these turbulent coefficients is limited because there are no good formulations [Ishii & Hibiki, 2006].

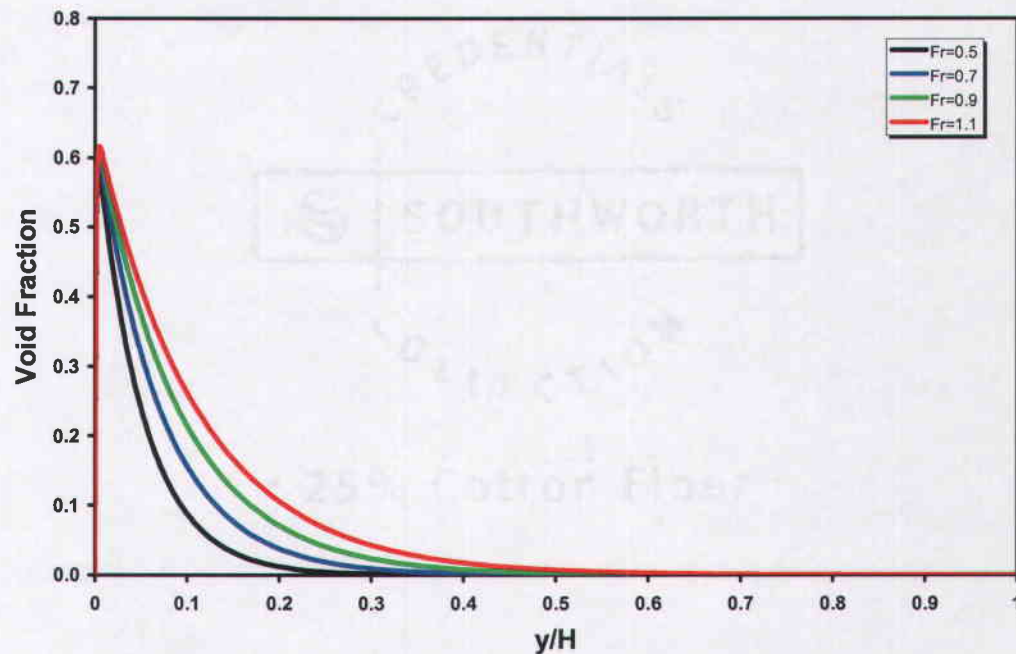


Figure 4.5: Void Fraction Swell (Froude Number Variation)

Figure 4.5 shows Froude number variation effects: a relative variation of two-fluid flow buoyancy to liquid-phase inertial force. When the inertia force dominates and overcomes the buoyancy force, the void profiles approach a stratified flow case. In

the opposite case, they would approach a swollen void fraction profile of the mixed two-fluid flow. In order to obtain exact profiles, Froude numbers in conjunction with flow coefficients, turbulent-diffusion, and turbulent ratio coefficient must be acquired locally.

4.5 VOID DISTRIBUTION IN TWO-FLUID MIXTURE LAYER

By applying the concept of the proposed homogenous mixture two-fluid flow, the void distribution equation can incorporate the void interactions, convection, and diffusion. Assuming a nearly stationary state of two-fluid flow, adding each phase momentum equation, and proposing a turbulent-void gradient relation, the net momentum equation becomes a second order differential equation. The parametric void fraction equation provides more insight than a conventional one, these insights being taken out by a parametrical study. With these parametrical studies, the proposed void diffusion-transport model is performed on the two-fluid fraction distribution in previous sections. By modifying expected coefficient values with observations of experimental results or incorporation of an appreciable void distribution profile, the natural characters of disperse phase distributions can be achieved. It is shown that a dispersed phase distribution can be modeled by several turbulent related coefficients, including Froude numbers. It is also shown that the amount of void diffusivity is inversely proportional to the continuous liquid turbulent strength, thus diffusion coefficient. While in reality, the coefficient represents the sweeps of the disperse voids through out the control domain. The amount of sweeping is represented in the incorporated coefficient. Even if liquid-phase turbulence plays a key role on the magnitude of peak void fraction, both liquid-phase inertia and gravity play main roles in profiling the void fraction distribution in the whole mixture domain as well shown in the previous section. A higher buoyancy force can result in a higher void fraction on the top. Unlike the diffusivity, they are directly related to body forces.

In considering all these parameters, it is found that the obtained two-fluid overall configurations show similarity. This similarity is not surprising knowing that the Froude number is much smaller than unity. Physically the amount of void dispersions is proportional to the liquid-phase inertial force or carrier diffusivity, a net effect of turbulence strength between the continuous and the disperse phase. Another important aspect that needs to be taken into account is an effect of the movements of the dispersed void itself. A long wave movement in the upward direction could be covered by buoyancy effects.

Furthermore, additional work is needed to validate the proposed model to minimize uncertainties, which can be introduced by a measured diffusivity or turbulence strength coefficients. There is also need to verify that the turbulent gradient, which will vary significantly from the liquid or disperse turbulence near the interface, while the turbulent strength of the continuous side will be higher than that of the disperse side [Carruthers and Hunt, 1985]. In order to assess the prediction capabilities of the void distribution model, void distribution data of the mixing layer is needed. The coefficients of the void distribution equation can be benchmarked against the void fraction data. In analytical modeling, these parameters will play a key role in a one-dimension two-fluid horizontal flow model. In the mixture flow zone, the momentum balance will depend on the mixture buoyancy, inertia, and turbulence even if the interface momentum sources cancel each other as shown previously. In the following section, a proposed one-dimension two-fluid pressure model will be described, allowing a unification of flow regime changes. This will provide not only one set of unified equations to solve, but will also allow smooth change of flow regimes. Thus, it will reduce or eliminate the numerical oscillations caused by sudden changes in flow regime or flow instability. The performances of the model can be verified by the characteristic system analysis.

5 UNIFIED ONE-DIMENSION HORIZONTAL FLOW MODEL

As shown previously research, time-averaging approaches are the most effective methods to find a two-fluid model, which handle two-fluid fraction variation. In deriving a one-dimension two-fluid flow model, the derived equation set is interrelated with a couple of interfacial transfer conditions. That will be a main mechanism to construct a unified one-dimension two-fluid flow model.

The considered models may have simple-unified constitutive relations in order to unify the stereotypes of two-fluid flows. They can allow smooth transitions between the various two-fluid regimes and permit correct determination of these variations, even if the original local instantaneous equation does not have the same kinds of simple constitutive relationships. The model equations have the capability of calculating the flow variations such as velocity, pressure, and pressure gradient without any instability problems, and determine the average pressure and the average interfacial pressure, even in one-dimension incompressible flow, at a given void fraction profile.

Two-fluid pressures distribution over the cross-section could follow certain two-fluid fraction distribution profiles. This would be a rather drastic assumption which can enable manufacturing of stereotypes of two-fluid flow structure in unification. In case of a separate two-fluid flow, some specific void heights can be calculated using the one-dimension conservation equations [Taitel and Duker, 1977]. They show a relationship between the equilibrium void height and equilibrium pressure in separate flows. Independently, the pressure distribution over an individual wave was calculated using a mathematical model, which was based on physical interpretation of roll waves. This also shows some equilibrium pressure relationships [Miya and Hanratty 1971]. When the interface surface of the two-fluid is not aligned in the direction of mean motion, there is an apparent mass force in accelerating inviscous flows [Wallis & Dobson, 1973; Wallis, 1969]. Based on hydrostatic assumptions, a unified parameter has been discussed by Dr. Kojasony and Dr. Ishii. The parameter would be dependent

on the void fraction profile of two-fluid flow types. All of the above are main mechanisms to be used in a unified void-pressure model.

A theoretical derivation of the unified pressure model is illustrated by assuming a linear variation of void profiles. More specifically, a unified void-pressure relationship will be shown with a linear void fraction profile over the mixture layer. These works are performed in two main sections: First, making a unified pressure model with a set of two-fluid flow governing equations; second, performing verification of the model by characteristic system analysis. Physically, the pressures between the two fluids would be in local equilibrium when considering static pressure. In considering the hypostatic body forces, there would be significant pressure differences between phase pressure and interface pressure. With the above descriptions, a theoretical void distribution model can be made understandable, explaining void fraction weight average process. The theoretical void-pressure expression will be acquired in conjunction with real experimental data.

5.1 VOID FRACTION VARIATIONS

A local void fraction distribution profile and its effects on two-fluid flow types should be known in order to develop the unified model. In another way, any different types of flow could be expressed in a unified model or in a unified expression form. In the case of a single-fluid zone, there is no interface and no void fraction gradient as expected. The single-fluid zone flow can be observed to obey their single-fluid governing laws. In the mixture flow regions, above or below the interface of the two single-fluid zones, the fraction of two-fluids would vary from zero to one. These void fraction distributions are evaluated by proposing a linear profile. The furthest position of the penetrating lighter upper fluid into the heavier bottom fluid can be explained by two-fluid momentum balance. The furthest boundary of the lighter upper fluid could create a mixing layer on the way, thus the local void fraction distribution is explained by overall momentum balancing in the direction.

5.1.1 Void Fraction Weighted Average

In considering the theoretical model of two-fluid fraction profiles, these trends need to manufacture mathematical associations. From this mathematical model, the estimation of the associate-value weighted averaging can be made analytically. As well known, time-averaging of the single-phase index or single-fluid conservation qualities give local void fractions or local void fraction weighted conservation qualities, respectively. Further, averaging them over the flow cross-section leads to area-averaged single-fluid occupations or one-dimension conservation qualities. In mathematical expression, the associated void fraction and the void fraction weighted average variable can be defined:

$$\begin{aligned}
 \frac{1}{A_A} \int \alpha_k dt &\equiv \langle \alpha_k \rangle \\
 \frac{1}{A_A} \int \alpha_k u_k dA &\equiv \langle \langle u_k \rangle \rangle \langle \alpha_k \rangle \\
 \frac{1}{A_A} \int \alpha_k p_k dA &\equiv \langle \langle p_k \rangle \rangle \langle \alpha_k \rangle
 \end{aligned}
 \tag{5.1}$$

All of the above expressions show that these mean values are a function of void fraction profile and can be used in one-dimension two-fluid conservations equations.

5.1.2 Two-Fluid Flow Interfacial Pressure

Interface pressure only occurs where the local two-fluid wave interface surface or the time-averaged interfaces are present with some degrees of void fraction variations. In order to evaluate the interface pressures of two-fluid flow, there needs to be a weight-average with interfacial wave surface area or void fraction at the interface. However, it is very difficult to calculate local interfacial surface area or local void fraction, even if they are greatly related to void fraction profiles. The difficulty lies in

the fact that the interfacial terms are only defined on the associated interfacial surfaces. Furthermore, the local two-fluid conservation qualities are present with big changes at their interfaces. This happens wherever interfaces occur. A gradient of local void fractions represents the probability variation of a single-fluid occupation at their interfaces. This is the reason that a void fraction gradient weighted interfacial pressure term should be used. From the definition of the interfacial average, the averaged interface pressure can be expressed:

$$\langle\langle p_{ki} \rangle\rangle \equiv \int_A \left(\frac{\partial \alpha_k}{\partial x} \right) p_i dA / \int_A \left(\frac{\partial \alpha_k}{\partial x} \right) dA \quad (5.2)$$

In the above definition of an average interface pressure, it is exact only if the interface is not flat. This is the main cause of redefining the average interfacial pressure term. This means that mean interfacial pressure only exists with the local void fraction gradients. The pressure term can be a mixture of two-fluid density, local two-fluid fraction and local two-fluid fraction gradient. The above interfacial expression is more reasonable than using a local void fraction since the interface pressure is a surface related quantity. In this way, any interfacial properties of a single interface or multiple interfaces can be consistently evaluated.

5.1.3 Void Fraction Integral Parameters and Unification

The evaluation of integral parameters can be shown by accounting the pressure difference caused by a gravity head and considering a momentum balance of horizontal two-fluid flow. The development of the unified model can be started with the previously derived two-fluid governing conservation equations. In the one-dimension two-fluid horizontal flow, the pressure difference between the phase pressure and interfacial pressure, delta pressure, should be in equilibrium in the two-fluids. In these cases, the delta pressure term is always in a coefficient of the void

fraction gradient term of the one-dimension momentum equation. A mathematical expression is given in the following:

$$\Delta p_k \frac{\partial \langle \alpha_k \rangle}{\partial x} \quad (5.3)$$

As already explained in previous sections, the coefficient of which equation is a very important term governing the growth or decay of void fraction and its stability. The pressures can be generalized by its body force by incorporating the influences of two-fluid structure and their involved forces. With the definition of the one-dimension two-fluid horizontal flow notations, the two pressures can be written:

$$\begin{aligned} \langle\langle p \rangle\rangle &= p_r + \frac{1}{A} \int_A \int_0^y \rho_m g dy \alpha dA - \frac{1}{A} \int_A \alpha dA \\ \langle\langle P_i \rangle\rangle &= P_r + \frac{1}{A} \int_A \int_0^y \rho_m g dy \left(\frac{\partial \alpha}{\partial x} \right) dA - \frac{1}{A} \int_A \left(\frac{\partial \alpha}{\partial x} \right) dA \end{aligned} \quad (5.4)$$

In the above equation, P_r is a reference pressure at the top of the two-fluid flow geometry, A is the two-fluid flow cross-section area, and y is the vertical distance measured from the top. The equations can be expanded by the definition of mixture density and gravity:

$$\begin{aligned} \rho_m &= \rho_1 \alpha + \rho_2 (1 - \alpha), \\ p(y) &= p_r + \int_0^y \rho_m g dy \end{aligned} \quad (5.5)$$

In a rectangular channel flow case, the integration can be expanded to a channel height, H . By assuming that the pressure variation due to gravitational head is only a function of vertical distance in incompressible limit, the pressure equation sets can be greatly

simplified. By giving void profiles, both pressure equations can be evaluated explicitly:

$$\begin{aligned} \langle\langle p \rangle\rangle &= p_r + \rho_1 g \frac{\int_H \int_0^y \alpha dh dy}{\int_H \alpha dh} + \rho_2 g \frac{\int_H \int_0^y (1 - \alpha) dh dy}{\int_H \alpha dh} \\ \langle\langle p_i \rangle\rangle &= p_r + \rho_1 g \frac{\int_H \int_0^y \alpha dh \left(\frac{\partial \alpha}{\partial x} \right) dy}{\int_H \left(\frac{\partial \alpha}{\partial x} \right) dh} + g \rho_2 \frac{\int_H \int_0^y (1 - \alpha) dh \left(\frac{\partial \alpha}{\partial x} \right) dy}{\int_H \left(\frac{\partial \alpha}{\partial x} \right) dh} \end{aligned} \quad (5.6)$$

Physically, the phase and interfacial two-fluid consist of a lighter fluid plus a heavier fluid. The gravitational force is proportional to fluid densities and the displacements from a reference value. Simplifying of the above equations further, new integral parameters are defined as various integral forms of local void fraction and local void fraction gradient such as:

$$\begin{aligned} \theta_1 &\equiv \int_H \int_0^y \alpha dh dy / H \int_H \alpha dy \\ \theta_2 &\equiv \int_H y \alpha dy / H \int_H \alpha dy \\ \delta_1 &\equiv \int_H \int_0^y \alpha dh \left(\frac{\partial \alpha}{\partial x} \right) dy / H \int_H \left(\frac{\partial \alpha}{\partial x} \right) dy \\ \delta_2 &\equiv \int_H \int_0^y dh \left(\frac{\partial \alpha}{\partial x} \right) dy / H \int_H \left(\frac{\partial \alpha}{\partial x} \right) dy \end{aligned} \quad (5.7)$$

Using the previous integral parameters, the one-dimension interfacial and phase pressures are given by a simple form:

$$\begin{aligned} \langle\langle p \rangle\rangle - P_r &= -(\rho_2 - \rho_1) g H \theta_1 + \rho_2 g H \theta_2 \\ \langle\langle p_i \rangle\rangle - P_r &= -(\rho_2 - \rho_1) g H \delta_1 + \rho_2 g H \delta_2 \end{aligned} \quad (5.8)$$

The above equations show that pressure terms are composite in their substantial forces, buoyancy and gravity. The advantage of this arrangement is that the pressure contributions of two-fluid flow can be identified, buoyancy and heavier fluid gravitational head in a linear function of integral parameters. The integral parameters could appear as a virtual displacement, even if it is usually difficult to deal with the integrations of local void fraction distributions. Evaluation of the integral parameter is the main key in constructing a unified two-fluid model. These integral parameters could be approximated using a reasonable assumption or empirical relationships of void fraction profiles. The integral parameters can be simplified in a series of mathematical manipulations with a linear void fraction profile.

5.2 LINEAR LOCAL VOID FRACTION MODEL

It is important to note that void fraction distribution profiles can be evaluated by momentum balancing for any number of interfaces. These corresponding interface conditions would not be dependent on flow types. The proposed linear void fraction is very useful in taking account of locally distributed interfaces in these integral parameter evaluations. In two-fluid horizontal flow, there are wavy, slug, and bubbly flow as graphically shown in Figure 5.1. These figures show the characteristics of void fraction profiles, which is needed for the unification model. Any flow type is somewhere between stratified separate flow and well-mixed bubbly flow, even if some of them would be existence for a very short time. The main difference between wavy and slug flow is the number of interfaces. In two-fluid modeling, it can be assumed that these interfaces are distributed over the mixture zone, even if the interface of wavy flow is well distributed on the wave surface. Different types of overall void fraction profiles depend on the type of two-fluid flow. A void fraction model is needed to evaluate these void fraction profiles. Using the linear void fraction model, the identification of the flow characteristics can be attained with some manageable precision and be reduced to a simple form.

5.2.1 Stratified Separate and Well-Mixed Bubbly Flow

Mathematically, the interfacial pressure relationships have been attained in the previous sections to develop one-dimension two-fluid horizontal flow models. The definition of the interfacial pressure is a summation of the local interfacial pressure variation over the interface surface or the average of void fraction gradient weighted pressure. Sometimes, the average interface pressure could not be evaluated since the void fraction variation is ignorable small or infinitely large depending on the two flow types. There is need for a crude approximation of a one-dimension pressure difference equilibrium condition and a momentum equilibrium condition between two-fluid fluid flows, as well as an assumption of manageable void fraction gradient.

Both flow types have no gradient void fraction profiles, near symmetric, because the both fluids represent the same amount of momentum exchange between the fluids. By definition, the interfacial pressure would be considerably large depending on the two-fluid flow types. With a relatively large local void fraction variation flow or a relatively large interfacial pressure, the pressure difference would be constant:

$$\Delta P = \text{Constant} \quad (5.9)$$

By definition in well-mixed flow, there would be no interfacial pressure since the symmetrical geometric void distributions. There is no significant pressure difference between the two-fluids. Thus, the average interfacial pressures would be relatively zero. The delta pressure would be equal to the phase average static pressure:

$$\Delta P = \frac{\rho_1 g H}{2} \langle \alpha \rangle + \frac{\rho_2 g H}{2} (1 - \langle \alpha \rangle) \quad (5.10)$$

It is worth mentioning that there is no significant pressure difference between the phase and interface. It has been shown that interfacial pressure occurs where a void

fraction variation. Mathematically, this is because making an interface pressure can be not presentable with the void fraction variations. In a simple case of stratified separate flow, the delta pressure would always remain limited due to the difference of the hydrostatic head. In the fully mixed flow case, the pressure is equal to continuous flow pressure, as expected. By taking these mathematical operations over the newly introduced parameters, detailed analytical expression can be obtained. The parameters could be approximated to manageable levels using reasonable assumptions and/or empirical relationships. The evaluated value is a one-dimension pressure difference instead of the interface itself pressure. This is another form of the momentum balancing conditions, which is expressing the vertical pressure difference. All results are based on a one-dimension two-fluid flow definition mathematically and would be true in any case of two-fluid horizontal flow. The pressure would be continuous at any flow regime. A more detailed delta pressure model will be developed and compared in each of the flow regimes in the following section.

5.2.2 Wavy Flow

In wavy flow, there is a significant mean interfacial pressure by the mathematical definition. The phase pressure is proportional to the amount of fluid fraction. As soon as a surface wave appears, the average interface pressure term could be calculated. It has been illustrated by some measurements of the local interfacial pressure of the wave surfaces [Miya, 1971], where the interfacial pressure is plotted as a function of position along the wave. There would be a different interfacial pressure value depending on the wave shape.

As expected in wavy flow, there are two characteristic void fraction variations: a constant and a continuous variation zone. Based on the assumption of a smoothly varying void fraction profile over a mixture flow, a linear slope void fraction distribution model can be constructed as shown in Figure 5.1. Actually, the model needs three variables, maximum void fraction and two max-min void locations. These

variables can be chosen to describe the linear void model in a sufficient equilibrium two-fluid flow state. It is very convenient to impose a linear void variation when modeling the void fraction profiles in theoretical pressure calculations.

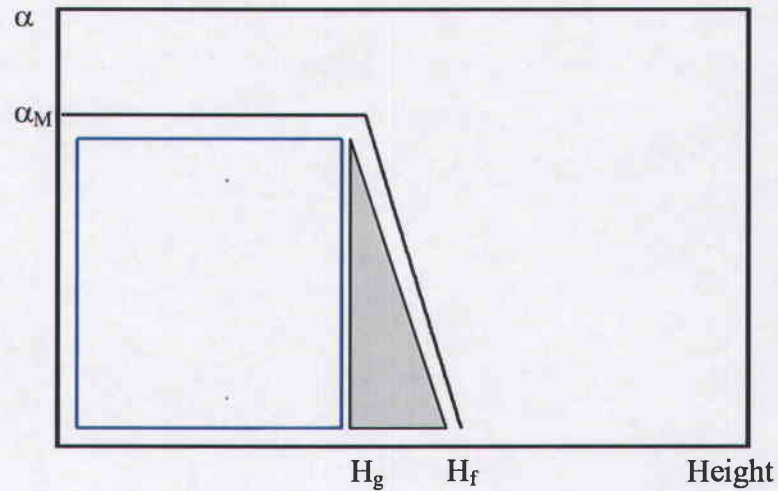


Figure 5.1: Linear Void Fraction Profile Model-Wavy Flow

As illustrated in Figure 5.1, the proposed void fraction profile model can replace a real void fraction profile by these linear variations and replacing the void fraction max-min heights with integral parameters, which can be rewritten by fixed-value formulations [Appendix D]. In the case of wavy flows, the integral parameters can be found:

$$\begin{aligned}
 \delta_1 &= \frac{\alpha_M (H_f^2 + H_g H_f - 2H_g^2)}{6H(H_f - H_g)} \\
 \delta_2 &= \frac{(H_f + H_g)}{2H} \\
 \theta_1 &= \frac{\langle \alpha \rangle}{2H} \\
 \theta_2 &= \frac{5H_g^2 + 2H_f H_g + 2H_f^2}{3H(3H_g + H_f)}
 \end{aligned} \tag{5.11}$$

All evaluating integral parameters can be restricted within the specific mathematic formulation condition, any derivative value from the fixed void fraction formulations reduced to second order error. By combining these integral parameters for delta pressure, they can be greatly simplified to a physically understandable expression. This is appeared as an important relationship between the delta pressure and the linear void fraction profile:

$$\Delta p = K \left(\frac{\rho_f}{3\alpha^M} - \frac{\rho_f - \rho_g}{6} \right) \langle \alpha \rangle g \quad (5.12)$$

It is shown that the delta pressure is dependent on two basic variables, mean void fraction and maximum void fraction. On physical interpretations, the delta pressure is expressed as two two-fluid main forces and their mixture ratio. The first represents the gravity, and the second accounts for the buoyancy force.

5.2.3 Mixed Flow

The delta pressure expression of mixed type flows can be evaluated by using the same linear void fraction model, basing on a physical interpretation of the mixture flow as shown in the pervious sections. As expected in mixture flows, there is a unique characteristic void fraction variation, a continuous variation zone. Based on the assumption of a smoothly varying void fraction profile over a mixture flow, a uniform slope void fraction profile model can be constructed as shown in Figure 5.2. The model needs three variables, maximum void fraction and two max-min heights. These variables can be chosen to describe the linear void model in a sufficient equilibrium two-fluid flow state. It is very convenient to impose a linear void variation when modeling the void fraction profiles, and evaluating with integral parameters.

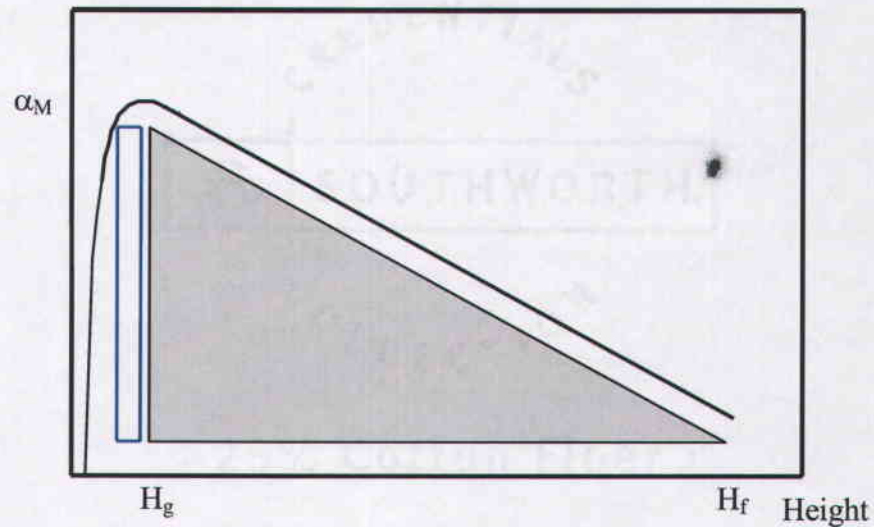


Figure 5.2: Linear Void Fraction Profile Model-Mixed Flow

As shown in the previous section, the void fraction profile shows a linear variation over a vertical distance. At a sufficient two-fluid equilibrium state, the void fraction profile has three related linear model parameters, max-min void heights and maximum void fraction. Similarly after a series of mathematic manipulations, the delta pressure integral parameters can be rewritten [Appendix E].

$$\begin{aligned}
 \delta_1 &= \frac{\alpha_M(H_f^2 + H_g H_f - 2H_g^2)}{6H(H_f - H_g)} \\
 \delta_2 &= \frac{(H_f + H_g)}{2H} \\
 \theta_1 &= \frac{\langle \alpha \rangle}{2H} \\
 \theta_2 &= \frac{2(H_f^2 + H_f H_g + H_g^2)}{3H(H_f + H_g)}
 \end{aligned} \tag{5.13}$$

It is worth noting that these integral parameters can be written in simplified forms. By combining these integral parameters, a relationship between delta pressure and the integral parameters of mixed flow can be written:

$$\Delta p = K \left(\frac{\rho_f}{3\alpha^M} - \frac{\rho_f - \rho_g}{6} \right) \langle \alpha \rangle g \quad (5.14)$$

In the above equation, all of the parts are exactly the same form as in the previous case, including the proportional factor which is the ratio of the peak to the average void fraction. From the above two delta pressure relationships, the modeling results show a possible connection in making a unified model.

By linear theoretical examination of the void fraction profile, a simple relationship of the delta pressure expression is found. In the same frame of void fraction profile examinations, the complex integration parameters can be put into a simple delta pressure expression. These results can be applied to a unified delta pressure formulation of one-dimension two-fluid horizontal flow. The delta pressure model can be greatly used in describing a characteristic analysis of the two-fluid flows. It is important to note that the analytical fixed value formulation efficiently closes all integral parameter relationships, handling a unified delta pressure model for a single or multiple interface flow case.

5.3 DELTA PRESSURE ON INSTABILITY ANALYSIS

It is well known that when a heavier fluid flowing over a lighter fluid at any velocity, a physical instability occurs at the layer of the two-fluid interfaces. In case of a lighter fluid moving over a heavier fluid, a physical instability can occur at a specific relative velocity on the layer of the two-fluid interfaces. The instability results from transitions from one flow type into another flow type, displaying different types of void fraction profiles. A physical mechanism behind the regime transition is interfacial

surface instability. These interfacial instabilities have been investigated, to the growth of the interface surface reaching the top of the flowing area [Trapp, 1986; Kosasony, 1985]. When the lighter upper fluid exceeds the critical relative velocity, the inertia forces pull upon these interfaces. This means that the force overcomes the gravity force of the bottom heavier fluid, and pulls the crest of the heavier fluid surface to the top. Physically, the more interesting parts of instability lie on the prediction of the flow regime transitions.

A stability analysis is needed to determine under what conditions the model remains instable and where the instability transition point would be. For this stability analysis, the mean flow conditions of the two-fluid flows should be known and could be simplified such as neglecting source terms. In the horizontal two-fluid flow, there is a mass generation source and no external body force source acting in the flow direction, even if the two-fluid flow occupational area is exchanging. Since these area variations greatly affect the mean momentum of two-fluid horizontal flow, including hydrostatic pressure that should be considered in varying interfaces. In these relationships, void fraction distribution concepts and gravity are very important in evaluating equivalent forces. Furthermore, they show reason why the interface pressure should be weighted by interfacial void fraction variation. In order to determine the impact of the variations on stability of one-dimension two-fluid horizontal flows, the governing equation needs to be expressed in a matrix:

$$\begin{vmatrix} \rho_1(\lambda - u_1) & -\alpha\rho_1 & 0 & 0 \\ \rho_2(\lambda - u_2) & 0 & (1-\alpha)\rho_2 & 0 \\ \rho_1 u_1(\lambda - u_1) & \alpha\rho_1(\lambda - 2u_1) & 0 & \alpha \\ \rho_2 u_2(\lambda - u_2) + \Delta P & 0 & (1-\alpha)\rho_2(\lambda - 2u_2) & (1-\alpha) \end{vmatrix} = 0 \quad (5.15)$$

Based on the prescribed characteristic analysis process, the solutions of the above matrix equation can be reduced to an investigation of the roots of the determinant. In

order for the determinant to be equal to zero and keep the solution nontrivial, the determinant becomes a second order quadratic equation:

$$\lambda_{1,2} = \frac{\left(\frac{\rho_1 u_1}{\alpha} + \frac{\rho_2 u_2}{1-\alpha}\right) \pm \sqrt{-\frac{\rho_1 \rho_2}{\alpha(1-\alpha)}(u_1 - u_2)^2 + \frac{\Delta p}{1-\alpha} \left(\frac{\rho_1}{\alpha} + \frac{\rho_2}{1-\alpha}\right)}}{\left(\frac{\rho_1}{\alpha} + \frac{\rho_2}{1-\alpha}\right)} \quad (5.16)$$

For the solution to remain in real, the quadratic equation would be hyperbolic and well-posed, and the square root term of the quadratic equation must be real positive value. As long as the square root part of above equation keeps positive, two real characteristic roots can exist. If the root's evaluation term with the delta pressure term behaves in such a way that the inequality is always met, the two-fluid flow model becomes well-posed:

$$u_1 - u_2 \leq \pm \sqrt{\Delta p \left(\frac{1}{\rho_2} + \frac{\alpha}{\rho_1(1-\alpha)} \right)} \quad (5.17)$$

When the inequality of the above equation is violated, additional momentum interactions due to inertial force would presumably appear. In analyzing the system real stable limit ranges, a real formulation or a real value of the delta pressure is needed. Using the preceding linear void fraction profile model, one of an exact form of the delta pressure can be expressed theoretically. A further characteristic analysis can be performed by substituting in the delta pressure formulation, and the above criterion expression turn into:

$$u_1 - u_2 \leq \pm \sqrt{kH \left(\frac{\rho_2}{3\alpha_m} - \frac{\Delta p}{6} \right) \left(\frac{1}{\rho_1} + \frac{\alpha}{\rho_2(1-\alpha)} \right)} \quad (5.18)$$

Furthermore just after the transition to a slug flow, the coefficient k is keeping to one and the well known peak void fraction is going to:

$$\alpha^M = 2/3 \quad (5.19)$$

The transition point of flow regimes should be somewhere between a separate flow and a mixed flow and the delta pressure would be continuous between them. From the all above relationships, the criterion for slug transiting flow becomes:

$$u_2 - u_1 \leq \pm \sqrt{\frac{Hg\alpha}{\rho_1} \left(\frac{\rho_2 - \Delta\rho}{2} - \frac{\Delta\rho}{6} \right) \left(\frac{\rho_1 + \alpha}{\rho_2 + 1 - \alpha} \right)} \quad (5.20)$$

By assuming that the light upper fluid density is much less than heavier bottom fluid like an air-water flow case, the above hyperbolic criterion can be further simplified:

$$u_1 - u_2 \leq 0.57 \sqrt{\frac{\alpha}{1 - \alpha}} \sqrt{\frac{\Delta\rho g \alpha H}{\rho_1}} \quad (5.21)$$

In the range of relative velocity, the two-fluid flow is a well-posed system. This result is similar to the previously obtained well known Kelvin-Helmholtz instability criteria, showing that gravity force stabilized the two-fluid flow over a significant inertial force.

5.4 UNIFIED ONE-DIMENSION HORIZONTAL FLOW MODEL

The linear void fraction model has been used in order to unify one-dimension two-fluid horizontal flow problems. The continuous void fraction distribution profiles can be simplified by replacing with an approximate linear void distribution. By

replacing the void fraction characteristic variation by a linear variation model, a new vertical direction momentum relationship can be obtained with the function of the mean void fraction and the peak void fraction of two-fluid flows. In considering stereo types of local void fraction profiles that are dependent on two-fluid flow regimes, it is found that there is a unique relationship in balancing the vertical momentum.

In a mathematic derivation of the integral parameters of the one-dimension two-fluid equations with the linear void fraction model, the delta pressure, vertical momentum balancing relation, can be written:

$$\Delta p = K \left(\frac{\rho_2}{3\alpha^M} - \frac{\rho_2 - \rho_1}{6} \right) \langle \alpha \rangle g \quad (5.22)$$

The expression is always consistent through the flow regimes in any of the cases of two-fluid flow types, and the amount of the delta pressure force is proportional to the fluid density difference and these displacements. It should be recognized that it is also convenient to take the proportional coefficient as the ratio of average void fraction to maximum peak void fraction in some apparent mass effects being included. Furthermore, the delta pressure would be continuous at any flow regime, including an unstable transition point even if the flow situation continuously exists or not.

6 RESULTS

The unified one-dimension two-fluid horizontal model has been developed and can be applied to any flow types. In the development of a unified correlation, the one-dimension horizontal flow model is getting stabilities. The model is tested to the relative velocity limit of two-fluid stable system by the characteristic system analysis. By comparing the theoretical linear void profiles model with experimental void profile data, the test results are verified. For verifications of the theoretical linear void profiles model, a numerical integral of the empirical real void fraction profiles are treated, even if all the data is dependent on these flow regimes. If the previous approximations and assumption in the theoretical model developments are correct, a numerical or a theoretical constitutive relationship for two-fluid flow will be reduced to a unique pattern.

In the unified flow modeling with hydrostatic body force, it is no longer appropriate to apply the pressure jump at the two-fluid interfaces and/or flow type transitions point even if in a one-dimension sense. These intentions can be evaluated by the delta pressure model, which has continuous pressure changing between flow types. Since all these possible discontinuous transition regions can be replaced by the mean continuous properties, all these results may be in a physical stable condition, continuous flow transition, and be allowed the instability to remain hyperbolic in naturally. A detailed comparison of the hydrostatic relations will be discussed in the next section.

6.1 VOID FRACTION DISTRIBUTION

In steady-state with no-phase change two-fluid flow, the empirical void fraction distribution profiles have been measured by various methods. Some void fraction measurement devices result in an average value over a given flow domain, and others do not. If two-fluid flow structures show fast-changing along the flow direction, the

two-fluid fraction measurements would not be the same. It would happen near a sudden instability region between before and after it. They also require two- and/or three-dimensional void fraction measurements, allowing the local measurements over the whole flow cross-section areas.

For theoretical or analytical usages of the void fraction profiles, the most effective and simplest methods are numerical estimating approach or a simple approximation method of local void fraction measurements. The basic concept of the approximation method is choosing a known functional form of the void fraction distribution profiles or a known form of the void fraction differential equations, and to adjust its consequent form of parameters so that the non-linear void profile is numerically or analytically satisfied as close as possible. These methods should be easier than calculating with the actual profile, but won't contain much information about void fraction mechanisms that can be created by the actual profiles. But these will mimic actual void fraction distribution profiles and be a good analytical usage in comparing to a linear void fraction distribution profile model.

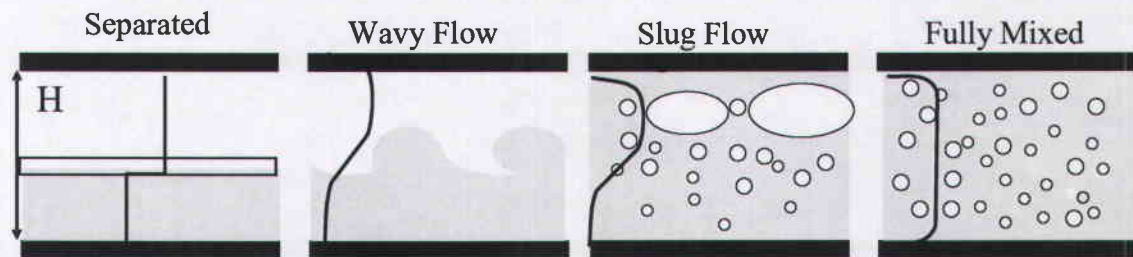


Figure 6.1: Mixture Flow Layer of Different Flow Regimes

Figure 6.1 shows visualized two-fluid structure and its correspondence to conceptual mixture layers, which are obtained by evaluation of these local void fraction profiles or time-averaging local instantaneous two-fluid horizontal flows in various two-fluid flow regimes.

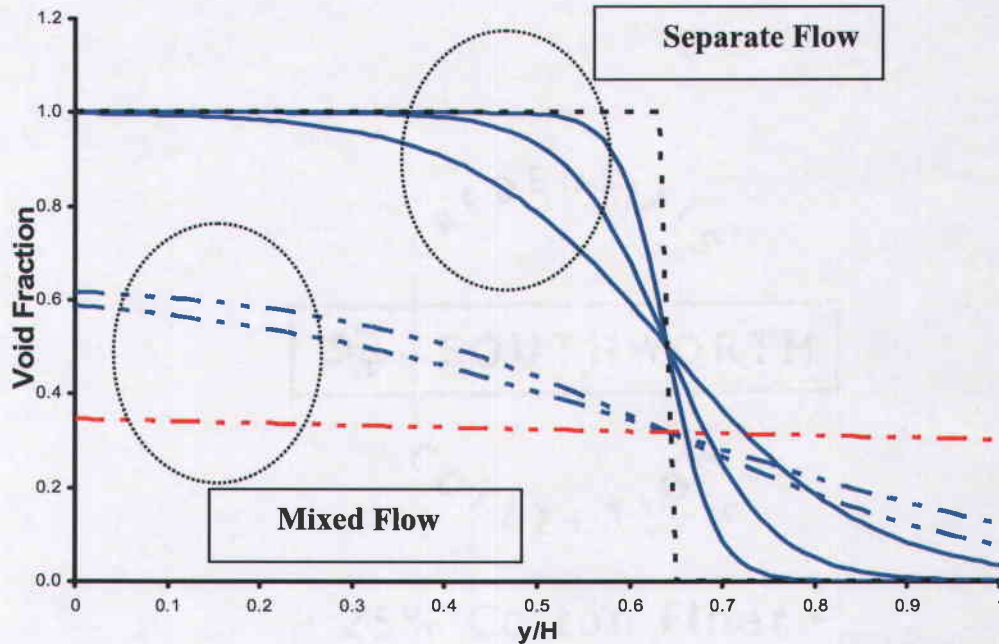


Figure 6.2 Contours of Void Fraction Distribution

In these horizontal two-fluid flows, void profiles characterize the spatial trend of void concentrations, which would locally transport into one another according to involved forces. In considering a local void distribution profile as a time-averaged two-fluid interface, the interfaces are replaced by a homogenous mixture with a direct parallel to two-fluid flow as shown in Figure 6.2. In mixture layer, there are two important common contours, separate and mixed flow, in view of void variation over the whole vertical distance. The blue-solid lines of Figure 6.2 represent local void fraction distributions of separated flows. The maximum of these void fractions is dependent on two-fluid flow rates, even if there is a very small mixing zone in the middle of the flow cross-section. The blue-dotted lines represent the expected void fraction profiles of mixed flow. The outside of blue-lines, the dotted black and red lines, represent expected void profiles of a stratified and a bubbly flow, respectively.

6.2 LOCAL VOID FRACTION PROFILE

The actual void fraction profile measurements are represented in the following few sections. The measured void fraction distributions will provide better insight of local two-fluid flow construction, local two-fluid volume ratios. In quasi-steady-state, the local two-fluid flow combinations are seen, since the two-fluid fraction is a time-average fraction of the two-fluids. From the local void fraction measurements of a separate flow, it is easily expected that the void fraction will have a constant zone near the top wall. The constant void fraction is the peak maximum void fraction, which also has the transit point from a constant to a continuous void fraction variation in the vertical direction of horizontal flow. In these void fraction profiles, there is a void fraction variation zone, the time-average of interface mixing layer. As shown in the previous chapters, these profiles are very similar to the solutions of the void distribution model or the profiles of the linear void fraction model.

These void fraction distributions explain the involved body forces, which cause same amount of void to move upside to balance all the concerned force terms physically. These fractions are the maximum at a much higher point in two-fluid flows, and are monotonically or suddenly changed thorough the interface mixing region until a region occupying only one heavier fluid. Even if the actual measured profiles have much more meaningful characteristics, the mixing layer thickness can grow with those void fraction profiles variations and these growth rates are not proportional to the variations. This is because the two fluids have different velocities, densities, and are less dependent on void concentrations. Also, suddenly occurring two-fluid instabilities significantly affect overall void fraction distribution profiles. These void distribution profiles have less information of the two-fluid instability: far away from the instability, the void fraction profiles have a constant void fraction, just after the instability the maximum peak void fraction is 0.65 (2/3). There is no known method to find an exact solution of these void distribution profiles, even if some analytical methods are good at approximation they are still under research. As shown previously, the delta pressure model is one of candidates.

6.2.1 Void Fraction Profiles

Under a steady-state two-fluid horizontal flow, the flow may have two typical types of void fraction profiles. As shown in Figure 6.3 and 6.4, both void fraction profiles are the function of two-fluid flow rates. They correspond to net momentum balancing results, while some voids are pushed downwards by turbulent force near the mixing layer with the maximum void fraction at the topside. The continuous constant void fraction is likely intercepted at the mixing layer boundary, which is always found at the topside of separate flows. With their higher average void fraction, a monotonically changing void zone is observed from the topside of the mixing layer to the lower part as expected. In more detail, the topside of the two-fluid flow area is mostly occupied by a lighter fluid with a constant two-fluid fraction

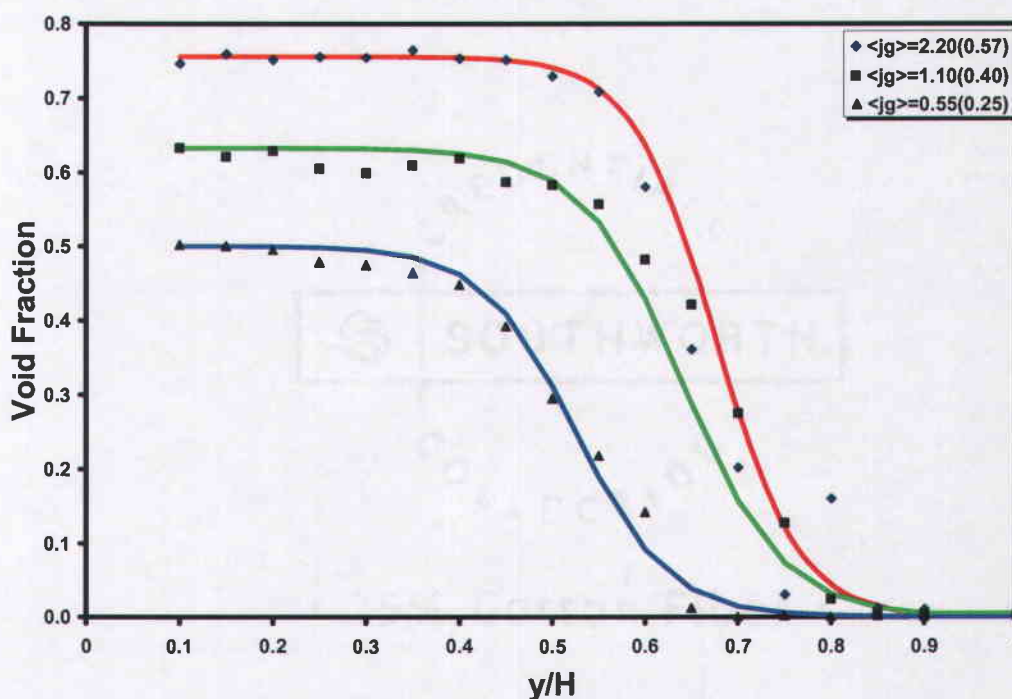


Figure 6.3: Experimental Void Fraction Profiles, $\langle j_r \rangle = 1.65 \text{ m/s}$

Similarly, the bottom part is occupied by a heavier fluid with constant local two-fluid fractions. Between these top and bottom regions, a monotonically two-fluid fraction variation region exists until the boundaries of the areas occupied by one specific fluid. Approximately, the two-fluid fraction corresponds to the balance of inertia and buoyancy, while some rates of voids are pushing downwards by flow turbulence near the mixing layer. A net effect of these forces results in void fraction distribution: if the inertia of the lighter fluid overcomes the buoyancy force, the higher part of the two-fluid flow area is prevailing with the light-weight fluid that would be responsible for the separating two-fluid flow. With actual measurements, Figure 6.3 shows what percentage of the single-fluid flow area is occupied by separate two-fluid flow. The three solid lines show a numerical curve fitting corresponded to these void fraction distributions, where three void fraction distribution profiles are compared with their three air flow rates.

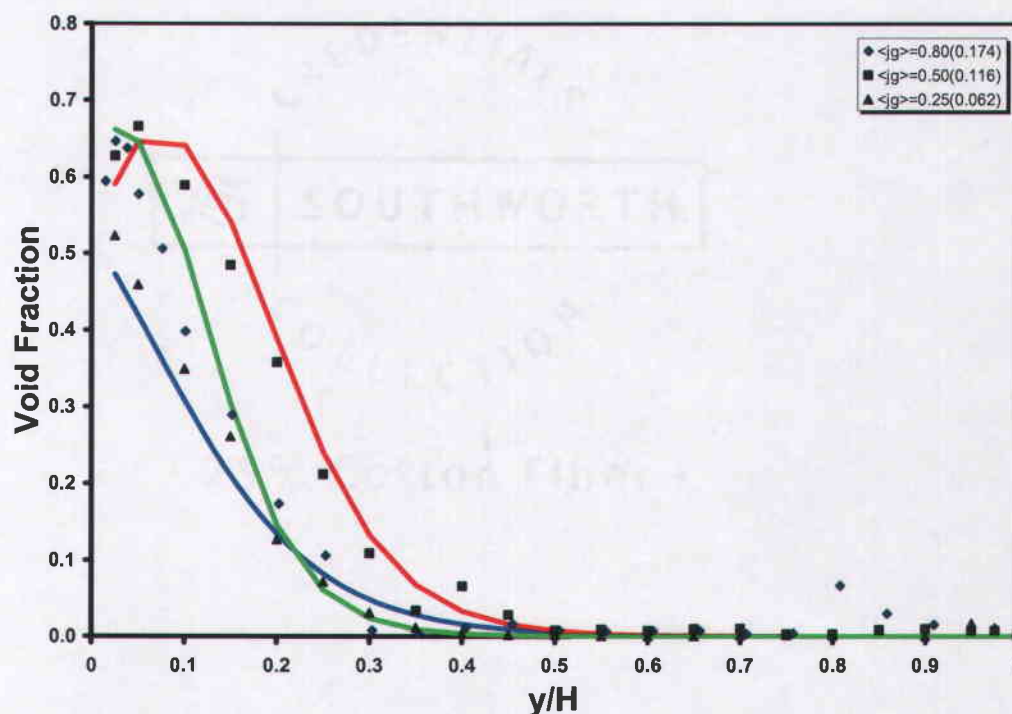


Figure 6.4: Experimental Void Fraction Profiles, $\langle j_f \rangle = 3.8 \text{ m/s}$

They exhibit continuous variations all over their mixture layers. They will happen until the average fraction of air is approximately up to a quarter. After that point, a separation mechanism is no longer stable: the overall void fraction profile transitions from having partial constant trend to whole variation two-fluid mixture trend flowing as shown in Figure 6.4.

All actual measurements [Kocamustafagullari and Wang, 1991; Kojasony and Hung, 1994; Kocamustafagullari et al., 1994 Iskandrani and Kojasony, 2001] suggest that the topside local void fraction is larger than in the bottom and these differences make an asymmetric void distribution profile, which is strongly related to a mean two-fluid mixture flow condition. A large portion of air is flowing along the upper part of the flow area, the air fraction is nearly constant, and continuously decreases over the vertical direction. Also, a strong mixing action is made by a rapidly growing instability and a whole area mixture flow situation is constructed after the instability, sharply re-establishing the void fraction trend. This strongly suggests that local void fraction distribution profiles could be dependent on their mixture flow situations and be changed by the two-fluid flow conditions. These void fraction profiles also have a characteristic slope as a function of mean void fraction, even if the slope is continuously changing. These characteristic void fraction slopes could be introduced by balancing two-fluid total momentum, which takes account of turbulence and gravity. With a total momentum balance concepts in two-fluid mixture layer, an equivalent hydrostatic pressure should be in existence with the function of equilibrium local void fraction distribution. It is important to note that there is no difference between applying these concepts on any of the two-fluid flow regimes. From these relations, a unified theoretical pressure relation has been developed.

6.2.2 Void Fraction Profiles of Mixed Flow

In void fraction measurements of mixed flows, there are no constant void fraction zones. The void fraction zone will change in a continuously varying

distribution. Also it has been observed that all void fraction profiles have very similar overall shape with a peak void fraction peak near the topside as shown in Figures 6.5. Specifically in air-water horizontal flow, it is well known that the maximum peak void fraction is about 0.65 just after the transition from separated to mixed flow. It has been expected that the maximum fraction is a maximum packing factor of equal-size spherical bubbles in an equilibrium force state. Physically, the turbulent force overcomes the surface tension of a larger bubble and the accumulated bubbles near the top would be broken into smaller bubbles. The creation of smaller bubbles can establish new bubble upward forces, buoyancy forces, made to balance the liquid turbulence force.

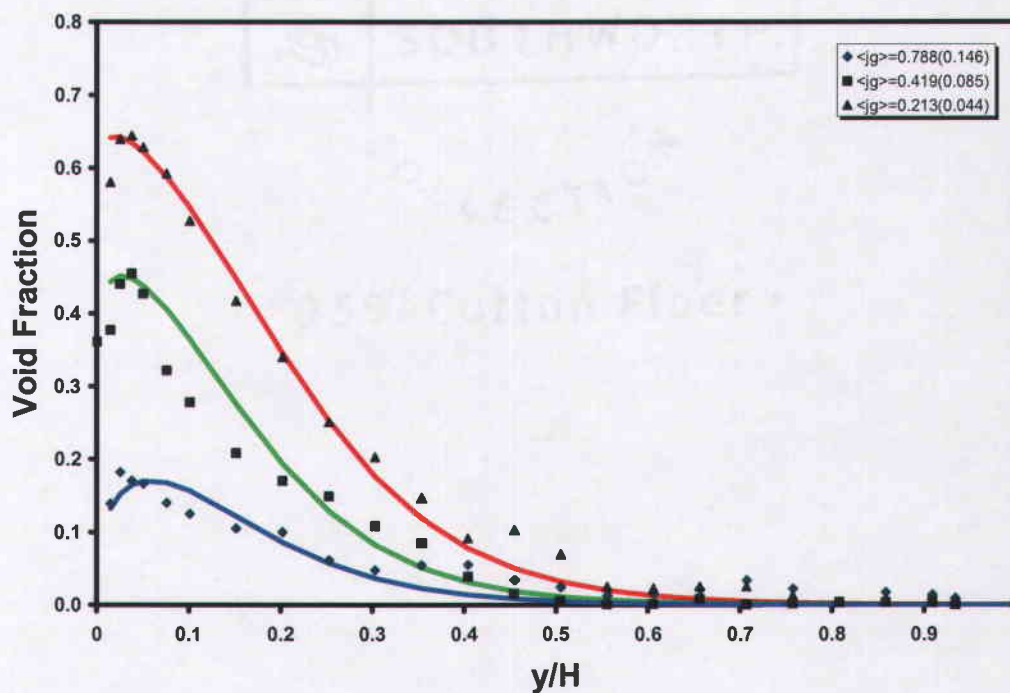


Figure 6.5: Experimental Void Fraction Profiles, $\langle j_f \rangle = 4.67$ m/s

As the liquid flow rate is increased, the dispersed bubbles become diffusive and wider by increasing the continuous fluid inertia, thus liquid turbulence, as shown in Figure 6.6. Even if the void distribution profiles look like half of a Gaussian distribution curve, they may or may not represent a statistic distribution. They simply come from a characteristic trend of void distribution with two-fluid momentum balancing in mixture flow layer. It is important to note that the different between the void fractions have been shown with different values of air flow rates. The maximum void fraction is decreased and occurs at more or less intermediate position as air flow rates are decreased, even though the overall shapes of void fraction distribution has no affect. At the void fraction peaks and these locations are decreased and deeper as continuous phase flow rates are increased.

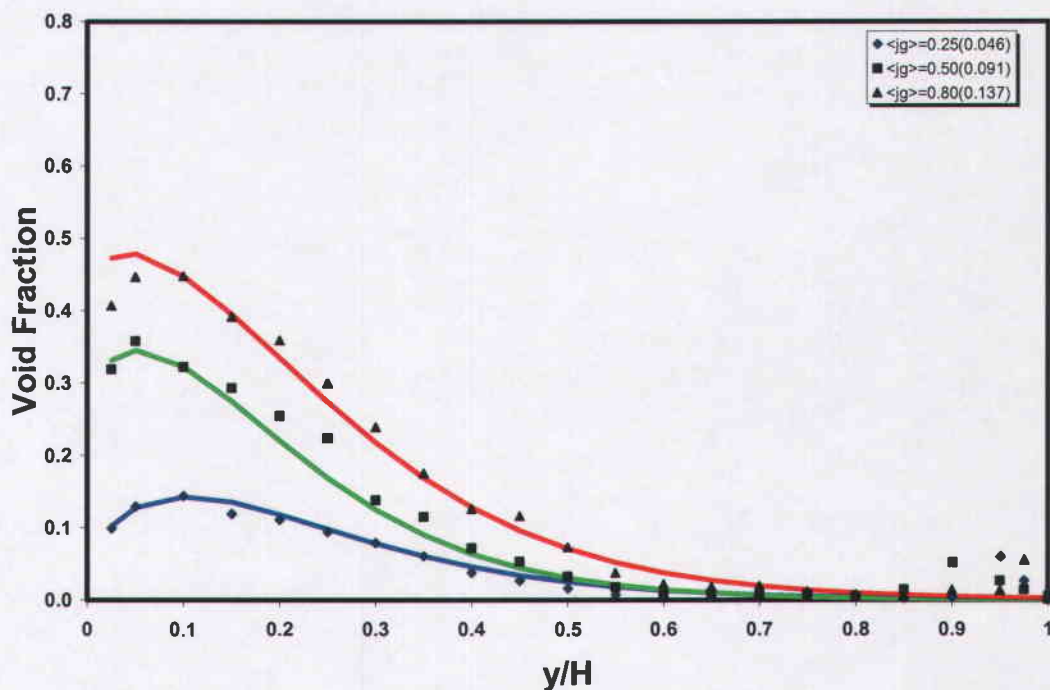


Figure 6.6: Experimental Void Fraction Profiles, $\langle j_f \rangle = 5.0$ m/s

6.3 DELTA PRESSURE VERIFICATION

All above figures show that the visualized flow structures observed by actual void fraction measurements and numerical re-constructions of the two-fluid fraction distributions. To evaluate the actual interfacial momentum balancing forces, delta pressures, a set of real experimental data is required. In the evaluation of any two-fluid flow regime, a linear void fraction profiles have been used as one of the candidates. The actual measurements can be used in evaluations of void fractions, thus delta pressure, both correspond to the numerical approximations.

In the void profiles of well-mixed flow and stratified separated flow, it is expected that the gradient of the two-fluid fractions would be nearly zero and very large respectively. In these two cases, the interface pressures are not well known. Only when two-fluid flow diverges from stratified or well-mixed flow, the influence of void fraction gradients on the vertical force balancing relations can become evident. For the verification of these void fraction models, the actual evaluation results are needed to compare to the actual measurement data. For comparison purposes, the actual void fraction profiles from actual measurement data can be numerically approximated by fitting the coefficients of the void diffusion-transport model based on the homogenous flow approximation. By estimating actual void fraction distribution profiles over the flow cross-section, the real characteristic trend of two-fluid flow structures can be shown.

With the same mathematical definition of theoretical delta pressure, a numerical delta pressure can be evaluated with real measurement data. The experimentally evaluated delta pressures, red-dots, are shown for comparisons purpose in Figure 6.7, where the theoretical delta pressures, blue-dots, are found with the concepts of linear void fraction profile and its equivalent gravitational body force. All of these evaluated pressures are relative to the static pressure of the fully channeled single-liquid pressure. This means that all these experimental and numerical delta pressures are normalized by the full height liquid pressure.

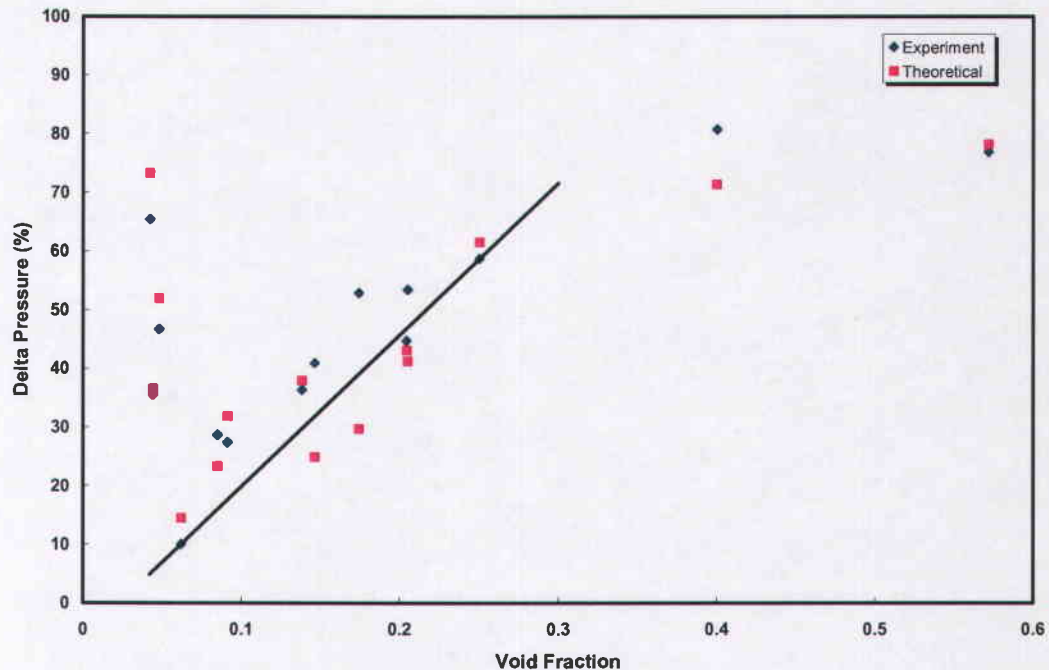


Figure 6.7: Comparison of Experimental and Theoretical Delta Pressures

Within a number of significant digits, both delta pressures are very similar, even if there are some differences at lower void fraction values. The differences between them could be attributed to the fact that small errors or uncertainties of measurement might amplify the difference between the predicted and measured values in evaluating the spatially void distributions. It is believed that given these uncertainties, the agreements are well matched. As shown by the solid black line in Figure 6.7, the overall trend of delta pressures is to decrease with the mean void fraction. This means that delta pressure is decreased as being the generation of a surface wave and void mixture wave, and their amplitude growth in vertical direction as they are going to well mixed situation.

These delta pressure results can be used in system characteristic stability analysis for the verification of the theoretical delta pressure model. The flow characteristic analysis is focused on a role of delta pressure relating the momentum balance of different two-fluid flow regimes. In cases of perfectly-stratified and well-mixed two-fluid flow, the stable relative velocities could be hard to evaluate by the facts that the void fraction gradients are infinite and zero respectively, even if all these could be estimated in numerical evaluation of experimental void fraction data. Considering a linear void fraction profile, the functional relationship of delta pressure can be greatly simplified with an asymptotical approach to real gravitational momentum balancing problems. Furthermore, there would not be suddenly changing forces with a possible unphysical instability by unifying the interfacial momentum balancing relations.

6.4 STABILITY LIMIT

It has been shown that the delta pressure plays a main role in stabilizing the one-dimension two-fluid horizontal flow formulations, where overall void fraction profile is considered with its equivalent stabilizing gravity force. Basically, the gravitational delta pressure expresses the momentum balance of two-fluid flow in the gravitational direction, and increases the stable relative velocity significantly. In a mixed two-fluid flow, the two-fluid flow will decrease the stable relative velocity to the point where the dispersed fluid velocity is slightly faster than the continuous fluid one. The dispersed fluid would have enough inertial force to overcome buoyancy force along the horizontal flow channel and also has its own unique stable constant relative velocity. As the flow situations diverge from a well-mixed flow, a finite void gradient shows up and a calculable interface pressure appears, thus another newly stable relative velocity comes up. All these results are related to the variations of effective momentum in the force balancing of the two-fluid flow, affecting on the neutral stability of the flow.

The most promising way to find the above characteristic effects is a direct investigation of the delta pressure relations to the two-fluid instability. For the characteristic stability analysis, the delta pressure expression should be recast in an evolution equation set forms or equivalent values. By considering two-fluid effective gravity, the delta pressures can be theoretically expressed in terms of two-fluid volume ratios and densities. For verification purposes, experimental delta pressures are numerically illustrated in the instability analysis. These are evaluated by numerically approximating the actual measured void fraction profile, numerically adjusting their associated coefficients or parameters to perform the analysis determine under what condition the flow has stability numerically.

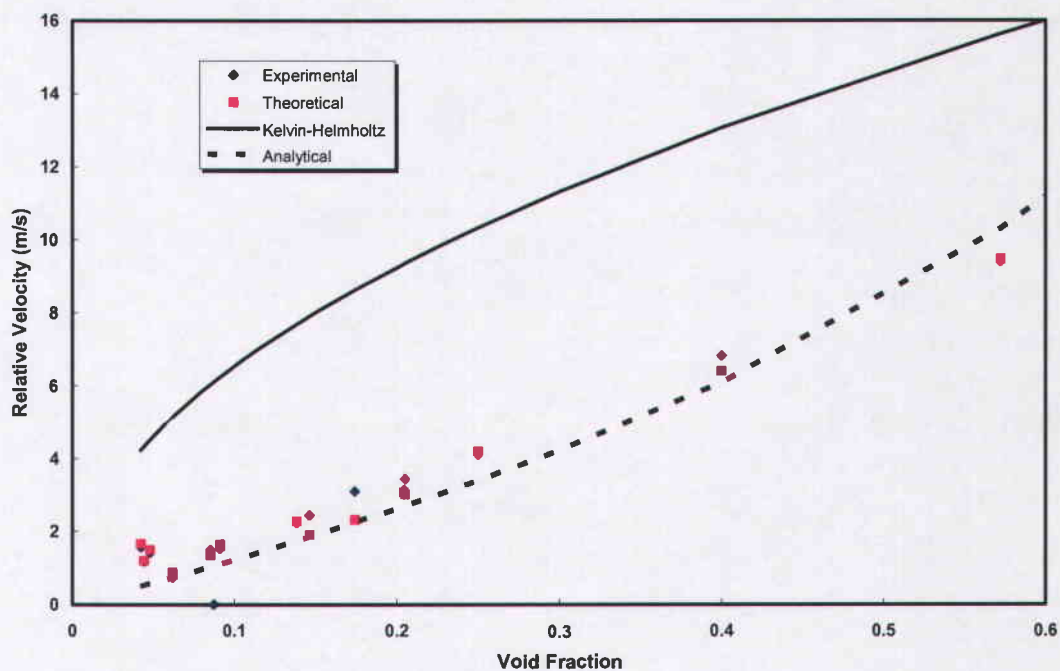


Figure 6.8: Comparison of Stability Limits (Experimental, Theoretical, Analytical, and Kelvin-Helmholtz)

As shown in Figure 6.8, the theoretical and experimental relative velocity criterion to keep the two-fluid flow hyperbolic is obtained. The theoretically achieved velocity limits are calculated with red dots and the numerically evaluated velocity limits are represent with blue dots. Both the experimental and theoretical evaluation results are well matched over all two-fluid flow regimes. The instability limit is mostly identical to the criterion of the actual relative velocity [Wu, Q. & Ishii, M., 1996].

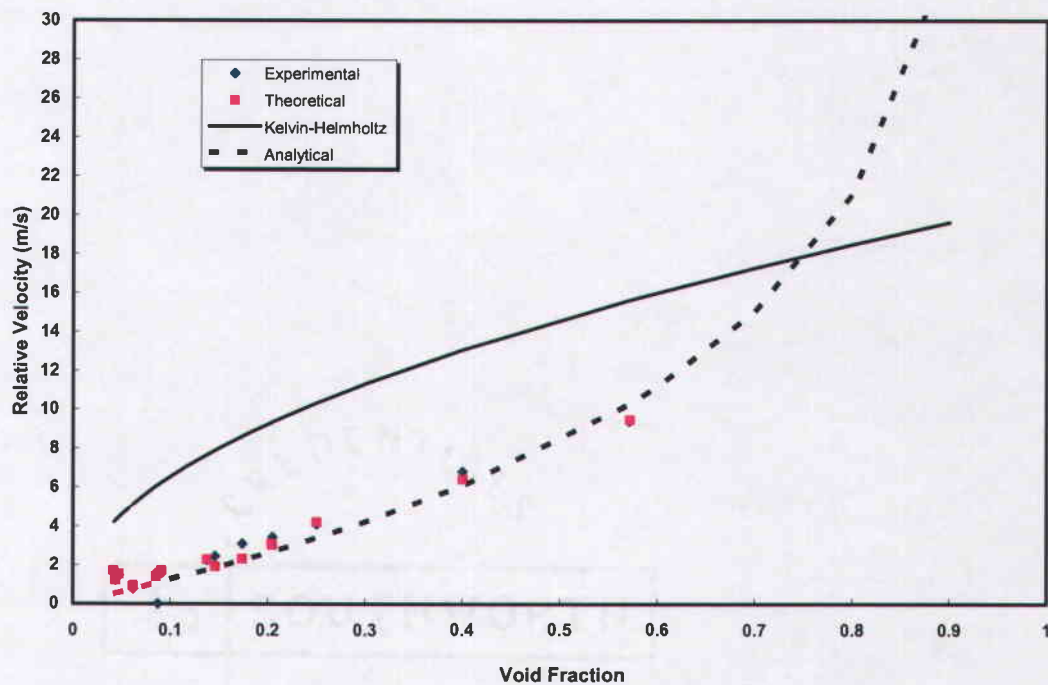


Figure 6.9: Expansion of Analytical Stability Criteria Lines

In evaluation of velocity criteria, the solid black line represents the stability line predicted by the Kelvin-Helmholtz instability limit and the dotted black line represents the analytically predicted instability limit. All these instability limits can be used as a very important reference in physical instability criteria of two-fluid flow. Some

discrepancies could be interpreted as the theoretical criterion is calculated with the linear void fraction profile approximations, thus these solutions would be asymptotically approached. All previous results show two unique consistencies that were previously expected. As shown in Figure 6.9, two-fluid flow is stabilized by gravity force over the whole ranges of void fractions, and furthermore is accounting for the unified model improving the two-fluid unphysical system stability. For a relative velocity which is lower than the above criterion, the one-dimension two-fluid horizontal flow would be stable. Physically, they do appear realistic with stabilizing gravity force, and maintaining against the possibility of instability.

7 DISCUSSION AND FUTURE WORK

Taking two general conservational single-fluid flow balance relations, adding them and averaging them over a time and space respectively, a one-dimension two-fluid horizontal flow model has been created. All of the conservational properties of two-fluid flows are balanced within the two-fluid system status in constructing the two-fluid flow, which consists of a virtual mixture layer and two single-flow layers. A physical explanation of these features is interpreted as a steady-state expansion of the mixing of steady-state two-fluid construction of two single-fluid boundaries. They arise from a force balancing of buoyancy, liquid-turbulence and its gradients, etc, thereby gravitational local void fraction profile representations. Naturally taking into account the gravitational force with the two-fluid fraction representations, a new stability-enhanced one-dimension two-fluid horizontal model can be obtained.

To find the one-dimension constitutive explicitly, a linear void fraction model is used. With the theoretical development of two-fluid integral parameters, an important unique value formula, applicable to any two-fluid flow regime, is deduced. While keeping the formula in derivation of the integral parameter, the encountered void fraction integral parameters are linearly combined in order to create a unified model. The major advantages of this model are, first of all, it can explicitly unify any distributed multiple interface flow including any single interface flow and, second it has reasonably simple formulation. They make the unified theoretical correlation of the interfacial force of two-fluid horizontal flow possible. Thus the unified correlation can apply to any two-fluid flow types, allowing a transition of flow types or transition back if required. The proposed unified model further enhances a hyperbolic nature by fixing the unphysical instability problems of two-fluid.

After the development of the one-dimensional model, the model's stability is tested. The stability of the new one-dimension model is tested by a characteristic system analysis method. By comparing these results with the measurement results, the proposed model has good agreement with experimental data and the correlation works

for a wide range of horizontal flow conditions, even within the evaluations of interfacial forces based upon a linear void fraction. In order to keep the derivations reasonably simple, the two interface layer boundaries are assumed to have slower enough variation that any dispersion terms could be neglected. For the same reason, the interfacial shear stress is assumed to be small enough so that drag force is negligible. This would avoid the potentially nonlinear variations of the variables across the interfaces, and the property variations simply follow a gravity long wave variation. The success of the simple linear model may be explained by the fact that the turbulent dispersion and drag force forces were negligible, thus leaving us only with a two relative strong forces, turbulence and gravity.

There is future work that can archive more stability enhanced one-dimension two-fluid horizontal flow model developments and verifications. A phenomenological void fraction relationship of two-fluid interface mixing has been proposed as a unified interface force balancing model, with the developments of a mixture layer concept. As seen in flow compatible linear void fraction profile modeling procedures, further work is required to find void distribution mechanisms as well as two-fluid interfacial area transport mechanisms, the mechanisms of the generation, deformation, and propagation of void waves and two-fluid surface waves. From these wave distribution mechanisms, vertical profiles and their variations could be evaluated, correlated, and projected into the one-dimension forms. The void distribution mechanisms would need to include turbulence shear stress and its gradient, even if it has been introduced in the mixing layer void distribution equation in a previous section. Additionally, there is need to conduct work that is related to interfacial area, its transports, and its implementation of different two-fluid flow structures. More theoretical and experimental work is needed to verify these relationships, including the other interfacial area transport relationships between transverse interfacial area concentrations and corresponding interfacial pressures.

It is also required to take care of these applications for other two-fluid flow geometries like a tilted two-fluid flow and to create an analytical solution or an exact

formulation. There is need for a more detailed theoretical interfacial pressure relationship for determining exact interfacial terms of two-fluid flow. Especially when a two-fluid flow has similar densities or a small change of void fraction distribution, more exact correlation evaluation becomes more important. All these additional tasks works are required to develop these closure relationships. Results for a more smoothly varying structure over a wide range of flow conditions would significantly improve the modeling of fully mixed flow. The creation of a good model can eliminate subjectively the instability that could be associated with numerical calculation near a transition point. All these results will need to be incorporated in the one-dimension two-fluid difference equations and these efforts could eliminate the non-hyperbolic nature of the previous one-dimension two-fluid single-pressure model.

8 CONCLUSIONS

With the previous work, two-fluid flow models have been considered as the superposition of two single-fluid flows separated by interfaces. In one-dimension two-fluid horizontal flow, a more advanced mode has been considered in a long time since the previous one-dimension two-fluid single-pressure models have instability problems. The main cause of the unphysical instability is due to a failure to express an interface force and to model its interfacial transfer distribution in dealing with the two-fluid flow. This would be a governing force of two-fluid flow surface stability. As the indication of a system instability analysis, the interfacial factors play a main dominant role in void fraction growth.

By starting from the view point that the instability comes from the oversimplified void fraction profile results of the previous model, a proper consideration of local void fraction profiles can allow a unified model to overcome the instability. Considering one-dimension modeling, the main focus is on the relation of the actual void fraction profile to gravity. This natural approach allows combinational relationships between the void fraction profiles with the average pressure variation in the vertical direction in a horizontal two-fluid channel flow. Physically, the system of two-fluid flow consists of two regions with a large number of boundaries or a single interface. In order to determine the value of the pressure and the interfacial pressure, changing the two-fluid horizontal flow to three virtual zones, two single-fluid flow zones and a mixed-fluid flow zone, is needed. Determining effective forces of these zones is important in closing the total momentum balance and creating a unified one-dimension two-fluid model with flow regime transitions. An analytical expression of the interfacial factor is derived as a function of average void fraction, two-fluid densities, and peak void fraction by considering gravity and a linear two-fluid distribution profiles. By incorporating the physically reasonable approaches, the unified one-dimension two-fluid model has two distinct interfacial forces. On these bases, this pressure model has very desirable physical properties and reasonably well

describable stability velocity criteria. In extending previous convectional one-dimension two-fluid horizontal flow equations, the characteristic test is performed to the determinate if physical stability has been achieved.

This research has demonstrated that a stability-enhanced one-dimension two-fluid flow equation can be derived with the mixture layer concepts. These equations describe the mean two-fluid flow behaviors in the time-averaged mixture layer. The mixture layer concepts can be used in unifying a one-dimension two-fluid horizontal flow formulation, even if there are sufficiently thin interface thicknesses dependent on the two-fluid flow types. The proposed unified one-dimension two-fluid horizontal flow formulation is introduced with virtual thick mixture layer concepts to produce the static interfacial pressure. The results are shown to be much better than that of the Kelvin-Helmholtz instability criterion. The unified two-fluid model has significantly improved the stability, achieving physical stability and contributing to remove unphysical instability. Removing instability problems will improve the numerical stability of thermal-hydraulic codes because the computer codes will no longer need the more subjective flow regime maps or flow regime dependence correlations. Eliminating the unphysical oscillations that can occur near flow regime transition boundaries and a smooth transiting from one flow regime type can be possible. All of these properties indicate that the proposed model would be one of the promising one-dimension two-fluid horizontal flow models. With the unified two-fluid model, it can also naturally overcome the unphysical stability of a one-dimension two-fluid horizontal flow.

BIBLIOGRAPHY

1. Abel, Kent C., "Stability Improvement of the One-Dimensional Two-Fluid Model for Horizontal Two-Phase Flow with Model Unification," OSU Ph.D Thesis, 2005
2. Ardron K.H., "One-Dimensional Two-Fluid Equations for Horizontal Stratified Two-Phase Flow," *Int. J. Multiphase Flow*, vol. 6, pp. 295-304, 1980.
3. Ansari, M.R., "Effect of Pressure on Two-Phase Stratified Flow Modeling," *Journal of Nuclear Science and Technology*, Vol. 41, No. 7, pp. 709-714, 2004.
4. Beattie, D.R.H., "Flow Characteristics of Horizontal Bubbly Pipe Flow", *Nuclear Engineering and Design*, Vol. 163, pp. 207-212, 1996.
5. Benjamin, T.B., "Gravity Currents and related phenomena," *Journal of Fluid Mechanics*, vol. 31, Part 2, pp. 209-248, 1968.
6. Biesheuvel, A. and Wijngaarden, L. Van, "Two-Phase Flow Equations for a Dilute Dispersion of Gas Bubbles in Liquid," *Journal of Fluid Mechanics*, vol. 148, pp. 301-318, 1984.
7. Bostjan Koncar, Ivo Kljenak, Borut Mavko, "Modelling of Local Two-Phase Flow Parameters in Upward Subcooled Flow Boiling at Low Pressure, " *Int. J. Multiphase Flow*, Vol. 47, pp. 1499-1513, 2004.
8. Brackbill, J.U., Kothe, D.B., Zemach, C.A. "A continuum method for modeling surface tension," *J. Comput. Phys.* Vol. 100, pp. 335-354, 1992.

9. Carruthers D. J., Hunt, J. C. R., "Turbulence and Wave Motions Near an Interface Between a Turbulent Region and a Stably Stratified Layers", *Turbulence and Diffusion in Stable Environments*, Oxford, pp. 29-60, 1985.
10. Buckingham, M. J., "Sound Speed and Void Fraction Profiles in the sea Surface Bubble layer," *Applied Acoustics*. Vol. 51, No. 3, pp. 225-250, 1997.
11. Chang, P.C. and Plate E.J., Hidy G.M., "Turbulent air flow over the Dominant Component of Wind-Generated Water Waves," *Journal of Fluid Mechanics*, vol. 47, pp. 183-208, 1971.
12. Chen, I.Y., Downing, R.S., Parish, R., Keshock, E., "A Reduced Gravity Flight Experiment: Observed Flow Regimes and Pressure Drops of Vapor and Liquid Flow in Adiabatic Piping," *AIChE Symposium Series*, Vol. 84, pp. 203-216, 1988.
13. Chen, Y.M., Fan, L.S., "Drift Flux in Gas-Liquid-Solid Fluidized Systems from the Dynamics of Bed Collapse," *Chemical Engineering Science*, Vol. 45, No. 4, pp. 935-945, 1990.
14. Chung, M.S., Lee, S.J., Lee, W.J., Chang, K.S., "An Interfacial Pressure Jump Model for Two-Phase Bubbly Flow," *Numerical Heat Transfer, Part B*, Vol. 40, pp. 83-97, 2001.
15. Chung, M.S., Pak, S.K., Chang, K.S., "A Numerical Study of Two-Phase Flow using a Two-Dimensional Two-Fluid Model," *Numerical Heat Transfer, Part A*, Vol. 45, pp. 1049-1066, 2004.
16. Delhaye, J.M., "Jump Conditions and Entropy Sources in Two-Phase Systems: Local Instant Formulation," *Int. J. Multiphase Flow*, Vol. 1, pp. 395-409, 1974.

17. Drew, D.A., "Average field Equations for two-phase media," *Studies in Applied Mathematics*, Vol. L, N0. 2. MIT, Cambridge, Ma. 1971.
18. Drew, D.A., "Mathematical modeling of two-phase flow," *Annu. Rev. Fluid Mech.* 15, pp.261-291, 1983.
19. D.A. Drew, S.L. Passman, "Theory of Multicomponent Fluids," *Applied Mathematical Sciences* 135, Springer, New York, 1999.
20. Egely, G., Saha, P., "A Study of Momentum Transfer in Two-Fluid Formulation of Two-Phase Flow," *Multi-Phase Flow and Heat Transfer* 3, Proceedings of the 3rd Symposium-Workshop, Part A: Fundamentals, pp. 79-101, 1984.
21. Franca, F., Lahey, R.T. Jr., "The Use of Drift-Flux Techniques for the Analysis of Horizontal Two-Phase Flows," *Int. J. Multiphase Flow*, Vol. 18, No. 6, pp. 787-801, 1992.
22. Fukano, T., Ousaka, A., "Prediction of the Circumferential Distribution of Film Thickness in Horizontal and Near-Horizontal Gas-Liquid Annular Flows," *Int. J. Multiphase Flow*, Vol. 15, No. 3, pp. 403-419, 1989.
23. Gardner, G.C. "Onset of Slugging in Horizontal Ducts," *Int. J. Multiphase Flow*, Vol. 5, pp. 201-209, 1979.
24. Ghiaasiaan, S.M., Kamboj, B.K., Addel-Khalik, S.I., "Two-Fluid Modeling of Condensation in the Presence of Noncondensables in Two-Phase Channel Flows," *Nuclear Science and Engineering*, Vol. 119, pp. 1-17, 1995.

25. Gidaspow, D., "Modeling of Two-Phase Flow," Round Table Discussion, Proceedings of the 5th International Heat Transfer Conference, VII, pp. 163-168, 1974.
26. Gidaspow, D., Rasouli, F., Shin, Y.W., "An Unequal Velocity Model for Transient Two-Phase Flow by the Method of Characteristics," Nuclear Science and Engineering, Vol. 84, pp. 179-195, 1983.
27. Hewitt, G.F., Roberts, D.N., "Studies of Two-Phase Flow Patterns by Simultaneous X-ray and Flash Photography," AERE-M2159, 1969.
28. Hibiki, T., Hogsett, S., Ishii, M., "Local Measurement of Interfacial Area, Interfacial Velocity, and Liquid Turbulence in Two-Phase Flow," Nuclear Engineering and Design, Vol. 184, pp. 287-304, 1998.
29. Hibiki, T., Ishii, M., "Experimental Study on Interfacial Area Transport in Bubbly Two-Phase Flows," Int. J. Heat Mass Transfer, Vol. 42, pp. 3019-3035, 1999.
30. Hibiki, T., Ishii, M., "Two-Group Interfacial Area Transport Equations at Bubbly-to-Slug Flow Transition," Nuclear Engineering and Design, Vol. 202, pp. 39-76, 2000.
31. Hibiki, T., Ishii, M., Zheng, X., "Axial Interfacial Area Transport of Vertical Bubbly Flows," Int. J. Heat Mass Transfer, Vol. 44, pp. 1896-1888, 2001.
32. Hibiki, T., Takamasa, T., Ishii, M., "Interfacial Area Transport of Bubbly Flow in a Small Diameter Pipe," Journal of Nuclear Science and Technology, Vol. 38, No. 8, pp. 614-620, 2001.

33. Ishii, M., "Thermally Induced Flow Instabilities in Two-Phase Mixtures in Thermal Equilibrium," Ph.D. Thesis, School of Mechanical Engineering, Georgia Institute of Technology, 1971.
34. Ishii, M., "Thermo-Fluid Dynamic Theory of Two-Phase Flow," Eyrolles, Paris, 1975.
35. Ishii, M., "Foundation of Various Two-phase Flow Models and Their Limitations," EPRIWS-81-212, pp. 3-47, 1981.
36. Ishii, M., Mishima, K., "Two-Fluid Model and Hydrodynamic Constitutive Relations," Nuclear Engineering and Design, Vol. 82, pp. 107-126, 1984.
37. Ishii, M., Hibiki, T, "Thermo-Fluid Dynamic of Two-Phase Flow," Springer, 2006.
38. Iskandrani, A., Kojasoy, G., "Local Void Fraction and Velocity Field Description in Horizontal Bubbly Flow," Nuclear Engineering and Design, Vol. 204, pp. 117-128, 2001.
39. Jepson, W.P., Taylor, R.E., "Slug Flow and its Transitions in Large-Diameter Horizontal Pipes," Int. J. Multiphase Flow, Vol. 19, No. 3, pp. 411-420, 1993.
40. Kang, H.C., Kim, M.H., "The Relation between the Interfacial Shear Stress and the Wave Motion in A Stratified Flow," Int. J. Multiphase Flow, Vol. 19, No. 1, pp. 35-49, 1993.

41. Kaminaga, F., "Assessment of Void Fraction Correlations for Vertical Two-Phase Flow in Small Diameter Tube at Low Liquid Velocity," *Journal of Nuclear Science and Technology*, Vol. 29, pp. 695-698, 1992.
42. Kataoka, I., Ishii, M., "Drift Flux Model for Large Diameter Pipe and New Correlation for Pool Void Fraction," *Int. J. Heat Mass Transfer*, Vol. 30, pp. 1927-1939, 1987.
43. Kataoka, Y., Suzuki, H., Murase, M., "Drift-Flux Parameters for Upward Gas Flow in Stagnant Liquid," *Journal of Nuclear Science and Technology*, Vol. 24, pp. 580-586, 1987.
44. Khan, H.J., Ye, W., Pertmer, G.A., "Numerical Calculation of Gas-Liquid Transient Flow in Channels and Bends," *American Society of Mechanical Engineers, Fluids Engineering Division (Publication) FED*, Vol. 144, *Multiphase Flow in Wells and Pipelines*, pp. 113-123, 1992.
45. Kim, S., Fu, X.Y., Wang X., Ishii, M., "Study on Interfacial Structures in Slug Flows Using a Miniaturized Four-Sensor Conductivity Probe," *Nuclear Engineering and Design*, Vol. 204, pp. 45-55, 2001.
46. Kocamustafaogullari, G., "Thermo-Fluid Dynamics of Separated Two-Phase Flow," Ph.D. Thesis, School of Mechanical Engineering, Georgia Institute of Technology, 1971.
47. Kocamustafaogullari, G., "Two-Fluid Modeling in Analyzing the Interfacial Stability of Liquid Film Flows," *Int. J. Multiphase Flow*, Vol. 11, pp. 63-89, 1985.

48. Kocamustafaogullari, G., Huang, W.D., "Internal Structure and Interfacial Velocity Development for Bubbly Two-Phase Flow," Nuclear Engineering and Design, Vol. 151, pp. 79-101, 1994.
49. Kocamustafaogullari, G., Huang, W.D., Razi, J., "Measurement and Modeling of Average Void Fraction, Bubble Size and Interfacial Area," Nuclear Engineering and Design, Vol. 148, pp. 437-453, 1994.
50. Kocamustafaogullari, G., Wang, Z., "An Experimental Study on Local Interfacial Parameters in a Horizontal Bubbly Two-Phase Flow," Int. J. Multiphase Flow, Vol. 17, No. 5, pp. 553-572, 1991.
51. Kynch G. J., "A theory of sedimentation," Trans. Faraday Soc., Vol. 48, pp. 166-176, 1952.
52. Lafi, A.Y. and Reyes, J.N. Jr., "Phenomenological Models for Fluid Particles Coalescence and Breakage," Technical Report, OSU-NE-9120, Department of Nuclear Engineering, Oregon State University, Corvallis, Oregon, 1991.
53. Lahey, R.T. Jr., "Void Wave Propagation Phenomena in Two-Phase Flow," AIChE J., Vol. 37, No. 1, pp. 123-135, 1991.
54. Lahey, R.T. Jr., Lopez de Bertodano, M., Jones, Jr., "Phase Distribution in Complex Geometry Conduits," Nuclear Engineering and Design, Vol. 141, pp. 177-201, 1993.
55. Lamb, H., "Hydrodynamics," 6th edition, Cambridge University Press, 1932.

56. Lee, S.J., Chang K.S. Kim, S.J., "Surface Tension Effect in Two-fluids Equation System," *Int. J. Heat Mass Transfer*, Vol. 41, pp. 2821-2816, 1998.
57. Leung, W.H., Revankar, S.T., Ishii, Y., Ishii, M., "Axial Development of Interfacial Area and Void Concentration Profiles Measured by Double-Sensor Probe Method," *Int. J. Heat Mass Transfer*, Vol. 38, pp. 445-453, 1995.
58. Lewis, S., Fu, W.L., Kojasoy, G., "Internal Flow Structure Description of Slug Flow-Pattern in a Horizontal Pipe," *Int. J. Heat Mass Transfer*, Vol. 45, pp. 3897-3910, 2002.
59. Lopez de Bertodano, M., Lee, S-J., Lahey, R.T. Jr., Drew, D.A., "The Prediction of Two-Phase Turbulence and Phase Distribution Phenomena Using a Reynolds Stress Model," *J. of Fluids Engineering*, Vol. 112, pp. 107-113, 1990.
60. Lopez de Bertodano, M., Lahey, R.T. Jr., Jones, O.C., "Phase Distribution in Bubbly Two-Phase Flow in Vertical Ducts," *Int. J. Multiphase Flow*, Vol. 20, No. 5, pp. 805-818, 1994.
61. Lopez de Bertodano, M., Moraga, F.J., Drew, D.A., Lahey, R.T. Jr., "The Modeling of Lift and Dispersion Forces in Two-Fluid Model Simulations of a Bubbly Jet," *J. of Fluids Engineering*, Vol. 126, pp. 573-577, 2004.
62. Long R.R. "Solitary Waves in One- and Two-fluid System," *Tellus*. Vol. 8, pp. 460-472, 1956.
63. Lyczkowski, R.W., Gidaspow, D., Solbrig, C.W., Hughes, E.D., "Characteristics and Stability Analyses of Transient One-Dimensional Two-Phase Flow Equations

- and their Finite Difference Approximations," Nuclear Science and Engineering, Vol. 66, pp. 378-396, 1978.
64. Mandhane, J.M., Gregory, G.A., Aziz, K., "A Flow Pattern Map for Gas-Liquid Flow in Horizontal Pipes," Int. J. Multiphase Flow, Vol. 1, No. 4, pp. 537-553, 1974.
65. Miles J.W, "On the Generation of Surface Waves by Shear Flows," Journal of Fluid Mechanics, vol. 6, pp. 583-592, 1959.
66. Mishima, K., Ishii, M., "Theoretical Prediction of Onset of Horizontal Slug Flow," Journal of Fluids Engineering, Transactions of the ASME, Vol. 102, pp. 441-445, 1980.
67. Morel, C., Goreaud, N., Delhaye, J.M., "The Local Volumetric Interfacial Area Transport Equation: Derivation and Physical Significance," Int. J. Multiphase Flow, Vol. 25, pp. 1099-1128, 1999.
68. Morriss, S.L., Hill, A.D., "Ultrasonic Imaging and Velocimetry in Two-Phase Pipe Flow," Journal of Energy Resources Technology, Transactions of the ASME, Vol. 115, No. 2, pp. 108-116, 1993.
69. Murata, S., Minato, A., Yokomizo, O., "Development of Three-Dimensional Analysis Code for Two-Phase Flow Using Two-Fluid Model," J. Nuclear Science and Technology, Vol. 28, pp. 1029-1040, 1991.
70. Miya, M., Woomansee D.E. Hanratty, T., "A Model for Roll Waves in Gas-Liquid Flow," Chem. Engr. Science, Vol. 26, pp. 1915-11931, 1971

71. Park, J.W., Drew, D.A., Lahey, R.T. Jr., "Void Wave Dispersion in Bubbly Flows," *Nuclear Engineering and Design*, Vol. 121, pp. 1-10, 1990.
72. Pauchon C., Banerjee, S., "Interphase Momentum Interaction Effects in the Averaged Multifield Model, Part 1: Void Fraction Propagation in Bubbly Flows," *Int. J. Multiphase Flow*, Vol. 12, No. 4, pp. 559-573, 1986.
73. Pauchon C., Banerjee, S., "Interphase Momentum Interaction Effects in the Averaged Multifield Model, Part 2: Kinematic Waves and Interfacial Drag in Bubbly Flows," *Int. J. Multiphase Flow*, Vol. 14, No. 3, pp. 253-264, 1988.
74. Picart, A. Berlemont, A., Gouesbet, G., "Modeling and Predictions Turbulence Fields and the Dispersion of Discrete Particles Transports By Turbulent Flows," *Int. J. Multiphase Flow*, Vol. 12, No. 2, pp. 237-261, 1985.
75. Prandtl, L., Tietjens, O.G, "Applied Hydro- and Aeromechanice," New York, McGraw-Hill 1934.
76. Rousseau J.C. and Ferch R.L., "A Note on Two-Phase Separated Flow Models," *Int. J. Multiphase Flow*, vol. 5, pp. 489-493, 1979.
77. Ramshaw, J.D. and Trapp, J.A., "Characteristics, Stability, and Short-Wave Length Phenomena in Two-Phase Flow Equation Systems", *Nuclear Science and Engineering*, vol. 66, pp. 93-102, 1978.
78. Ransom, V.H., Hicks, D.L., "Hyperbolic Two-Pressure Models for Two-Phase Flow," *Journal of Computational Physics*, Vol. 53, pp. 124-151, 1984.

79. Ransom, V.H., Hicks, D.L., "Hyperbolic Two-Pressure Models for Two-Phase Flow Revisited," *Journal of Computational Physics*, Vol. 75, pp. 498-504, 1988.
80. Reinecke, N., Petritsch, G., Boddem, M., Mewes, D., "Tomographic Imaging of the Phase Distribution in Two-Phase Slug Flow," *Int. J. Multiphase Flow*, Vol. 24, No. 4, pp. 617-634, 1998.
81. Revankar, S.T., Ishii, M., "Local Interfacial Area Measurement in Bubbly Flow," *Int. J. Heat Mass Transfer*, Vol. 35, pp. 913-925, 1992.
82. Revankar, S.T., Ishii, M., "Theory and Measurement of Local Area Using a Four Sensor Probe in Two-Phase Flow," *Int. J. Heat Mass Transfer*, Vol. 36, pp. 2997-3007, 1993.
83. Riznic, J.R., Lewis, S.P., Kojasoy, G., "Experimental Studies of Interfacial Area in Horizontal Slug Flow," *American Society of Mechanical Engineers, Heat Transfer Division, (Publication) HTD*, Vol. 334, No. 3, Proceedings of the ASME Heat Transfer Division, pp. 27-37, 1996.
84. Sadatomi, M., Kawaji, M., Lorencez, C.M., Chang, T., "Prediction of Liquid Level Distribution in Horizontal Gas-Liquid Stratified Flows with Interfacial Level Gradient," *Int. J. Multiphase Flow*, Vol. 19, No. 6, pp. 987-997, 1993.
85. Serrin, J., "Mathematical principles of classical fluid mechanics," *Encyclopedia of Physics*, Vol. 3, Springer, 1959.
86. Shi, J., Kocamustafaogullari, G., "Interfacial Measurements in Horizontal Stratified Flow Patterns," *Nuclear Engineering and Design*, Vol. 149, pp. 81-96, 1994.

87. Song, J.H., Ishii, M., "The Well-Posedness of Incompressible One-Dimensional Two-Fluid Model," *Int. J. Heat Mass Transfer*, Vol. 43, pp. 2221-2231, 2000.
88. Song, J.H., Ishii, M., "On the Stability of a One-Dimensional Two-Fluid Model," *Nuclear Engineering and Design*, Vol. 204, pp. 101-115, 2001.
89. Song, J.H., "A Linear Stability Analysis for an Improved One-Dimensional Two-Fluid Model," *Journal of Fluids Engineering, Transactions of the ASME*, Vol. 125, No. 2, pp. 387-389, 2003.
90. Steinbach, I., Pezzolla, F., "A Generalized Field Method for Multiphase Transformations Using Interface Fields," *Physica D*, vol. 134, pp. 385-393, 1999.
91. Stewart, H.B. "Stability of Two-Phase Flow Calculation using Two-Fluid Models," *Journal of Computational Physics*, vol. 33, pp. 259-270, 1979.
92. Taitel, Y., Dukler, A.E., "A Model for Predicting Flow Regimes Transition in Horizontal and Near Horizontal Gas-Liquid Flow," *AIChE J.*, Vol. 22, pp. 47-55, 1976.
93. Taitel, Y., Dukler, A.E., "A Model for Slug Frequency During Gas-Liquid Flow in Horizontal and Near Horizontal Pipes," *Int. J. Multiphase Flow*, Vol. 3, pp. 585-596, 1977.
94. Taitel, Y., Dukler, A.E., "A Theoretical Approach to the Lockhart-Martinelli Correlation for Stratified flow," *Int. J. Multiphase Flow*, Vol. 2, pp. 591-595, 1976.

95. Tam, K., W., "The Drag on a cloud of spherical particles on low Reynolds number Flow," *J. Fluid Mech.* Vol. 38, pp. 537-546, 1969.
96. Travis J.R. Harlow, F.H. Amsden, A.A, "Numerical Calculation of Two-Phase Flows," *Nuclear Science and Engineering*, vol. 61, pp. 1-10, 1976.
97. Trapp, J.A., "The Mean Flow Character of Two-Phase Flow Equations," *Int. J. Multiphase Flow*, Vol. 12, No. 2, pp. 263-276, 1986.
98. Ulke, A., "Study of a Two-Component, Two-Phase Flow System in One Dimension," *Multi-Phase Flow and Heat Transfer 3*, Proceedings of the 3rd Symposium-Workshop, Part A: Fundamentals, pp. 59-77, 1984.
99. Wallis, G.B., Dobson, J.E., "The Onset of Slugging in Horizontal Stratified Air-Water Flow," *Int. J. Multiphase Flow*, Vol. 1, pp.173-193, 1973.
100. Wallis, G.B "One-dimensional Two-phase Flow," McGraw-Hill Book Company, pp.3-16, 1969.
101. Wu, Q., Ishii, M., "Interfacial Wave Stability of Concurrent Two-Phase Flow in a Horizontal Channel," *Int. J. Heat Mass Transfer*, Vol. 39, No. 10, pp.2067-2075, 1996.
102. Wu, Q., Ishii, M., "Sensitivity Study on Double-Sensor Conductivity Probe for the Measurement of Interfacial Area Concentration in Bubbly Flow," *Int. J. Multiphase Flow*, Vol. 25, pp.153-173, 1999.
103. Zuber, N., Findley, J.A., "Average Volumetric Concentration in Two-Phase Flow Systems," *J. Heat Transfer*, pp. 453-468, Nov., 1965.

NOMENCLATURE

A	flow area
a_i	interfacial area concentration
C_o	distribution parameter
C_{vk}	momentum covariance term
d_{sm}	Sauter mean diameter
g	gravity acceleration constant
H	flow channel height
j	superficial velocity
k	wave number
L_s	length scale at interface
\dot{m}	mass flow rate
n	surface normal vector
p	pressure
Q	volumetric flow rate
\dot{q}	heat flux
t	time
u, v	velocity
V_{gj}	drift velocity of the jth interface
x	vapor quality
x, y, z	spatial coordinates

Greek Symbols

α	void fraction
Δ	difference between two terms
Γ	mass generation rate per unit volume
ρ	density
θ	void distribution parameter
τ	shear stress

ω	angular frequency
φ	angle from vertical, rates of change of the bubble number density
Φ	dissipation, rates of change of the interfacial area concentration
ξ	wetted perimeter
ψ	bubble shape factor

Subscripts

d, c, i	dispersed fluid , continuous fluid , interface
m, n	index
r	relative
t	unit time
x, y, z	spatial coordinates
0	reference

Mathematical operators

$\langle \rangle$	area averaged quantity
$\langle\langle \rangle\rangle$	void fraction weighted area averaged quantity
$\langle\langle \rangle\rangle_{\partial\Omega}$	void fraction gradient weighted area averaged quantity

APPENDICES

WEDNESDAY
MAY 19 1900
SOUTH WORTH
COLLECTOR
S. ALLEN FISHER

APPENDIX A: VOID FRACTION EQUATION

To derive a basic void fraction equation, a time-averaged indication function, a limit form of Leibnitz rule and Gauss theorem [Ishii, 1975; Delhay 1981] can be used:

- Leibnitz Rule:

$$\int_{T_k} \frac{\partial f_k}{\partial t} dt = \frac{\partial}{\partial t} \int_{T_k} f_k dt - \sum_{T_k} \frac{\mathbf{u}_i \cdot \mathbf{n}_k}{|\mathbf{u}_i \cdot \mathbf{n}_k|} f_k \quad (\text{A.1})$$

- Gauss Theorem:

$$\int_{T_k} \nabla \cdot f_k dt = \nabla \cdot \int_{T_k} f_k dt + \sum_{T_k} \frac{\mathbf{n}_k}{|\mathbf{u}_i \cdot \mathbf{n}_k|} f_k \quad (\text{A.2})$$

T_k : Occupational time of k-fluid

\mathbf{n}_k : Normal vector of k-fluid

\mathbf{u}_i : Local instantaneous interface surface velocity.

- First Term :

$$\begin{aligned} \int_{T_k} \frac{\partial M_k}{\partial t} dt &= \frac{\partial}{\partial t} \int_{T_k} M_k dt - \sum_{T_k} \frac{\mathbf{u}_i \cdot \mathbf{n}_k}{|\mathbf{u}_i \cdot \mathbf{n}_k|} M_k \\ \frac{\partial}{\partial t} \left(\frac{T_k}{T_t} \right) &= \frac{1}{T_t} \sum_{T_k} \frac{\mathbf{u}_i \cdot \mathbf{n}_k}{|\mathbf{u}_i \cdot \mathbf{n}_k|} \\ \frac{\partial}{\partial t} \alpha_k &= \frac{1}{T_t} \sum_{T_k} \frac{\mathbf{u}_i \cdot \mathbf{n}_k}{|\mathbf{u}_i \cdot \mathbf{n}_k|} \end{aligned} \quad (\text{A.3})$$

- Second Term:

$$\int_{T_k} \nabla \cdot \mathbf{M}_k dt = \nabla \cdot \int_{T_k} \mathbf{M}_k dt + \sum_{T_k} \frac{\mathbf{n}_k}{|\mathbf{u}_i \cdot \mathbf{n}_k|} M_k$$

$$\nabla \cdot \left(\frac{T_k}{T_i} \right) = -\frac{1}{T_i} \sum_{T_k} \frac{\mathbf{n}_k}{|\mathbf{u}_i \cdot \mathbf{n}_k|} \quad (\text{A.4})$$

$$\nabla \cdot \alpha_k = -\frac{1}{T_i} \sum_{T_k} \frac{\mathbf{n}_k}{|\mathbf{u}_i \cdot \mathbf{n}_k|}$$

Combining the first terms and the second terms:

$$\frac{\partial \alpha_k}{\partial t} + \mathbf{u}_i \cdot \nabla \alpha_k = 0 \quad (\text{A.5})$$

APPENDIX B: TWO-FLUID CONSERVATION EQUATIONS

Applying the limit form of Leibnitz rule and Gauss theorem [Appendix A]:

- First Term :

$$\begin{aligned}
 \frac{1}{T_t} \int_{T_i} \frac{\partial \rho_k \psi_k M_k}{\partial t} dt &= \frac{1}{T_t} \int_{T_k} \frac{\partial \rho_k \psi_k}{\partial t} dt \\
 &= \frac{\partial}{\partial t} \left(\frac{1}{T_t} \int_{T_k} \rho_k \psi_k dt \right) - \frac{1}{T_t} \sum_{T_i} \frac{\mathbf{u}_i \cdot \mathbf{n}_k}{|\mathbf{u}_i \cdot \mathbf{n}_k|} \rho_k \psi_k \\
 &= \frac{\partial}{\partial t} \left(\frac{1}{T_t} \frac{T_k}{T_k} \int_{T_k} \rho_k \psi_k dt \right) - \frac{1}{T_t} \sum_{T_i} \frac{\mathbf{u}_i \cdot \mathbf{n}_k}{|\mathbf{u}_i \cdot \mathbf{n}_k|} \rho_k \psi_k \\
 &= \frac{\partial}{\partial t} \left(\frac{\alpha_k}{T_k} \int_{T_k} \rho_k \psi_k dt \right) - \frac{1}{T_t} \sum_{T_i} \frac{\mathbf{n}_k \cdot \mathbf{u}_i}{|\mathbf{n}_k \cdot \mathbf{u}_i|} \rho_k \psi_k
 \end{aligned} \tag{B.1}$$

- Second Term:

$$\begin{aligned}
 \frac{1}{T_t} \int_{T_i} \nabla \cdot (\rho_k \psi_k \mathbf{u}_k M_k + \mathbf{J}_k M_k) dt \\
 &= \frac{1}{T_t} \int_{T_k} \nabla \cdot (\rho_k \psi_k \mathbf{u}_k + \mathbf{J}_k) dt \\
 &= \nabla \cdot \left(\frac{1}{T_t} \int_{T_k} (\rho_k \psi_k \mathbf{u}_k + \mathbf{J}_k) dt \right) + \sum_{T_i} \frac{\mathbf{n}_k \cdot (\rho_k \psi_k \mathbf{u}_k + \mathbf{J}_k)}{T_k |\mathbf{n}_k \cdot \mathbf{u}_i|} \\
 &= \nabla \cdot \left(\frac{T_k}{T_t} \frac{1}{T_k} \int_{T_k} (\rho_k \psi_k \mathbf{u}_k + \mathbf{J}_k) dt \right) + \sum_{T_i} \frac{\mathbf{n}_k \cdot (\rho_k \psi_k \mathbf{u}_k + \mathbf{J}_k)}{T_k |\mathbf{n}_k \cdot \mathbf{u}_i|} \\
 &= \nabla \cdot \left(\frac{\alpha_k}{T_k} \int_{T_k} (\rho_k \psi_k \mathbf{u}_k + \mathbf{J}_k) dt \right) + \sum_{T_i} \frac{\mathbf{n}_k \cdot (\rho_k \psi_k \mathbf{u}_k + \mathbf{J}_k)}{T_k |\mathbf{n}_k \cdot \mathbf{u}_i|}
 \end{aligned} \tag{B.2}$$

Combining them:

$$\begin{aligned} & \frac{\partial}{\partial t} \left(\frac{\alpha_k}{T_k} \int_{T_k} \rho_k \psi_k dt \right) + \nabla \cdot \left(\frac{\alpha_k}{T_k} \int_{T_k} (\rho_k \psi_k \mathbf{u}_k + \mathbf{J}_k) dt \right) - \frac{\alpha_k}{T_k} \int_{T_k} s_k dt \\ & = \frac{1}{T_t} \sum_{T_i} \frac{\mathbf{n}_k \cdot \mathbf{u}_i}{|\mathbf{n}_k \cdot \mathbf{u}_i|} \rho_k \psi_k - \sum_{T_i} \frac{\mathbf{n}_k \cdot (\rho_k \psi_k \mathbf{u}_k + \mathbf{J}_k)}{T_k |\mathbf{n}_k \cdot \mathbf{u}_i|} \end{aligned} \quad (\text{B.3})$$

With a time-averaged quantity definitions;

$$\begin{aligned} \frac{1}{T_k} \int_{T_k} \rho_k \psi_k dt & \equiv \overline{\rho_k \psi_k}^T \\ \frac{1}{T_k} \int_{T_k} \rho_k \psi_k \mathbf{u}_k dt & \equiv \overline{\rho_k \psi_k \mathbf{u}_k}^T \\ \frac{1}{T_k} \int_{T_k} \mathbf{J}_k dt & \equiv \overline{\mathbf{J}_k}^T \\ \frac{1}{T_k} \int_{T_k} s_k dt & \equiv \overline{s_k}^T \\ \rho_k (\mathbf{u}_k - \mathbf{u}_i) \cdot \mathbf{n}_k & \equiv \dot{m}_k \end{aligned} \quad (\text{B.4})$$

The time-averaged general conservation equation can be reduced to:

$$\begin{aligned} & \frac{\partial}{\partial t} (\alpha_k \overline{\rho_k \psi_k}^T) + \nabla \cdot (\alpha_k \overline{\rho_k \psi_k \mathbf{u}_k}^T + \alpha_k \overline{\mathbf{J}_k}^T) - \alpha_k \overline{s_k}^T \\ & = \frac{1}{T_t} \sum_{T_i} \frac{-1}{|\mathbf{n}_k \cdot \mathbf{u}_i|} (\dot{m}_k \psi_k + \mathbf{n}_k \cdot \mathbf{J}_k) \end{aligned} \quad (\text{B.5})$$

APPENDIX C: ONE-D TWO-FLUID CONSERVATION EQUATIONS

C.1: Mass Conservation Equation

With the definition of the conservation quantity, flux, and source terms;

$$\begin{aligned}\Psi_k &= 1 \\ J_k &= 0 \\ S_k &= 0\end{aligned}\tag{C.1}$$

the integral form of mass conservation equation becomes:

$$\frac{1}{A} \int_A \frac{\partial \alpha_k \rho_k}{\partial t} dA + \frac{1}{A} \int_A \nabla \cdot \alpha_k \rho_k \mathbf{u}_{xk} dA = - \frac{1}{A} \int_A \frac{1}{T_t} \sum_{T_k} \frac{\dot{m}}{|\mathbf{n}_k \cdot \mathbf{u}_i|} dA\tag{C.2}$$

By applying Leibnitz rule and Gauss theorem, the first and second term of the conservation equation can be rewritten;

- First Term :

$$\frac{1}{A} \int_A \frac{\partial \rho_k \alpha_k}{\partial t} dA = \frac{\partial}{\partial t} \frac{1}{A} \int_A \alpha_k \rho_k dA - \frac{1}{A} \int_{C_i} \alpha_k \rho_k (\mathbf{u}_i \cdot \mathbf{n}_x) dC\tag{C.3}$$

- Second Term:

$$\frac{1}{A} \int_A \nabla \cdot \rho_k \mathbf{u}_{xk} \alpha_k dA = \frac{\partial}{\partial x} \left(\frac{1}{A} \int_A \rho_k \mathbf{u}_{xk} \alpha_k dA \right) + \frac{1}{A} \int_{C_i} \mathbf{n}_k \cdot \rho_k \mathbf{u}_{xi} \alpha_k dC\tag{C.4}$$

By combining these two terms, a differential form of the mass conservation equation can be written:

$$\frac{\partial}{\partial t} \frac{1}{A} \int \rho_k \alpha_k dA + \frac{\partial}{\partial x} \left(\frac{1}{A} \int \rho_k \mathbf{u}_{xk} \alpha_k dA \right) = - \frac{1}{A} \int \frac{1}{T_t} \sum \frac{\dot{m}}{|\mathbf{n}_k \cdot \mathbf{u}_i|} dA \quad (\text{C.5})$$

Assuming that the density change is very small over the flow cross sectional area, the mass conservation equation can be reduced:

$$\underbrace{\frac{\partial}{\partial t} \frac{\rho_k}{A} \int \alpha_k dA}_{[1]} + \underbrace{\frac{\partial}{\partial x} \left(\frac{\rho_k}{A} \int \mathbf{u}_{xk} \alpha_k dA \right)}_{[2]} = - \underbrace{\frac{1}{A} \int \frac{1}{T_t} \sum \frac{\dot{m}}{|\mathbf{n}_k \cdot \mathbf{u}_i|} dA}_{[3]} \quad (\text{C.6})$$

Using an averaged void fraction and the void fraction weight averaged quantities, each term of the mass equation can be rewritten as follows:

$$[1] \quad \frac{\partial}{\partial t} \frac{\rho_k}{A} \int \alpha_k dA = \frac{\partial}{\partial t} \rho_k \langle \alpha_k \rangle \quad (\text{C.7})$$

$$[2] \quad \frac{\partial}{\partial x} \left(\frac{\rho_k}{A} \int \mathbf{u}_{xk} \alpha_k dA \right) = \frac{\partial}{\partial x} \left(\frac{\rho_k}{A} \int \mathbf{u}_{xk} \alpha_k dA \right) = \frac{\partial}{\partial x} \rho_k \langle \alpha_k \rangle \langle \mathbf{u}_{xk} \rangle \quad (\text{C.8})$$

$$[3] \quad - \frac{1}{A} \int \frac{1}{T_t} \sum \frac{\dot{m}}{|\mathbf{n}_k \cdot \mathbf{u}_i|} dA = \frac{1}{A} \int \Gamma_k dA = \langle \Gamma_k \rangle \quad (\text{C.9})$$

$$\Gamma_k \equiv -\frac{1}{T_t} \sum_{T_i} \frac{\dot{m}}{|\mathbf{n}_k \cdot \mathbf{u}_i|} \quad (\text{C.10})$$

Combining the first term, second term, and the area averaged source term, the one dimensional mass conservation equation reduced to:

$$\frac{\partial}{\partial t} \rho_k \langle \alpha_k \rangle + \frac{\partial}{\partial x} \rho_k \langle \alpha_k \rangle \langle \langle \mathbf{u}_{xk} \rangle \rangle = \langle \Gamma_k \rangle \quad (\text{C.11})$$

C.2: Momentum Conservation Equation

By taking the definition of the conservation quantity term, flux term, and source term;

$$\begin{aligned} \Psi_k &\equiv \mathbf{u}_k \\ \bar{\mathbf{J}}_k &\equiv p_k \bar{\mathbf{I}} - (\bar{\boldsymbol{\tau}}_k + \overline{\mathbf{u}'_k \mathbf{u}'_k{}^T}) \equiv p_k \bar{\mathbf{I}} - \bar{\boldsymbol{\tau}}_k{}^T \\ s_k &\equiv F_k \end{aligned} \quad (\text{C.12})$$

By taking the dot product in the x-direction normal unit vector for one dimensional equation and integrating the time-averaged momentum conservation equation;

$$\begin{aligned} &\int_A \frac{\partial \rho_k \mathbf{u}_{xk} \alpha_k}{\partial t} dA + \int_A \nabla \cdot \alpha_k (\rho_k \mathbf{u}_k \mathbf{u}_{xk} + \mathbf{n}_x \cdot p_k \bar{\mathbf{I}} - \mathbf{n}_x \cdot \bar{\boldsymbol{\tau}}_k{}^T) dA \\ &= \int_A F_{xk} \alpha_k dA - \int_A \frac{1}{T_t} \sum_{T_i} \frac{\mathbf{n}_x}{|\mathbf{n}_k \cdot \mathbf{u}_i|} (\dot{m} \mathbf{u}_k + \mathbf{n}_k \cdot p_k \bar{\mathbf{I}} - \mathbf{n}_k \cdot \bar{\boldsymbol{\tau}}_k{}^T) dA \end{aligned} \quad (\text{C.13})$$

The area-averaged one dimensional momentum conservation equation can be obtained as following:

$$\begin{aligned}
& \frac{1}{A_A} \int \frac{\partial \rho_k \mathbf{u}_{xk} \alpha_k}{\partial t} dA + \frac{1}{A_A} \int \nabla \cdot \alpha_k (\rho_k \mathbf{u}_k \mathbf{u}_{xk} + \mathbf{n}_x \cdot \mathbf{p}_k \bar{\mathbf{I}} - \mathbf{n}_x \cdot \bar{\boldsymbol{\tau}}_k^T) dA \\
& = \frac{1}{A_A} \int \mathbf{F}_{xk} \alpha_k dA - \frac{1}{A_A} \int \frac{1}{T_t} \sum_{T_t} \frac{\mathbf{n}_x}{|\mathbf{n}_k \cdot \mathbf{u}_i|} (\dot{m} \mathbf{u}_k + \mathbf{n}_k \cdot \mathbf{p}_k \bar{\mathbf{I}} - \mathbf{n}_k \cdot \bar{\boldsymbol{\tau}}_k) dA
\end{aligned} \tag{C.14}$$

Applying Leibnitz rule for the first term and Gauss theorem for the second, third, and fourth terms of the momentum conservation equation;

- First Term :

$$\begin{aligned}
\frac{1}{A_A} \int \frac{\partial \rho_k \mathbf{u}_{xk} \alpha_k}{\partial t} dA & = \frac{\partial}{\partial t} \frac{1}{A_A} \int \alpha_k \rho_k \mathbf{u}_{xk} dA - \frac{1}{A_C} \int (\mathbf{n}_k \cdot \mathbf{u}_c) \alpha_k \rho_k \mathbf{u}_{xk} dC \\
& = \frac{\partial}{\partial t} \frac{1}{A_A} \int \alpha_k \rho_k \mathbf{u}_{xk} dA - \frac{1}{A_{C_i}} \int (\mathbf{n}_k \cdot \mathbf{u}_i) \alpha_k \rho_k \mathbf{u}_{xk} dC
\end{aligned} \tag{C.15}$$

- Second Term:

$$\begin{aligned}
\frac{1}{A_A} \int \nabla \cdot \alpha_k \rho_k \mathbf{u}_k \mathbf{u}_{xk} dA & = \frac{\partial}{\partial x} \left(\frac{1}{A_A} \int \mathbf{n}_x \cdot \alpha_k \rho_k \mathbf{u}_k \mathbf{u}_{xk} dA \right) + \frac{1}{A_C} \int \mathbf{n}_k \cdot \alpha_k \rho_k \mathbf{u}_k \mathbf{u}_{xk} dC \\
& = \frac{\partial}{\partial x} \frac{1}{A_A} \int \alpha_k \rho_k u_{xk}^2 dA + \frac{1}{A_{C_i}} \int \mathbf{n}_k \cdot \alpha_k \rho_k \mathbf{u}_i \mathbf{u}_{xk} dC
\end{aligned} \tag{C.16}$$

- Third Term:

$$\begin{aligned}
\frac{1}{A_A} \int \nabla \cdot \alpha_k \mathbf{p}_{xk} dA & = \frac{\partial}{\partial x} \left(\frac{1}{A_A} \int \mathbf{n}_x \cdot \alpha_k \mathbf{p}_{xk} dA \right) + \frac{1}{A_C} \int \mathbf{n}_k \cdot \alpha_k \mathbf{p}_{xk} dC \\
& = \frac{\partial}{\partial x} \frac{1}{A_A} \int \alpha_k p_k dA + \frac{1}{A_{C_i}} \int \mathbf{n}_x \cdot \alpha_k \mathbf{p}_k dC
\end{aligned} \tag{C.17}$$

● Fourth Term:

$$\begin{aligned}
 \frac{1}{A_A} \int \nabla \cdot \alpha_k \bar{\bar{\tau}}_{xk}^T dA &= \frac{\partial}{\partial X} \frac{1}{A_A} \int \mathbf{n}_x \cdot \alpha_k \bar{\bar{\tau}}_{xk}^T dA + \frac{1}{A_C} \int \mathbf{n}_C \cdot \alpha_k \bar{\bar{\tau}}_{xk}^T dC \\
 &= \frac{\partial}{\partial X} \frac{1}{A_A} \int \alpha_k (\bar{\bar{\tau}}_{xxk}^T + \bar{\bar{\tau}}_{xyk}^T + \bar{\bar{\tau}}_{zzk}^T) dA + \frac{1}{A_C} \int (\mathbf{n}_x \cdot \alpha_{ik} \bar{\bar{\tau}}_{ik}^T + \mathbf{n}_x \cdot \alpha_{wk} \bar{\bar{\tau}}_{wk}^T) dC \quad (C.18) \\
 &\cong \frac{\partial}{\partial X} \frac{1}{A_A} \int \alpha_k (\bar{\bar{\tau}}_{xxk} + \overline{\mathbf{u}'\mathbf{u}'_x}) dA + \frac{1}{A_{C_i}} \int \mathbf{n}_x \cdot \alpha_k \bar{\bar{\tau}}_k dC + \frac{4}{D_e} \alpha_{wk} \tau_{wk}
 \end{aligned}$$

In the fourth term, a wall shear must be used in modeling to obtain realistic transient response analysis for the mean well shear stress, τ_{wk} , with the wall wet perimeter.

Combining all of the above terms with the time-averaged source term;

$$\begin{aligned}
 &\frac{\partial}{\partial t} \frac{1}{A_A} \int \alpha_k \rho_k \mathbf{u}_{xk} dA + \frac{\partial}{\partial X} \frac{1}{A_A} \int \alpha_k \rho_k u_{xk}^2 dA \\
 &= -\frac{\partial}{\partial X} \frac{1}{A_A} \int \alpha_k p_k dA - \frac{4\alpha_{wk} \tau_{wk}}{D_e} - \frac{\partial}{\partial X} \frac{1}{A_A} \int \alpha_k (\bar{\bar{\tau}}_{xxk} + \overline{\mathbf{u}'\mathbf{u}'_x}) dA + \frac{1}{A_A} \int F_{xk} \alpha_k dA \quad (C.19) \\
 &\quad - \frac{1}{A_A} \int \frac{1}{T_t} \sum_{T_i} \frac{\mathbf{n}_x \cdot}{|\mathbf{n}_k \cdot \mathbf{u}_i|} (\dot{m}_{ki} + \mathbf{n}_k \cdot p_{ki} \bar{\bar{\mathbf{I}}} - \mathbf{n}_k \cdot \bar{\bar{\tau}}_{ki}) dA - \frac{1}{A_{C_i}} \int \mathbf{n}_x \cdot \alpha_k (p_k \bar{\bar{\mathbf{I}}} - \bar{\bar{\tau}}_k) dC
 \end{aligned}$$

Assuming that the density is not changed much over the flow cross section area and the averaged quantities are constant in the small x-direction distance, the conservation equation can be written as:

$$\begin{aligned}
& \underbrace{\frac{\partial \rho_k}{\partial t} \int_A \alpha_k \mathbf{u}_{xk} dA}_{[1]} + \underbrace{\frac{\partial \rho_k}{\partial X} \int_A \alpha_k u_{xk}^2 dA}_{[2]} \\
&= \underbrace{\frac{\partial}{\partial X} \frac{1}{A} \int_A \alpha_k p_k dA}_{[3]} - 4 \frac{\alpha_{wk} \tau_{wk}}{D_e} - \underbrace{\frac{\partial}{\partial X} \frac{1}{A} \int_A \alpha_k (\bar{\tau}_{xxk} + \overline{\mathbf{u}' \mathbf{u}'^T}_x) dA}_{[4]} + \underbrace{\frac{1}{A} \int_A F_{xk} \alpha_k dA}_{[5]} \quad (C.20) \\
&\underbrace{- \frac{1}{A} \int_A \frac{1}{T_i} \sum_{T_i} \frac{\mathbf{n}_x \cdot}{|\mathbf{n}_k \cdot \mathbf{u}_i|} (\dot{m} \mathbf{u}_{ki} + \mathbf{n}_k \cdot p_{ki} \bar{\mathbf{I}} - \mathbf{n}_k \cdot \bar{\tau}_{ki}) dA}_{[6]} - \frac{1}{A} \int_{C_i} \mathbf{n}_x \cdot \alpha_k (p_k \bar{\mathbf{I}} - \bar{\tau}_k^T) dC
\end{aligned}$$

$$[1]. \quad \frac{\partial \rho_k}{\partial t} \int_A \mathbf{u}_{xk} \alpha_k dA = \frac{\partial}{\partial t} \rho_k \langle \alpha_k \rangle \langle \mathbf{u}_{xk} \rangle \quad (C.21)$$

$$[2]. \quad \frac{1}{A} \int_A u_{xk}^2 \alpha_k dA = \langle \alpha_k \rangle \langle \mathbf{u}_{xk}^2 \rangle \equiv c_m \langle \alpha_k \rangle \langle \mathbf{u}_{xk} \rangle^2 \quad (C.22)$$

$$[3]. \quad \frac{\partial}{\partial X} \frac{1}{A} \int_A \mathbf{n}_x \cdot \alpha_k p_k \bar{\mathbf{I}} dA = \frac{\partial}{\partial X} \frac{1}{A} \int_A p_k \alpha_k dA = \frac{\partial}{\partial X} \langle \alpha_k \rangle \langle p_k \rangle \quad (C.23)$$

$$[4]. \quad \frac{\partial}{\partial X} \frac{1}{A} \int_A \alpha_k (\bar{\tau}_{xxk} + \overline{\mathbf{u}' \mathbf{u}'^T}_x) dA = \frac{\partial}{\partial X} \langle \alpha_k \rangle \langle \bar{\tau}_{xxk} + \overline{\mathbf{u}' \mathbf{u}'^T}_x \rangle \quad (C.24)$$

$$[5]. \quad \frac{1}{A} \int_A (F_k \cdot \mathbf{n}_x) \alpha_k dA = \frac{1}{A} \int_A F_{xk} \alpha_k dA = \langle \alpha_k \rangle \langle F_{xk} \rangle \quad (C.25)$$

The five parts of the sixth term can be written as followings:

- First Term :

$$\frac{1}{A} \int_A \frac{1}{T_t} \sum_{T_t} \frac{\dot{m} \mathbf{u}_{xk}}{|\mathbf{n}_k \cdot \mathbf{u}_i|} dA = \frac{1}{A} \int_A \Gamma_k \mathbf{u}_{xk} dA = \langle \Gamma_k \rangle \langle \mathbf{u}_{xk} \rangle \quad (\text{C.26})$$

- Second Term :

$$\begin{aligned} -\frac{1}{A} \int_A \frac{1}{T_t} \sum_{T_t} \frac{\mathbf{n}_k \cdot \mathbf{n}_x \mathbf{p}_{ki}}{|\mathbf{n}_k \cdot \mathbf{u}_i|} dA &= -\frac{1}{A} \int_A \frac{1}{T_t} \sum_{T_t} \frac{\mathbf{n}_k \cdot \mathbf{n}_x \mathbf{p}_{ki}}{|\mathbf{n}_k \cdot \mathbf{u}_i|} dA \\ &= \frac{1}{A} \int_A \mathbf{n}_x \mathbf{p}_{ki} \nabla \cdot \alpha_k dA \\ &= \frac{1}{A} \int_A \mathbf{p}_{ki} \frac{\partial \alpha_k}{\partial x} dA \\ &= \langle \mathbf{p}_{ki} \rangle \frac{\partial \langle \alpha_k \rangle}{\partial x} \\ \langle \mathbf{p}_{ki} \rangle &\equiv \left(\frac{1}{A} \int_A \mathbf{p}_{ki} \frac{\partial \alpha_k}{\partial x} dA \right) / \left(\frac{1}{A} \int_A \frac{\partial \alpha_k}{\partial x} dA \right) \end{aligned} \quad (\text{C.27})$$

- Third Term:

$$\begin{aligned} \frac{1}{A} \int_A \frac{1}{T_t} \sum_{T_t} \frac{\mathbf{n}_k \cdot \bar{\tau}_{xi}}{|\mathbf{n}_k \cdot \mathbf{u}_i|} dA &= \frac{1}{A} \int_A \frac{1}{T_t} \sum_{T_t} \frac{\mathbf{n}_k \cdot \mathbf{n}_x \bar{\tau}_i}{|\mathbf{n}_k \cdot \mathbf{u}_i|} dA \\ &= -\frac{1}{A} \int_A \bar{\tau}_i \mathbf{n}_x \nabla \cdot \alpha_k dA \\ &= -\frac{1}{A} \int_A \bar{\tau}_i \frac{\partial \alpha_k}{\partial x} dA \end{aligned} \quad (\text{C.28})$$

- Fourth Term :

$$\begin{aligned}
 -\frac{1}{A} \int_C \mathbf{n}_k \cdot \alpha_k \mathbf{p}_{xk} dC &= -\frac{1}{A} \int_{C_i} \mathbf{n}_i \cdot \alpha_k \mathbf{p}_{xk} dC - \frac{1}{A} \int_{C_w} \mathbf{n}_w \cdot \alpha_k \mathbf{p}_{xk} dC \\
 &= -\frac{1}{A} \int_{C_i} \mathbf{n}_i \cdot \mathbf{n}_x \alpha_k p_k dC \quad (C.29) \\
 &= -\frac{1}{A} \int_A \frac{\partial}{\partial x} \alpha_k p_{ki} dA = -\langle \mathbf{n}_x \cdot \nabla \alpha_k p_{ki} \rangle
 \end{aligned}$$

- Fifth Term:

$$\begin{aligned}
 \frac{1}{A} \int_{C_i} \mathbf{n}_x \cdot \alpha_k \bar{\tau}_k dC &= \frac{1}{A} \int_{C_i} \mathbf{n}_x \cdot \alpha_k \bar{\tau}_k dC \\
 &= \frac{1}{A} \int_A \frac{\partial}{\partial x} \alpha_k \bar{\tau}_{ki} dA \quad (C.30) \\
 &= \frac{1}{A} \int_A \bar{\tau}_{ki} \frac{\partial \alpha_k}{\partial x} dA + \frac{1}{A} \int_A \alpha_k \frac{\partial \bar{\tau}_{ki}}{\partial x} dA \\
 &= \langle \bar{\tau}_{ki} \nabla \alpha_k \cdot \mathbf{n}_x \rangle + \frac{1}{A} \int_A \alpha_k \frac{\partial \bar{\tau}_{ik}}{\partial x} dA
 \end{aligned}$$

Combing all the equations, another form of the one-dimensional two-fluid momentum conservation equation can be obtained such as:

$$\begin{aligned}
 \frac{\partial}{\partial t} \rho_k \langle \alpha_k \rangle \langle \mathbf{u}_{xk} \rangle + \frac{\partial}{\partial x} c_m \rho_k \langle \alpha_k \rangle \langle \mathbf{u}_{xk} \rangle^2 + \frac{\partial}{\partial x} \langle \alpha_k \rangle \langle \mathbf{p}_k \rangle - \langle \alpha_k \rangle \langle \mathbf{F}_{xk} \rangle \\
 = \langle \Gamma_k \rangle \langle \mathbf{u}_{xk} \rangle + \langle \mathbf{p}_{ki} \rangle \frac{\partial \langle \alpha_k \rangle}{\partial x} - \langle \mathbf{n}_x \cdot \nabla \alpha_k p_{ki} \rangle - \langle \bar{\tau}_{ki} \nabla \alpha_k \cdot \mathbf{n}_x \rangle - 4 \frac{\alpha_{wk} \tau_{wk}}{D_c} \quad (C.31)
 \end{aligned}$$

$$\begin{aligned}
& \frac{\partial}{\partial t} \rho_k \langle \alpha_k \rangle \langle \mathbf{u}_{xk} \rangle + \frac{\partial}{\partial x} c_m \rho_k \langle \alpha_k \rangle \langle \mathbf{u}_{xk} \rangle^2 + \frac{\partial}{\partial x} \langle \alpha_k \rangle \langle \mathbf{p}_k \rangle - \langle \alpha_k \rangle \langle \mathbf{F}_{xk} \rangle \\
& = \langle \Gamma_k \rangle \langle \mathbf{u}_{xk} \rangle + \langle \mathbf{p}_{ki} \rangle \frac{\partial \langle \alpha_k \rangle}{\partial x} - \langle \mathbf{M}_{xk}^d \rangle - 4 \frac{\alpha_{wk} \tau_{wk}}{D_c} \\
& \mathbf{M}_{xk}^d \equiv \mathbf{n}_x \cdot \nabla \alpha_k \mathbf{p}_{ki} - \bar{\bar{\tau}}_{ki} \nabla \alpha_k \cdot \mathbf{n}_x
\end{aligned} \tag{C.32}$$

C.3: Constitutive Equation

The local instantaneous form of the general conservation equation across the interface can be written:

$$\begin{aligned}
& \sum_{k=1}^2 [\dot{m}_k \psi_k + \mathbf{J}_k \cdot \mathbf{n}_k] = 0 \\
& \psi_k = 1 \\
& \mathbf{J}_k = 0
\end{aligned} \tag{C.33}$$

The interface mass jump condition can be derived:

$$\sum_{k=1}^2 \dot{m}_k = 0 \tag{C.34}$$

By multiplying the mass jump condition by an indication function and averaging this equation over a sampling time, the time-averaged interfacial mass transfer conditions can be obtained as follows.

$$\begin{aligned}
0 & = \sum_k \frac{1}{T_S} \int_{T_k} \dot{m}_k dt = \sum_k \frac{1}{T_k} \int \dot{m}_k dt \\
& = \sum_k \bar{\dot{m}}_k \frac{T_k}{T_S} = \sum_k \bar{\dot{m}}_k^T \alpha_k = \bar{\dot{m}}_k^T + (\bar{\dot{m}}_k^T - \bar{\dot{m}}_k^T) \alpha_k
\end{aligned} \tag{C.35}$$

With the mass balance equation and none zero void fraction, the interface mass jump condition can be reduced to the following time-average mass transfer rate conditions:

$$0 = \overline{\dot{m}}_k^T = \overline{\dot{m}}_k^T \quad (\text{C.36})$$

C.4: One-Dimensional Horizontal Flow Model

The averaged momentum equation can be simplified with the delta pressure definition as the averaged interfacial pressure and the averaged bulk pressure difference:

$$\langle F_x \rangle = 0 \quad (\text{C.37})$$

Without phase change conditions, the mass interface balance equation is the only statements of the local instantaneous interfacial velocity difference.

$$\langle \Gamma_k \rangle = 0 \quad (\text{C.38})$$

$$\Delta p_k \equiv \langle \langle p_{ki} \rangle \rangle - \langle \langle p_k \rangle \rangle \quad (\text{C.39})$$

After simplifications with no mass transfer and no-viscosity, the averaged momentum conservation equation can be written as:

$$\begin{aligned} \frac{\partial}{\partial t} \rho_1 \langle \alpha_1 \rangle \langle u_1 \rangle + \frac{\partial}{\partial x} c_m \rho_1 \langle \alpha_1 \rangle \langle u_1 \rangle^2 - \Delta p_1 \frac{\partial}{\partial x} \langle \alpha_1 \rangle &= -\frac{\partial}{\partial x} \langle p_1 \rangle \\ \frac{\partial}{\partial t} \rho_2 \langle \alpha_2 \rangle \langle u_2 \rangle + \frac{\partial}{\partial x} c_m \rho_2 \langle \alpha_2 \rangle \langle u_2 \rangle^2 + \Delta p_2 \frac{\partial}{\partial x} \langle \alpha_2 \rangle &= -\frac{\partial}{\partial x} \langle p_2 \rangle \end{aligned} \quad (C.40)$$

$$\frac{\partial}{\partial x} \langle p_1 \rangle = \frac{\partial}{\partial x} \langle p_2 \rangle$$

With simple notation, the one dimensional two-fluid momentum equations can be written:

$$\begin{aligned} \frac{\partial}{\partial t} \rho_1 \alpha_1 u_1 + \frac{\partial}{\partial x} c_m \rho_1 \alpha_1 u_1^2 - \Delta p_1 \frac{\partial}{\partial x} \alpha_1 &= -\frac{\partial}{\partial x} p_1 \\ \frac{\partial}{\partial t} \rho_2 \alpha_2 u_2 + \frac{\partial}{\partial x} c_m \rho_2 \alpha_2 u_2^2 - \Delta p_2 \frac{\partial}{\partial x} \alpha_2 &= -\frac{\partial}{\partial x} p_1 \end{aligned} \quad (C.41)$$

APPENDIX D: INTEGRAL PARAMETERS FOR SEPARATED FLOW

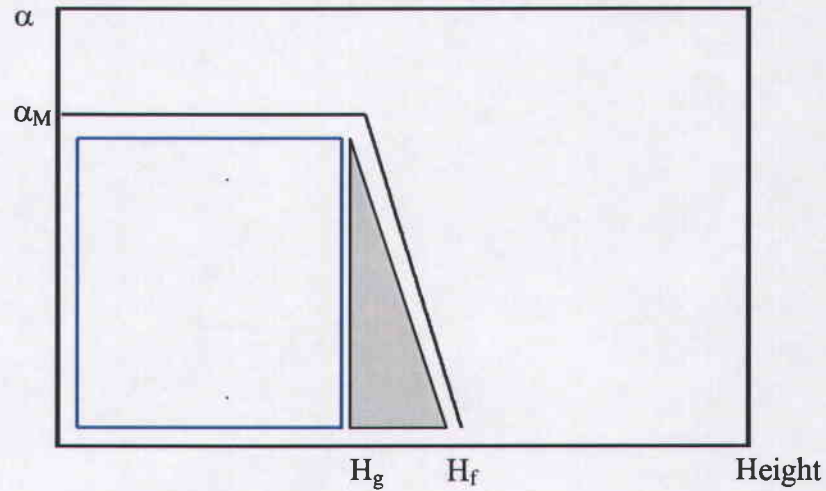


Figure D.1: Void Fraction Profile Model (Separated Flow)

$$\begin{aligned}
 \delta_1 &\equiv \frac{1}{H} \int_0^y \int_0^y \alpha \, dh \frac{\partial \alpha}{\partial x} \, dy / \int_0^y \frac{\partial \alpha}{\partial x} \, dy \\
 &= \frac{1}{H} \int_0^{H_g} \left(\int_0^y \alpha_M \, dh + \int_{H_g}^y \alpha^L \, dh \right) \frac{\partial \alpha}{\partial x} \, dy / \int_{H_g}^{H_f} \left(\frac{\partial \alpha}{\partial x} \right) \, dy \\
 &= \frac{1}{H} \int_{H_g}^{H_f} \left(\frac{\alpha^L}{2} (y^2 - H_g^2) \right) \left(\frac{\partial \alpha}{\partial x} \right) \, dy / \int_{H_g}^{H_f} \left(\frac{\partial \alpha}{\partial x} \right) \, dy \\
 &= \frac{1}{H} \int_{H_g}^{H_f} \left(\frac{\alpha^L}{2} (y^2 - H_g^2) \right) \, dy / \int_{H_g}^{H_f} \, dy \\
 &= \frac{\alpha^L \left(\frac{1}{3} (H_f^3 - H_g^3) - H_g^2 (H_f - H_g) \right)}{H (H_f - H_g)} \\
 &= \frac{\alpha_M (H_f^2 + H_g H_f + H_g^2 - 3H_g^2)}{6H (H_f - H_g)} \\
 &= \frac{\alpha_M (H_f^2 + H_g H_f - 2H_g^2)}{6H (H_f - H_g)}
 \end{aligned} \tag{D.1}$$

$$\begin{aligned}
\delta_2 &= \frac{1}{H} \int_H y \left(\frac{\partial \alpha}{\partial x} \right) dy / \int_H \left(\frac{\partial \alpha}{\partial x} \right) dy \\
&= \frac{1}{H} \int_{H_g}^{H_f} y \left(\frac{\partial \alpha}{\partial x} \right) dy / \int_{H_g}^{H_f} \left(\frac{\partial \alpha}{\partial x} \right) dy \\
&= \frac{1}{H} \int_{H_g}^{H_f} y \alpha^L dy / \int_{H_g}^{H_f} \alpha^L dy \quad (D.2) \\
&= \frac{1}{2H} (H_f^2 - H_g^2) / (H_f - H_g) \\
&= \frac{H_f + H_g}{2H}
\end{aligned}$$

$$\begin{aligned}
\theta_2 &\equiv \frac{1}{H} \int_H \alpha y dy / \int_H \alpha dy \\
&= \frac{1}{H} \int_H (\alpha_M + \alpha^L y) y dy / \int_H (\alpha_M + \alpha^L y) dy \\
&= \frac{1}{H} \frac{\frac{1}{2} \alpha_M H_g^2 + \frac{1}{3} \alpha^L (H_f^3 - H_g^3)}{\alpha_M H_g + \frac{1}{2} \alpha^L (H_f^2 - H_g^2)} \\
&= \frac{\alpha_M \frac{1}{2} H_g^2 + \frac{1}{3} (H_f^2 + H_f H_g + H_g^2)}{H \left(\alpha_M H_g + \frac{\alpha_M}{2} (H_f + H_g) \right)} \\
&= \frac{5H_g^2 + 2H_f H_g + 2H_f^2}{3H(H_f + 3H_g)} \quad (D.3)
\end{aligned}$$

$$\begin{aligned}
\theta_1 &\equiv \frac{1}{H} \int_H \int_0^y \alpha \, dh \, \alpha \, dy / \int_H \alpha \, dy \\
&= \frac{1}{H} \int_H \left(\int_0^{H_g} \alpha_M \, dh + \int_{H_g}^y \alpha^L \, dh \right) \alpha \, dy / \left(\int_0^{H_g} \alpha_M \, dy + \int_{H_g}^{H_f} \alpha^L \, dy \right) \\
&= \frac{1}{H} \int_H \left(\alpha_M H_g + \int_{H_g}^y \alpha^L \, dh \right) \alpha \, dy / \left(\int_0^{H_g} \alpha_M \, dy + \int_{H_g}^{H_f} \alpha^L \, dy \right) \\
&= \frac{\alpha_M \alpha_M H_g^2 + \frac{\alpha^L \alpha^L}{2} \left(\frac{1}{4} (H_f^4 - H_g^4) - \frac{1}{2} H_g^2 (H_f^2 - H_g^2) \right)}{\alpha_M H H_g + \alpha^L H (H_f^2 - H_g^2) / 2} \\
&= \frac{\alpha_M \alpha_M H_g^2 + \frac{\alpha_M \alpha_M}{4 (H_f - H_g)^2} \left(\frac{1}{2} (H_f^4 - H_g^4) - H_g^2 (H_f^2 - H_g^2) \right)}{\alpha^C H H_g + \alpha^C H (H_f + H_g) / 2} \\
&= \frac{\alpha_M H_g^2 + \frac{\alpha_M (H_f^2 - H_g^2)}{4 (H_f - H_g)^2} \left(\frac{1}{2} (H_f^2 + H_g^2) - H_g^2 \right)}{H H_g + H (H_f + H_g) / 2} \\
&= \frac{2 \alpha_M H_g^2 + \frac{\alpha_M (H_f + H_g)}{4 (H_f - H_g)} (H_f^2 - H_g^2)}{H H_g + H H_f} \\
&= \frac{8 \alpha_M H_g^2 + \alpha_M (H_f + H_g)^2}{4 H (3 H_g + H_f)} \\
&= \alpha_M \frac{H_f^2 + 2 H_f H_g + 9 H_g^2}{4 H (3 H_g + H_f)} \tag{D.4} \\
&= \frac{2 H_g \alpha_M + \alpha_M (H_f - H_g)}{4 H} + \alpha_M \frac{2 H_g (3 H_g - H_f)}{4 H (3 H_g + H_f)} \\
&= \frac{\langle \alpha \rangle}{2 H} \quad \text{if } 3 H_g = H_f
\end{aligned}$$

APPENDIX E: INTEGRAL PARAMETERS FOR MIXED FLOW

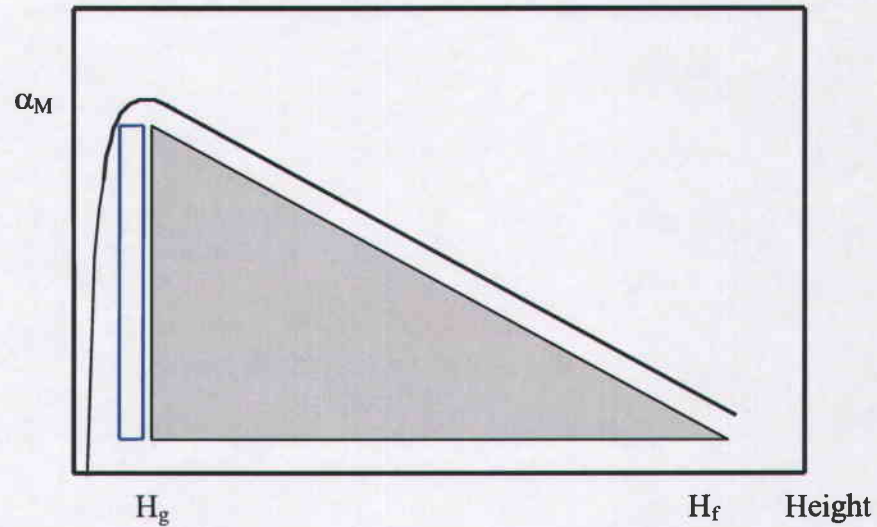


Figure E.1: Void Fraction Profile (Mixed Flow)

$$\begin{aligned}
 \delta_2 &= \frac{1}{H} \int_H y \left(\frac{\partial \alpha}{\partial x} \right) dy / \int_H \left(\frac{\partial \alpha}{\partial x} \right) dy \\
 &= \frac{1}{H} \int_{H_g}^{H_f} y \left(\frac{\partial \alpha}{\partial x} \right) dy / \int_{H_g}^{H_f} \left(\frac{\partial \alpha}{\partial x} \right) dy \\
 &= \frac{1}{H} \int_{H_g}^{H_f} y \alpha^L dy / \int_{H_g}^{H_f} \alpha^L dy \quad (E.1) \\
 &= (H_f^2 - H_g^2) / 2H(H_f - H_g) \\
 &= \frac{H_f + H_g}{2H}
 \end{aligned}$$

$$\begin{aligned}
\delta_1 &\equiv \frac{1}{H} \int_0^y \alpha \, dh \frac{\partial \alpha}{\partial x} \, dy / \int_H \frac{\partial \alpha}{\partial x} \, dy \\
&= \frac{1}{H} \int_H \left(\int_0^{H_g} \alpha_M \, dh + \int_{H_g}^y \alpha^L \, h \, dh \right) \frac{\partial \alpha}{\partial x} \, dy / \int_{H_g}^{H_f} \left(\frac{\partial \alpha}{\partial x} \right) \, dy \\
&= \frac{1}{H} \int_{H_g}^{H_f} \left(\frac{\alpha^L}{2} (y^2 - H_g^2) \right) \left(\frac{\partial \alpha}{\partial x} \right) \, dy / \int_{H_g}^{H_f} \left(\frac{\partial \alpha}{\partial x} \right) \, dy \\
&= \frac{1}{H} \int_{H_g}^{H_f} \left(\frac{\alpha^L}{2} (y^2 - H_g^2) \right) \, dy / \int_{H_g}^{H_f} \, dy \\
&= \frac{\alpha^L}{2H} \left(\frac{1}{3} (H_f^3 - H_g^3) - H_g^2 (H_f - H_g) \right) / (H_f - H_g) \\
&= \frac{\alpha_M (H_f^2 + H_g H_f + H_g^2 - 3H_g^2)}{6H (H_f - H_g)} \\
&= \frac{\alpha_M (H_f^2 + H_g H_f - 2H_g^2)}{6H (H_f - H_g)} \tag{E.2}
\end{aligned}$$

$$\begin{aligned}
\theta_2 &\equiv \frac{1}{H} \int_H \alpha y \, dy / \int_H \alpha \, dy \\
&= \frac{1}{H} \int_{H_g}^{H_f} (\alpha^L y) y \, dy / \int_{H_g}^{H_f} (\alpha^L y) \, dy \\
&= \frac{1}{H} \left(\frac{1}{3} \alpha^L (H_f^3 - H_g^3) \right) / \left(\frac{1}{2} \alpha^L (H_f^2 - H_g^2) \right) \tag{E.3} \\
&= \frac{1}{3H} (H_f^2 + H_f H_g + H_g^2) / \left(\frac{1}{2} (H_f + H_g) \right) \\
&= \frac{2(H_f^2 + H_f H_g + H_g^2)}{3H (H_f + H_g)}
\end{aligned}$$

$$\begin{aligned}
\theta_1 &\equiv \frac{1}{H} \int_{H_0}^y \alpha \, dh \alpha \, dy / \int_H \alpha \, dy \\
&= \frac{1}{H} \int_H \left(\int_{H_g}^y \alpha^L h \, dh \right) \alpha \, dy / \int_{H_g}^{H_f} \alpha^L h \, dh \\
&= \frac{1}{H} \int_H \left(\int_{H_g}^y \alpha^L h \, dh \right) \alpha \, dy / \frac{\alpha^L}{2} (H_f^2 - H_g^2) \\
&= \frac{1}{H} \int_{H_g}^{H_f} \left(\frac{\alpha^L}{2} (y^2 - H_g^2) \right) \alpha^L y \, dy / \frac{\alpha^L}{2} (H_f^2 - H_g^2) \\
&= \frac{1}{H} \int_{H_g}^{H_f} \left(\frac{\alpha^L \alpha^L}{2} (y^3 - H_g^2 y) \right) dy / \frac{\alpha^L}{2} (H_f^2 - H_g^2) \\
&= \frac{\alpha^L \alpha^L}{2H} \left(\frac{1}{4} (H_f^4 - H_g^4) - \frac{1}{2} H_g^2 (H_f^2 - H_g^2) \right) / \left(\frac{\alpha^L}{2} (H_f^2 - H_g^2) \right) \\
&= \frac{\alpha_M}{4H(H_f - H_g)} \left((H_f^4 - H_g^4) - 2H_g^2 (H_f^2 - H_g^2) \right) / (H_f^2 - H_g^2) \\
&= \frac{\alpha_M (H_f^2 - H_g^2) (H_f^2 + H_g^2 - 2H_g^2)}{4H(H_f - H_g)(H_f^2 - H_g^2)} \\
&= \frac{\alpha_M (H_f^2 - H_g^2)}{4H(H_f - H_g)} \\
&= \frac{\alpha_M (H_f + H_g)}{4H} \\
&= \alpha_M \frac{H_f - H_g}{4H} + \alpha_M \frac{2H_g}{4H} \\
&= \frac{\langle \alpha \rangle}{2H} \quad \text{if } H_g = 0
\end{aligned} \tag{E.4}$$

APPENDIX F: DELTA PRESSURE EVALUATION

With the integral parameters, the delta pressure can be written:

- **Separated flow**

$$\begin{aligned}
 \langle\langle p_i \rangle\rangle - \langle\langle p_g \rangle\rangle &= -(\rho_2 - \rho_1)gH(\theta_1 - \delta_1) - \rho_f gH(\theta_2 - \delta_2) \\
 &= -\frac{(\rho_f - \rho_g)g\alpha_M}{3} \left(\frac{H_g + \frac{1}{2}(H_f - H_g)}{2} + H_g - \frac{3H_f H_g}{(H_f + 3H_g)} \right) \\
 &\quad + \frac{\rho_f g}{3} \left(6H_g - \frac{2H_f^2 + 2H_f H_g + 6H_g^2}{(H_f + 3H_g)} + \frac{H_g^2}{(H_f + 3H_g)} \right) \quad (F.1) \\
 &= -\frac{(\rho_f - \rho_g)g}{3} \left(\frac{1}{2} H_g \alpha_M \right) + \frac{\rho_f g H_g}{3} + \frac{\rho_f g H_g}{18} \\
 &\cong -\frac{(\rho_f - \rho_g)g}{6} \left(\frac{1}{2} H_g \alpha_M \right) + \frac{\rho_f g H_g}{3}
 \end{aligned}$$

With the definition of the triangle void fraction area to total flow void fraction area ratio for linear wavy fraction void fraction model;

$$\frac{1}{2}(H_f - H_g)\alpha_M \equiv K\langle\alpha\rangle H \Rightarrow \frac{1}{2}(2H_g)\alpha_M = K\langle\alpha\rangle H \Rightarrow H_g = K \frac{\langle\alpha\rangle}{\alpha_M} H \quad (F.2)$$

The delta pressure of the wavy type flow can be written:

$$\langle\langle p_i \rangle\rangle - \langle\langle p_g \rangle\rangle = K \left(\frac{\rho_f g}{3\alpha_M} - \frac{\rho_f - \rho_g}{6} \right) g\langle\alpha\rangle H \quad (F.3)$$

● **Mixed flow**

$$\begin{aligned}
 \langle\langle p_i \rangle\rangle - \langle\langle p_g \rangle\rangle &= -(\rho_f - \rho_g)gH\alpha_M \left(\frac{H_f + H_g}{4H} - \frac{H_f^2 + H_g H_f - 2H_g^2}{6H(H_f - H_g)} \right) \\
 &\quad - \rho_f gH \left(\frac{2(H_f^2 + H_f H_g + H_g^2)}{3H(H_f + H_g)} - \frac{(H_f + H_g)}{2H} \right) \\
 &= -(\rho_f - \rho_g)gH\alpha_M \left(\frac{H_f - H_g}{12H} \right) + \rho_f gH \frac{(H_f - H_g)^2}{6H(H_f + H_g)} \quad (F.4) \\
 &= -(\rho_f - \rho_g)gH\alpha_M \left(\frac{H_f}{12H} \right) + \rho_f gH \left(\frac{H_f}{6H} \right) \\
 &= -(\rho_f - \rho_g)g\alpha_M \left(\frac{H_f}{12} \right) + \rho_f g \left(\frac{H_f}{6} \right)
 \end{aligned}$$

Similarly, with the triangle void fraction area condition for the linear slug flow void fraction model;

$$K \langle \alpha \rangle = \frac{1}{2} \frac{\alpha_M}{H_f} \frac{H_f^2}{H} \Rightarrow H_f = 2K \frac{\langle \alpha \rangle}{\alpha_M} H \quad (F.5)$$

the delta pressure term of slug flow can be written;

$$\langle\langle p_i \rangle\rangle - \langle\langle p_g \rangle\rangle = K \left(\frac{\rho_f}{3\alpha_M} - \frac{\rho_f - \rho_g}{6} \right) g \langle \alpha \rangle H \quad (F.6)$$